IDO-16807

32 5
12.27-6-2

MASTER

ORGANIC REACTOR TECHNOLOGY
QUARTERLY REPORT

April 1 - June 30, 1962

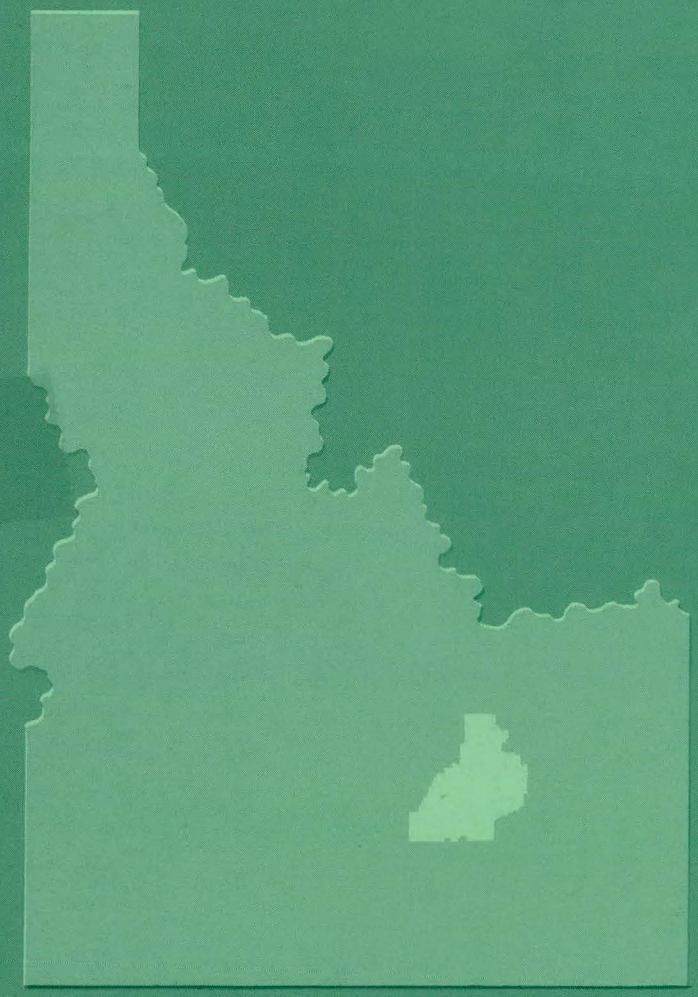

PHILLIPS PETROLEUM COMPANY

ATOMIC ENERGY DIVISION

NATIONAL REACTOR TESTING STATION

US ATOMIC ENERGY COMMISSION

DISCLAIMER

PRICE $2.25

Available from the
Office of Technical Services
U. S. Department of Commerce
Washington 25, D. C.

LEGAL NOTICE

Printed in USA

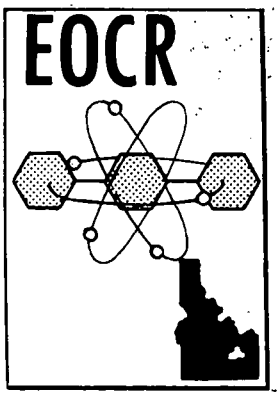

IDO-16807
AEC Research and Development Report
Reactor Technology
TID-4500 (17th Ed.)
Issued: October 15, 1962

ORGANIC REACTOR TECHNOLOGY
QUARTERLY REPORT
April 1 - June 30, 1962

J. R. Huffman
Assistant Manager, Technical

J. A. McBride
Manager, Chemical Technology

J. C. Hillyer
Manager, OCR Project, Bartlesville

J. W. Dykes
Superintendent, EOCR Operations

W. B. Lewis
Manager, EOCR Technical Branch

PHILLIPS
PETROLEUM
COMPANY

Atomic Energy Division
Contract AT(10-1)-205
Idaho Operations Office
U. S. ATOMIC ENERGY COMMISSION

Organic Coolant Research (Part I of this report) was carried out by Phillips Petroleum Company, Research and Development Department, Bartlesville, Oklahoma under Contract AT(10-1)-1080 with the Idaho Operations Office, U.S. Atomic Energy Commission.

Previous quarterly reports in this series, listed under the title "Organic Coolant Reactor Program Quarterly Report"

1960

Quarter	Number
4	IDO-16675

1961

Quarter	Number
1	IDO-16705
2	IDO-16713
3	IDO-16734
4	IDO-16761

1962

Quarter	Number
1	IDO-16787

ORGANIC REACTOR TECHNOLOGY
QUARTERLY REPORT
APRIL 1 - JUNE 30, 1962

SUMMARY

The deposition of film was studied in irradiated circulating loops, in which both grounded and insulated plates were in the irradiated coolant volume; purpose of these tests was to determine the effect on rate of film formation of charges generated on particulate matter or coolant molecules in the radiation field. Heavier deposits were found on the grounded plates and currents up to 30 microamp were measured flowing to this plate. Tests in the newly designed rocking cell showed that techniques are now available whereby this apparatus can be used with confidence to screen film-forming characteristics of coolant compositions.

It was demonstrated that iron percarbide ($Fe_{20}C_9$) could be made under conditions comparable to those in the OMRE. It was made from an iron chelate by carbon monoxide reduction and emphasizes the possible importance of oxygen containing chelate in the transport of iron and deposition of film.

The nature of the impurities occurring in commercial Santowax was examined and some highly colored, oxygenated material isolated. The hexaphenyls produced in irradiation of m- and p-terphenyls and in the reaction of polyphenyls with hydrogen atoms was studied.

Further work was initiated in the area of synthesis of reference hexaphenyls, but synthesis of new candidate coolants also was continued. Areas under study included non-benzenoid heterocyclics, fused ring compounds, and hydrogen donor compounds. Partially hydrogenated fused ring structures, such as dihydrophenanthrene, continue to look very promising. Stabilizer studies were directed largely toward this area also, but the stabilizer program was brought to a close.

The study of hydrocracking of high boiler was completed with a few additional catalyst tests. The treatment of unfractionated coolant was further developed and continued to look like the most desirable operation. Preliminary economic evaluations on the hydrocracking routes to reclamation were completed and looked attractive.

Design liaison on the Coolant Technology and Fuel Technology Loops and on loop handling equipment is nearing completion. Loop construction is about 13 percent completed. Overall completion of the basic EOCR was approximately 90 percent at the end of the reporting period.

The out-of-pile Component Development Test Loop has operated for Chempump testing with diphenyl-terphenyl eutectic fluid at temperatures up to 600°F.

Methods of attaching thermocouples to fuel plates and of leading them out of the fuel assembly have been studied. Both high temperature furnace brazing and resistance spot welding have been used for attachment in these studies,

and the brazing method has been selected as the preferred method for attaching thermocouples to the instrumented fuel plates. A detailed study of the locations of the thermocouples has been completed.

The practicability of using ethylene glycol as a displacement cleaner of fuel elements has been demonstrated. Studies on film formation from Santowax refluxed with chemically cleaned pipe sections have indicated that the passivation film dissolves in the organic and increases the film deposit. This effect is eliminated by one refluxing with Santowax.

Capsules for use in the MTR hydraulic rabbit facility have been designed and built. These will furnish heat by gamma absorption and permit organic samples to be irradiated at desired temperatures in a neutron field.

An improved capsule for pyrolytic fouling has been under test. Initial results have been satisfactory and indicate that useful heat transfer data on the coolant may be an unexpected dividend from use of this apparatus.

A draft of the EOCR Safety Analysis Review (formerly called Final Hazards Evaluation) was discussed informally with representatives of IDO and AEC from Washington. The final draft of this document is now in preparation, incorporating comments and requests received during the review.

Preparation of operating manuals and liaison with the EOCR construction contractor on component testing continue to require the major attention of the EOCR Operations Branch.

ORGANIC REACTOR TECHNOLOGY
QUARTERLY REPORT
APRIL 1 - JUNE 30, 1962

CONTENTS

FIGURES

TABLES

I. ORGANIC COOLANT RESEARCH

1. INTRODUCTION

The Research Division of Phillips Petroleum Co at Bartlesville, Okla, under Contract AT(10-1)-1080 with the Idaho Operations Office of the U. S. Atomic Energy Commission, as part of the Phillips' program on technology of organic-cooled and -moderated nuclear reactors, continued its study of the fundamentals of radiolytic breakdown of organic compounds, the deposition of film on fuel element surfaces, the selection of more resistant coolants, and the stabilization and reclamation of coolants.

Basic work on the radiolysis of terphenyls and on the mechanism and prevention of film formation continues to be the major effort. Work in the area of new coolants and in stabilizers have been closely coordinated with each other and with the fundamental radiolytic studies. Reclamation of damaged coolant by hydrocracking was extended to operation on the total coolant stream without prior separation of the high boiling waste fraction. Experimental work on this modification was in its final phases and economics were reevaluated on this basis.

2. RADIOLYTIC EXPERIMENTS

(P. S. Hudson, W. M. Hutchinson, R. B. Regier,
A. J. Moffat, R. A. Mengelkamp, P. W. Solomon)

2.1 Introduction

Continued emphasis has been directed toward the understanding of radiolysis of coolants, both to yield film and to high- and low-boiling degradation products. Attention also has been given to the radiation chemistry of aromatic mixtures, particularly coolants containing benzene. No work was done on dosimetry for the Linac, due to continued operating difficulties with the machine. Time and power available for the program were not adequate until the latter part of the quarter, for the same reason.

2.2 Film Deposition Under Irradiation

The objective of this investigation is to employ electron irradiation to cause radiolysis of coolant and deposit of a film on metal heat transfer surfaces, under controlled conditions so that the parameters involved in the OMRE experience with fouling can be systematically investigated. The OMRE conditions are most closely simulated by a circulating apparatus with a radiation cell with the same geometry as an OMRE fuel element coolant channel. Other loops, with radiation cells designed to investigate particular factors, extend the range studied, or achieve greater absorption of radiation, are in use. Study of the effect of coolant components is most readily done in a small noncirculating system, which lends itself to rapid screening on small samples.

2.21 Large Circulating Loop. Demonstration has been made of the deposition of film in the OMRE replica cell with typical used coolant containing high boilers and particulate matter high in iron content, and of lack of film when

clean coolant is in the system. Coolant velocity has been shown to have a direct effect on the thickness of film deposited. The apparatus has a very low ratio of in-beam to out-of-beam volume. Long irradiation times are required for deposition of appreciable films. It has been more profitable to direct research effort to other units giving more rapid film deposition during this quarter, particularly in view of the limited Linac power which prevailed during much of the time.

2.22 Small Circulating Loop. Using the small out-of-pile electron irradiation loop with the 1.75-inch-deep channel cell, a short series of exploratory tests was conducted. The objective of these tests was to study electrostatic effects on film formation. It has been postulated that beta current going to ground in the highly ionized reactor core might influence the deposition of film particulates on the fuel element surfaces. The deep channel cell with a grounded and non-grounded plate located 0.8 inch below the electron window in the coolant stream was utilized to test this hypothesis.

Tests REPL-3, -4, -5, and -6 - Effect of Grounding a Film Formation Surface

A third test in this series (REPL-3) was conducted with a charge of 3200 grams of coolant under the test conditions specified in Table I. The No. 1 condenser plate (outboard relative to cell) was grounded.

TABLE I

CIRCULATING LOOP TEST CONDITIONS FOR GROUNDED PLATE RUNS

Test No.	REPL-3	REPL-4	REPL-5	REPL-6
Coolant	CM-10235-64H(a)	CM-10235-50D(b)	CM-10235-64H	CM-10235-64H
Window temperature (°F)	850	850	890	850
Bulk coolant temperature (°F)	740	740	740	720
Velocity (ft/sec)	1.0	1.0	0.5	0.5
N_2 blanket pressure (psig)	200	200	200	200
Test period (hr)	18	18	18	18

(a) OMRE Core II coolant contained 10.2% high boiler, and 14-ppm Fe; 0.2% ferrocene was added to the coolant.

(b) OMRE Core II coolant contained 23% high boiler, and 50-ppm Fe; 0.2% ferrocene was added to the coolant.

Test results are shown in Table II. Electron beam current to the grounded plate was 30 microamp during the test. If the current flowed uniformly to the plate, the beta-current flux density was about 0.5 $\mu a/cm^2$. Measurements indicated 0.2 mil of film was formed on both the grounded electron window and on the grounded plate suspended vertically in the cell. The ungrounded plate had only 0.1 mil of film on it. The film on the electron window was uniform, indicating the electron beam was uniform over both grounded and ungrounded plates. Under these test conditions, a preferential deposit on the grounded

TABLE II

CIRCULATING LOOP TEST RESULTS OF GROUNDED PLATE RUNS

	Test No.			
	REPL-3	REPL-4	REPL-5	REPL-6
Window film thickness (mil)	0.2	0.2	0.4	0.1
Window film weight (mg)	2.3	6.0	16.2	2.0
Window film weight (mg/cm^2)	0.09	0.23	0.61	0.08
Window film X-ray diffraction analysis	Fe_3O_4, α-Fe	Fe_3O_4, α-Fe	Fe_3O_4	Fe_3O_4, α-Fe
Film composition				
%C	11.1	10.9	33.0	48.0
%H	3.3	2.0	1.2	3.6
C/H	0.28	0.45	2.3	1.1
%Ash	90	92	68	51
Grounded plate film thickness (mil)	0.2	0.14	0.3	0.1
Ungrounded film thickness (mil)	0.1	0.04	0.2	0.1
Grounded plate film weight (mg)	—	—	9.1	1.4
Ungrounded plate film weight (mg)	—	—	8.4	2.3
Total plate film weight (mg)	14.7	36.2	17.5	3.7
Total plate film weight (mg/cm^2)	0.25	0.62	0.30	0.06
Total plate film X-ray diffraction	Fe_3O_4, α-Fe	Fe_3O_4, α-Fe	Fe_3O_4	Fe_3O_4, α-Fe
Plate film				
%C	14.4	19.7	32.7	26.0
%H	0.94	1.1	1.6	2.0
C/H	1.3	1.5	1.7	1.1
%Ash	85	80	64	75
High boiler increase test (%)	10.4 to 14.4	23.2 to 26.5	10.2 to 14.1	10.5 to 12.5
Estimated dosage (rads)	6.5×10^8	5.4×10^8	6.1×10^8	2.5×10^8
Blanket gas mass spectrometer[a] (mol%)				
H_2	10.69	14.70	8.03	5.43
N_2	77.41	56.26	82.78	89.73
CO_2	3.17	8.54	1.64	1.69
O_2	0.11	0.17	2.05	0.06
C_1 and heavier	8.62	20.33	5.50	3.09

(a) Gas sample taken at end of test.

plate was indicated. Photographs of the window and condenser plates are shown in Figure 1.

Test severity with the small loop for an 18-hour run was equivalent to a 56-hour run in the large loop with the replica cell since the increase in high boiler was similar. Also the amount of film deposited in both tests was equal. Thus the REPL test procedure requires less time and gives good results which are comparable to previous tests.

Test REPL-4 was conducted on a Core 2 coolant which contained 23 percent high boiler and had originally 50-ppm iron. The iron content was increased by 600 ppm by adding 0.2 percent ferrocene to the coolant. This test was conducted at the same conditions as REPL-3 with the exception that the coolant contained more than twice the high boiler content and slightly more iron content. Test conditions are shown in Table I and test results are shown in Table II. Test results showed more than twice as much film weight on both the electron window and the condenser plates than in test REPL-3. This difference in film formation may be due to the higher concentration of high boiler in test REPL-4 coolant since the inorganic content was about the same.

Test results also showed about three times as much film on the grounded plate as on the ungrounded one. This was in general agreement with results obtained in test REPL-3. Photographs of the electron window and condenser plates are shown in Figure 2.

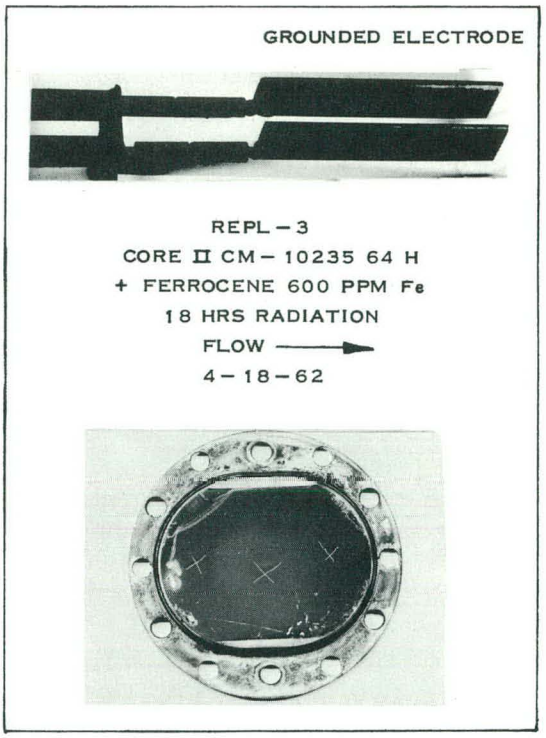

Fig. 1 Electron irradiation window and condenser plates from test REPL-3.

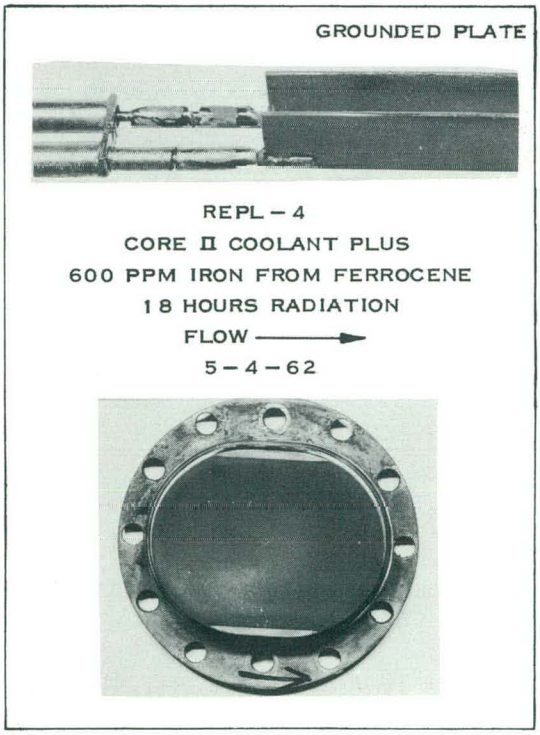

Fig. 2 Electron irradiation window and condenser plates from test REPL-4.

In order to increase the severity of the test procedure and produce heavier films, the magnetic field of the deflecting magnet at the end of the Linac accelerator tube was reduced. This reduced the diameter of the electron beam and focused it better. Coolant velocity also was reduced to 0.5 ft/sec. The test conditions are shown in Table I for REPL-5. Test results showed 0.4 mil of film on the window. Film weight on the window was 0.61 mg/cm^2. Thus, the combination of higher window temperature. reduced coolant velocity. and better focusing of the electron beam on the cell window appeared to increase test severity. In tests REPL-3 and -4, more film was noted per unit of area on the condenser plates than on the window. In test REPL-5 this was not the case. Film thickness in REPL-5 showed the grounded plate to have 0.3 mil as compared to 0.2 mil for the ungrounded plate. However, there was

only a small difference in weight of film between the two plates. The percent ash of the REPL-5 film was less than either REPL-3 or -4. Pyrolytic capsule data and other loop data indicate that as surface temperatures increased, the ash content of the film decreased. There was about two percent oxygen in the blanket gas after the test. This suggests an inadequate purge of the loop prior to the test. The oxygen may have affected film formation. Photographs of the window and plates are shown in Figure 3.

The effect of film deposition on condenser plates outside of the radiation zone was studied in REPL-6. Both the grounded and ungrounded condenser plates were assembled downstream of the radiation field in the exit portion of the deep-channel cell. During the initial part of the test the electron window thermocouple failed. This precluded the accurate monitoring of the window temperature and the electron beam power. The results, as indicated in Table II, show that the dosage was less than half that normally obtained and the amount of film formed was correspondingly low. No significant difference was noted in the amount of film collected on the grounded and ungrounded plates. The electron beam current to the grounded condenser plate was 0.5 microamp during the test.

The photographs of the window and plates are shown in Figure 4.

In all of the above tests a "pyrolytic" film was observed on the sides of the window assembly not exposed to the flow of coolant but wetted with static liquid film. The temperature of the sides of the window is not recorded but a temperature of at least 900°F would be expected in this region. After tests REPL-5 and -6, this static or pyrolytic film was removed and analyzed as shown in Table III.

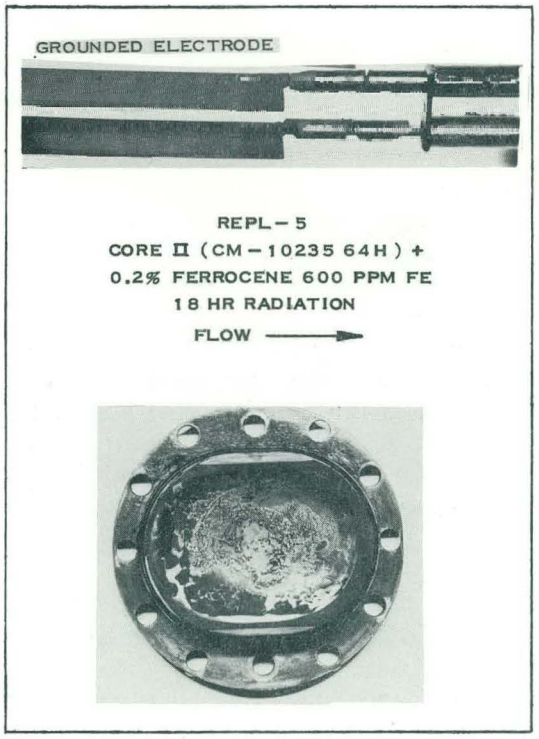

Fig. 3 Electron irradiation window and condenser plates from test REPL-5.

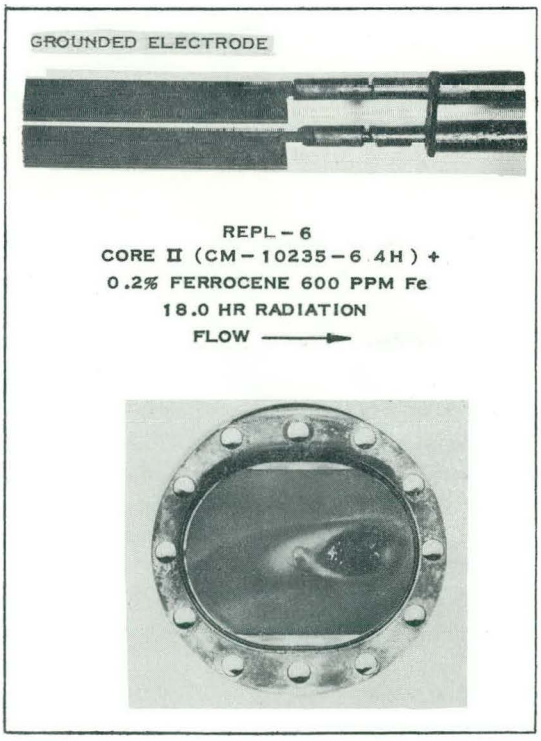

Fig. 4 Electron irradiation window and condenser plates from test REPL-6.

The films (Table III) were non-magnetic, indicating a low concentration of magnetite. In test REPL-5 the weight of pyrolytic film exceeded the dynamic film on the window (16 mg) or the film on the condenser plates (18 mg). In test REPL-6 the pyrolytic film also exceeded the dynamic window or condenser plate weights. Thus there is a striking difference in film composition on the window assembly depending on such parameters as temperature, radiation, and coolant velocity. In the future, the window walls will be adequately instrumented for better monitoring of temperatures during irradiations.

TABLE III

PYROLYTIC FILM ANALYSIS

	Test No.	
	REPL-5	REPL-6
Film weight (mg)	39	5
X-ray diffraction	Fe_3O_4	—
Film composition		
%C	95.1	96.0
%H	4.4	5.0
C/H	1.8	1.6
%Ash	0.3	0.1

Summary of Loop Test Results

Based on the circulating-loop-test data obtained during this quarter the following items summarize results and conclusions of the work:

(1) The small electron irradiation loop (REPL) with the 1.75-inch-deep coolant channel was as severe a test with regard to film and polymer formation in 18 hours as the larger EPL is in 56 hours.

(2) Grounded surfaces in electron radiation fields at coolant velocities of 1 ft/sec tend to collect more fouling film than ungrounded surfaces.

(3) OMRE coolant with 23 percent high boiler and 650-ppm iron formed twice as much film as OMRE coolant with 10.2 percent high boiler and 614-ppm iron. The higher concentration of high boiler may be the cause of more film formation.

(4) As surface temperature increased and coolant velocity decreased, ash content of the film decreased.

2.23 Rocking Irradiation Cell. A series of film formation experiments were completed which established the baseline conditions for further tests. Conditions were found under which virgin coolant produced little or no film, and OMRE Core II coolant or coolant with various additives caused film to deposit. Table IV lists some of the tests which have been completed and gives the important conditions under which these tests were carried out.

Runs 30 and 36 using Core II coolant resulted in the deposition of a hard shiny film on the hot section of the tube (located directly under the Linac beam).

In runs 32 and 34, the hot section of the tube was blued; however, a negligible amount of film was deposited. Runs 38, 40, and 42 demonstrated that either or both insoluble inorganic and insoluble organic materials will cause the

TABLE IV

ROCKER EXPERIMENTS

Run No.	Coolant	Additive	Bulk Temperature (°F)	Tube Temperature (°F)	Results
11306-30	Core II	—	488	955	film
11306-36	Core II	—	524	958	film
11306-32	OMP	—	505	958	no film
11306-34	OMP	—	452	951	no film
11306-38	OMP	0.25% 10899-12C(a) + 200-ppm Fe_3O_4	602	947	film
11306-40	OMP	0.25% 10899-12C(a)	650	949	film
11306-42	OMP	200-ppm Fe_3O_4	609	948	film
11306-44	OMP	20% 10899-10B(b)	550	954	trace
11306-46	OMP	20% 10899-12B(c)	555	951	trace
11306-48	OMP	0.25% 10587-59A(d)	546	950	film
11306-50	OMP	0.25% 10899-59A(e)	548	948	film
11306-52	OMP	0.25% 10899-12B(c)	537	950	film
11306-56	OMP	0.25% 10899-89D(f)	550	950	film

(a) 10899-12C is benzene insoluble fraction from 10899-12B.

(b) 10899-10B is soluble fraction from OMRE high boiler which was extracted with 50/50 benzene-cyclohexane.

(c) 10899-12B is insoluble fraction from OMRE high boiler after extraction with 50/50 benzene-cyclohexane and then dissolved in benzene.

(d) 10587-59A is benzene insoluble residue from OMRE high boiler distillation at 400°C and 1 mm.

(e) 10899-59A is hydrogenated 10899-12C, benzene soluble.

(f) 10899-89D is high mol wt. product (502) from the reaction of hydrogen atoms with m-terphenyl.

deposition of film. The film obtained with these additives had a fluffy, carbon-black type of appearance.

High boiler fractions soluble in Santowax OMP were used in runs 44 and 46 in large amounts (20 percent) with only a trace of film being deposited. An unusual result was obtained when film was deposited in run 52 where only

0.25 percent of the same material (10899-12B) was added to the Santowax OMP coolant. A possible explanation may be that large amounts of the additive solubilize the film-forming components which are produced via radiolysis.

In run 48, the insoluble character of the high boiler residue appears to be responsible for the deposited film. The additive in run 50 was a high boiler fraction, originally insoluble but which had been made soluble via hydrogenation. The insoluble high boiler probably was regenerated in the radiation field thus causing the film deposit.

Generally, film was obtained when insoluble matter was present (inorganic and organic). Little or no film was obtained with virgin coolant. Experiments in the pyrolytic capsule showed benzene insoluble fractions of high boiler increased fouling but soluble fractions did not. In the radiation rocking cell, benzene soluble fractions gave film. A possible explanation is that in the latter case radiolysis may have converted the additive to benzene insoluble materials.

2.24 Cells for Irradiation of Samples Under the Linac. The more sophisticated irradiation apparatus, mentioned in the last quarterly report [1] as necessary for more precise work under the Linac, has been in process of detail design and preparation of working drawings. Construction should be started shortly and be completed within the next quarter.

2.3 Fundamental Studies

2.31 The Radiation Chemistry of Aromatic Mixtures

General Approach. Radiolytic damage to the three isomeric terphenyls produces a wide variety of products, mainly included in a fraction known as "high boilers". Most of the high boilers are polyphenyls. It would be useful to know about the radiolytic mechanism and chemistry of the formation of high boiler polyphenyls from the simple polyphenyls and their mixtures. A program to study radiolysis of these simple mixtures is in progress.

In the initial phases of this program, only the simplest aromatic mixtures were studied because of the complex analytical problems involved in separating and identifying the numerous polphenyl products. A study has been made of the polphenyl product distribution from the irradiation (Linac electron) of biphenyl and mixtures of benzene-biphenyl, benzene-perdeuterobenzene, perdeutero-benzene-biphenyl, and benzene-meta-terphenyl. The various mixtures were analyzed via GSC (LiCl column) [2].

A simplified approach was developed to compare the reactivities of various polyphenyls to that of benzene. The basic reaction for a mixture of a given polyphenyl and benzene is postulated as:

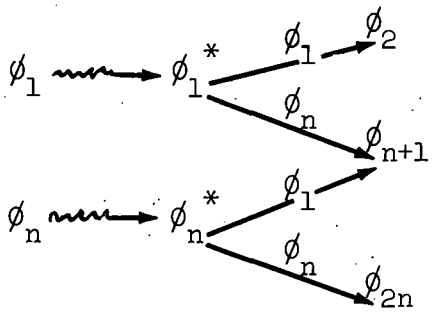

(1)

where ϕ_1 is benzene, ϕ_2 is biphenyl, etc, and the starred molecules are considered to be radicals, ions, or highly energetic molecules. It was assumed that a certain fraction, n, of the reactive species was from benzene molecules and a certain fraction (1-n) of the reactive species was from polyphenyl molecules. After the reactive species formed, it might react with either benzene, ϕ_1, or polyphenyl, ϕ_n. Further, it was assumed that β was the probability that either reactive species would react with benzene and $1-\beta$ was the probability that either would react with a polyphenyl.

The molar yields of ϕ_2, ϕ_{n+1}, and ϕ_{2n} can be measured with chromatographic analysis. The yields can be related to the probabilities by the following equations:

$$Y\,\phi_2 = n\,\beta \tag{2}$$

$$Y\,\phi_{n+1} = n\,(1-\beta) + (1-n)\,\beta \tag{3}$$

$$Y\,\phi_{2n} = (1-n)(1-\beta) \tag{4}$$

$Y\phi_2$ is the mole fraction of the yield of biphenyl and $Y\phi_{n+1}$ is the mole fraction yield of all the ϕ_{n+1} isomers. $Y\phi_{2n}$ is the mole fraction of all the dimeric isomers produced from ϕ_n.

The values of n and β (Table V) may be used to compare the various polyphenyls with benzene as to the relative probability for radical or ion formation:

$$\frac{P_r\,\phi_n^*}{P_r\,0_1^*} = \left(\frac{1-n}{n}\right) \tag{5}$$

TABLE V

RADICAL AND SCAVENGING PROBABILITIES IN AROMATIC MIXTURES

Equal Molar Mixtures	n	β	$(P_r\phi_n/P_r\phi_1)$	$(P_a\phi_n/P_a\phi_1)$
C_6H_6, C_6D_6	0.64	0.64	0.55	0.55
C_6H_6(a), $C_{12}H_{10}$	0.49	0.29	1.04	2.45
C_6H_6, m-$C_{18}H_{14}$	0.44	0.13	1.27	6.70
C_6D_6(a), $C_{12}H_{10}$	0.26	0.26	2.85	2.85

(a) These values were calculated using the relationship $Y\phi_2 = \frac{Z-1}{Z}$ which is described in Eq. 14-26 of this section. Carbon-14 labeled benzene is presently being used to determine $Y\phi_2$ directly.

The relative scavenging ability of ϕ_n compared to benzene may be calculated using:

$$\frac{P_a \phi_n}{P_a \phi_1} = \frac{(1-\beta)}{\beta} \tag{6}$$

Equations (5) and (6) provide an excellent means for comparing the radiation stabilities and scavenging abilities of individual polyphenyls in mixtures (the terphenyls, for example) simply by using the individual ratios and eliminating the benzene term:

$$(P_r\phi_n^*/P_r\phi_m^*) = (P_r\phi_n^*/P_r\phi_1^*)\ (P_r\phi_1^*/P_r\phi_m^*) \tag{7}$$

or

$$(P_a\phi_n/P_a\phi_m) = (P_a\phi_n/P_a\phi_1)\ (P_a\phi_1/P_a\phi_m) \tag{8}$$

It would have been impossible to obtain the probability ratios directly from the irradiation of ortho- and meta-terphenyl because of the difficulty in separating and identifying the great number of hexaphenyl isomer products.

Free Radical Determination of β

As a further check for the value of the $P_a(m\text{-}\phi_3)/P_a\phi_1$ ratio, phenyl radicals were generated (using a Hanovia mercury ultraviolet lamp) from phenyl iodide in a mixture of benzene and meta terphenyl. The products obtained were generated by the following reactions:

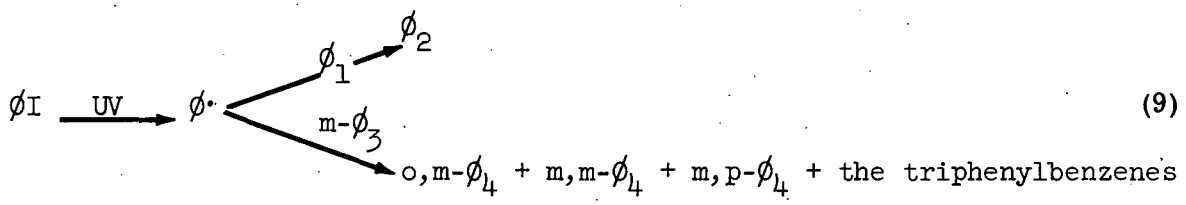

(9)

The value of β was then calculated from the mole fraction biphenyl yield, $Y\phi_2$.

Generating phenyl radicals in an equal molar mixture of benzene and biphenyl would give β.

$$\beta = Y\phi_2 \tag{10}$$

Since biphenyl is a product as well as a reactant, analysis would be impossible. Therefore, a p-biphenylyl radical was generated so products could be identified.

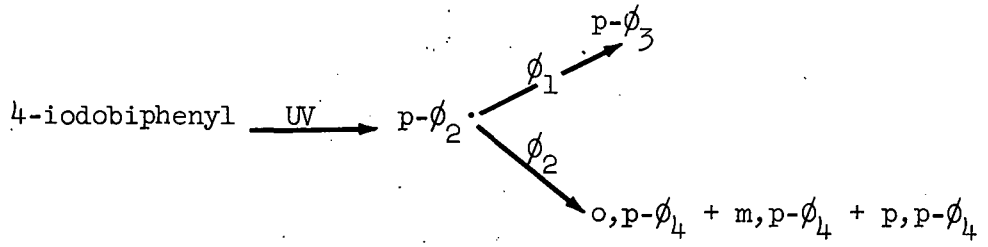

(11)

β was calculated from the mole fraction yield of para-terphenyl and for an equal molar mixture:

$$\beta = Y(p\text{-}\phi_3) \tag{12}$$

Table VI compares the values of β as were obtained from electron radiation and ultraviolet-generated radicals.

Good agreement was obtained between radical scavenging data and the scavenging of reactive species generated by radiation. This may indicate a radical process occurs during irradiation.

TABLE VI

RADIATION DATA FOR PROBABILITY OF BENZENE REACTING (β)

	Mixtures	
	$\phi_1 + \phi_2$	ϕ_1 + m-ϕ_3
Electron	0.29	0.13
Free radical	0.25	0.15

Detailed Analysis of the Benzene-Biphenyl Problem

The general reaction (see Equation 1) can be described in more detail for the benzene-biphenyl system by:

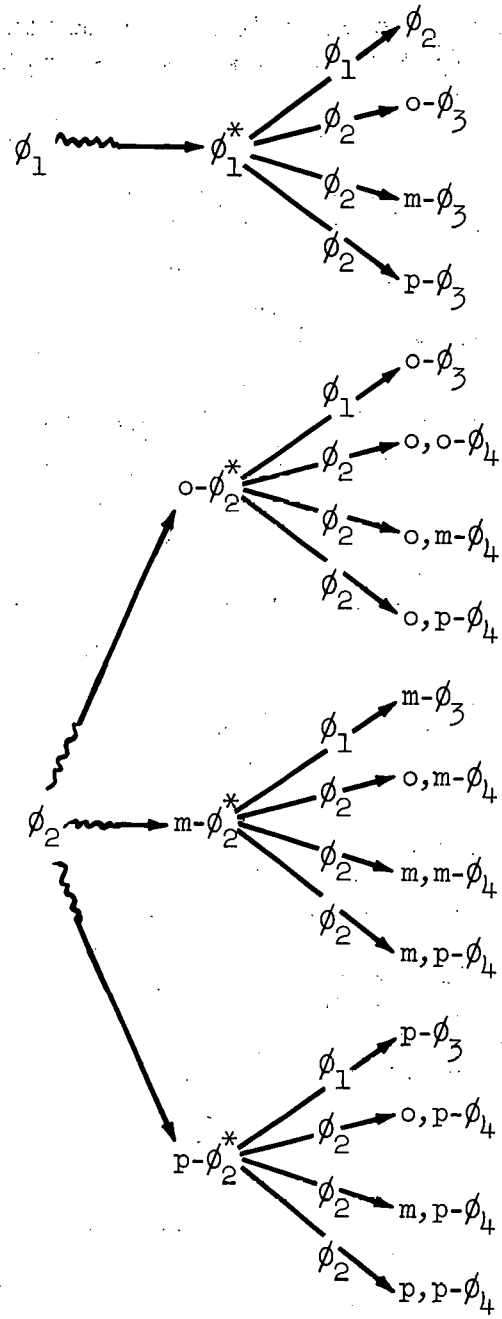

(13)

Let n be the mole fraction of reactive species generated from benzene. Then 1-n would be the mole fraction of the reactive biphenyl species. Specifically 1-n is the sum of the o,m and p-ϕ_2^* mole fractions which will be designated as a, b, and c, respectively. Any given reactive species (radical or ion) has the probability of reacting with either benzene or biphenyl. Let β be the probability that these radicals react with benzene. Then 1-β is the probability that the same reactive species would react with biphenyl. Then 1-β, which can be considered the scavenging probability of biphenyl, may be divided into three

parts. First, the ortho position may scavenge the radical (A), the meta position may scavenge the radical (B) or the para position (C). The complete GSC determination of the ten products is complicated because biphenyl (a reactant) is also a product. Thus, the analytical procedure excluded biphenyl and the factor Z was introduced to account for the unknown mole fraction of biphenyl formed during irradiation.

The nine unknowns a, b, c, n, A, B, C, β, and Z were used in conjunction with Equation (13) to derive the following set of relationships.

$$\frac{Y(o\text{-}\phi_3)}{Z} = a\beta + nA\,(1-\beta) \tag{14}$$

$$\frac{Y(m\text{-}\phi_3)}{Z} = b\beta + nB\,(1-\beta) \tag{15}$$

$$\frac{Y(p\text{-}\phi_3)}{Z} = c\beta + nC\,(1-\beta) \tag{16}$$

$$\frac{Y(o,o\text{-}\phi_4)}{Z} = aA\,(1-\beta) \tag{17}$$

$$\frac{Y(m,m\text{-}\phi_4)}{Z} = bB\,(1-\beta) \tag{18}$$

$$\frac{Y(p,p\text{-}\phi_4)}{Z} = cC\,(1-\beta) \tag{19}$$

$$\frac{Y(o,m\text{-}\phi_4)}{Z} = (aB + bA)\,(1-\beta) \tag{20}$$

$$\frac{Y(o,p\text{-}\phi_4)}{Z} = (aC + cA)\,(1-\beta) \tag{21}$$

$$\frac{Y(m,p\text{-}\phi_4)}{Z} = (bC + cB)\,(1-\beta) \tag{22}$$

$$\frac{Z-1}{Z} = n\beta \tag{23}$$

$$a + b + c + n = 1.00 \tag{24}$$

$$A + B + C = 1.00 \tag{25}$$

$$\sum_{3} Y(\phi_3) + \sum_{6} Y(\phi_4) = 1.00 \tag{26}$$

In Equation (23), (Z-1)/Z is the mole fraction biphenyl yield from the reaction of ϕ_1^* with benzene. Equations (14) through (22) provided the nine necessary independent equations to evaluate the nine unknowns. Equations (23) through (26) are a series of dependent equations which were found to be useful.

A program was developed for the IBM 7090 digital computer for the solution of nonlinear, algebraic, simultaneous equations of the type shown above. The original program was developed for analog computers. However, by using a Simulated Analog Computer (SAC) interpretative routine, access to the digital computer was obtained for the solution of the benzene-biphenyl radiolysis problem. This problem was set up principally by T. A. Matthews and S. A. Cunningham using SAC which was developed by M. Radd, Phillips Petroleum Co, Bartlesville, Okla. Some of the results are listed in Table VII.

TABLE VII

RELATIVE REACTIVE SPECIE GENERATION AND RELATIVE SCAVENGING ABILITIES OF BENZENE-BIPHENYL MIXTURES

Parameters	For Species	29.8 mole % Benzene	49.9 mole % Benzene	66.4 mole % Benzene	50.1 mole % Perdeuterobenzene
a	$P_r(o\text{-}\phi_2^*)$	0.142	0.088	0.103	0.172
b	$P_r(m\text{-}\phi_2^*)$	0.398	0.275	0.161	0.364
c	$P_r(p\text{-}\phi_2^*)$	0.193	0.151	0.098	0.187
n	$P_r\phi_1^*$	0.276	0.486	0.638	0.278
A	$P_a(o\text{-}\phi_2)$	0.421	0.429	0.359	0.404
B	$P_a(m\text{-}\phi_2)$	0.245	0.251	0.287	0.259
C	$P_a(p\text{-}\phi_2)$	0.334	0.320	0.354	0.337
β	$P_a\phi_1$	0.157	0.295	0.407	0.248
Z	—	1.046	1.167	1.352	1.075

Some information can be derived from the effect of concentration on the relative radical and scavenging probabilities. A linear relationship exists between the initial molar ratios of biphenyl and benzene and the radical and scavenging ratios (Figure 5). This relationship is expressed as:

$$\left(\frac{P_r\phi_2^*}{P_r\phi_1^*}\right)_x = \left(\frac{P_r\phi_2^*}{P_r\phi_1^*}\right)_{1.0} \left(\frac{\phi_2}{\phi_1}\right) \qquad (27)$$

and

$$\left(\frac{P_a\phi_2}{P_a\phi_1}\right)_x = \left(\frac{P_a\phi_2}{P_a\phi_1}\right)_{1.0}\left(\frac{\phi_2}{\phi_1}\right) \qquad (28)$$

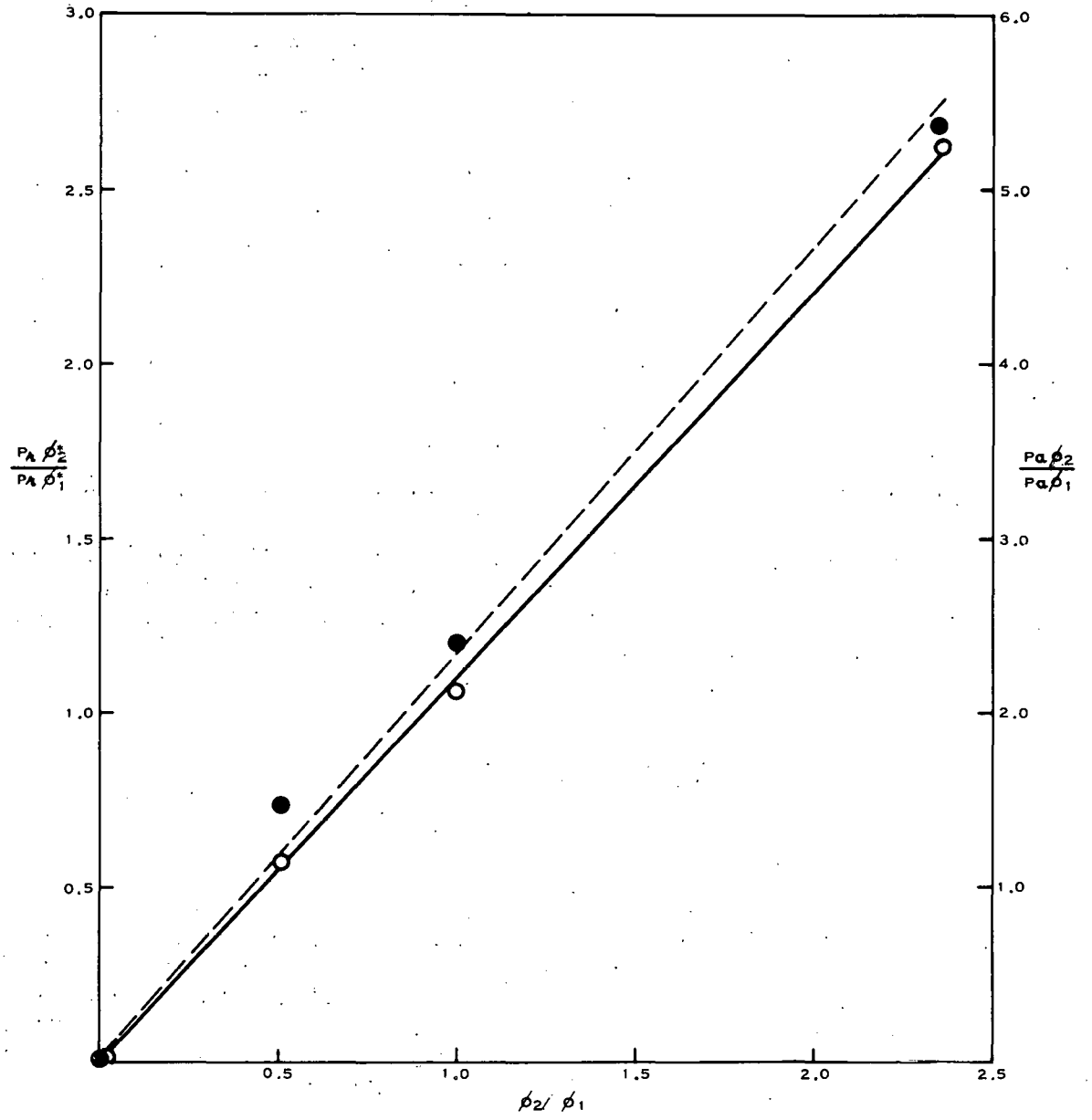

Fig. 5 $P_r\phi_2^*/P_r\phi_1^*$ and $P_a\phi_2/P_a\phi_1$ ratios as a function of the biphenyl-benzene molar ratios.

where the subscript x refers to the individual values at some mole ratio, (ϕ_2/ϕ_1). $(P_r\phi_2^*/P_r\phi_1^*)_{1.0}$ and $(P_a\phi_2/P_a\phi_1)_{1.0}$ are the radical and scavenging ratios for an equal-molar benzene-biphenyl mixture.

The partial rate factors for the scavenging and radical reactions were calculated from the data in Table VII and are listed in Table VIII. The average

partial rate factors from the benzene-biphenyl system agree remarkably with the perdeuterobenzene-biphenyl system.

TABLE VIII

PARTIAL RATE FACTORS FOR THE SCAVENGING AND RADICAL FORMATION REACTIONS OF BIPHENYL

Sample Composition	k_o	k_m	k_p	r_o	r_m	r_p
28.8% ϕ_1	1.72	1.00	2.73	0.36	1.00	0.97
49.9% ϕ_1	1.71	1.00	2.55	0.32	1.00	1.10
66.4% ϕ_1	1.25	1.00	2.47	0.64	1.00	1.22
50.1% C_2D_6	1.56	1.00	2.60	0.47	1.00	1.03
C_6H_6 average	1.56	1.00	2.58	0.44	1.00	1.10

This specific approach to the benzene-biphenyl problem has provided valuable information concerning radical or ion distribution ratios in aromatic mixtures. Also, the important scavenging reactions and relative scavenging ratios were related to non-radiolytic free radical reactions.

3. PYROLYTIC EXPERIMENTS

(P. S. Hudson, R. B. Regier, R. A. Mengelkamp, P. W. Solomon)

3.1 Film Deposition

The objective of the pyrolytic experimental program has been largely to support the radiolytic studies of film deposition by tests in which the effects of temperature are studied independently of the effects of radiation, an agent whose availability is limited. While it is not possible to equate directly the effects of these agents, the pyrolytic technique is in general use throughout the program, and tests have comparative value. Studies have been confined to the static capsule apparatus and to certain special tests.

3.11 Static Pyrolytic Film Apparatus

Test Procedure Development. Work has continued on the factors affecting film formation using a stainless steel heating element. In order to reduce the amount of coolant required for a test, a new capsule requiring only 600 grams of coolant was fabricated and a test procedure developed. This new procedure, designated SFB, is similar to the previous SF procedure in that maximum heater temperature was maintained at 950°F, but differs in that 700-psig blanket pressure was required to minimize nucleate boiling.

Data obtained during the test procedure development program are shown in Table IX.

TABLE IX

SFB TEST PROCEDURE DEVELOPMENT DATA

Test No.	Coolant	N_2 Blanket Pressure (psig)	Heater Temperature (°F)	Film (mg/hr)	Power Reduction (%)	C/H		Ash (%)	
						Outside Layer	Inside Layer	Outside Layer	Inside Layer
SFB-1	Core II	400	950	1.20	35	1.7	2.0	55	24
SFB-2	Core II	470	950	1.04	45	1.7	1.7	58	22
SFB-3	Core II	600	950	1.20	44	1.7	1.5	52	23
SFB-4	Core II(a)	700	900	0.33	27	—	1.5	—	67
SFB-5	Core II(a)	700	950	0.92	39	—	1.9	—	55
SFB-6	Core II(a)	700	950	0.80	40	—	1.7	—	58
SFB-13	Core II(a)	700	950	0.85	38	1.5	1.2	59	32
SFB-11	Core II	400	950	0.33	15	—	—	—	57
SFB-7	OMP	700	950	0.01	0	—	—	—	—
SFB-8	Core II 100-ppm Fe as Fe_3O_4	700	950	1.25	32	—	1.8	—	63

(a) New 5-gallon can of Core II coolant (CM 10235-50D).

The SFB procedure utilizes a three-inch, stainless steel, heater element as compared to a six-inch element with the SF procedure. Nucleate boiling occurred during test SFB-1 at 400-psig blanket pressure. Nucleate boiling was indicated by an increase in heater temperature as the blanket pressure increased. Also, examination of the film with a microscope showed craters and miniature volcanoes in the film body. Blanket pressure was increased in increments shown in Table IX. Trace boiling was noted at pressures up to and including 700 psig. In test SFB-4, the heater temperature was reduced to 900°F in order to minimize boiling, resulting in a reduction in film formation of a factor of three because of the cooler surface. The resulting fouling rates were too low to yield reliable data, so subsequent experiments were run at 950°F. Due to design limitations, 700 psig was considered to be a maximum permissible pressure when a bulk coolant temperature of 620°F was used. Tests SFB-1 through SFB-5 were conducted with one type of heater element holder. It should be noted that during these tests the change in heater temperature from 900 to 950°F resulted in a greater change in film formation than a change in pressure from 400 to 700 psig. In test SFB-6, a modification of the heater element holder eliminated one compression nut and ferrule. This made weighing and coolant removal after the test much easier. In this test the film formation rate was 0.80 mg/hr with a power reduction of about 40 percent. This was almost three times the film formation rate and power loss noted in test SF-11 using the older procedure. Test SFB-13, a duplicate test, showed good repeatability. In Table IX, C/H and ash values for the various tests are shown. Where it was possible, the inner layer of film next to the heater and the cooler outer layer of film were analyzed separately. There was no significant difference in the ratio but the percent ash of the inner and hottest layer of film was lower.

In Figure 6, the log of film thickness along the heater was plotted as a function of heater temperature for test SFB-6. It will be noted that film thickness increased exponentially with temperature. The slope of this curve is about the same as that obtained with the SF procedure.

Test SFB-7 was conducted with clean Santowax OMP in order to determine the spread between a clean and dirty coolant.

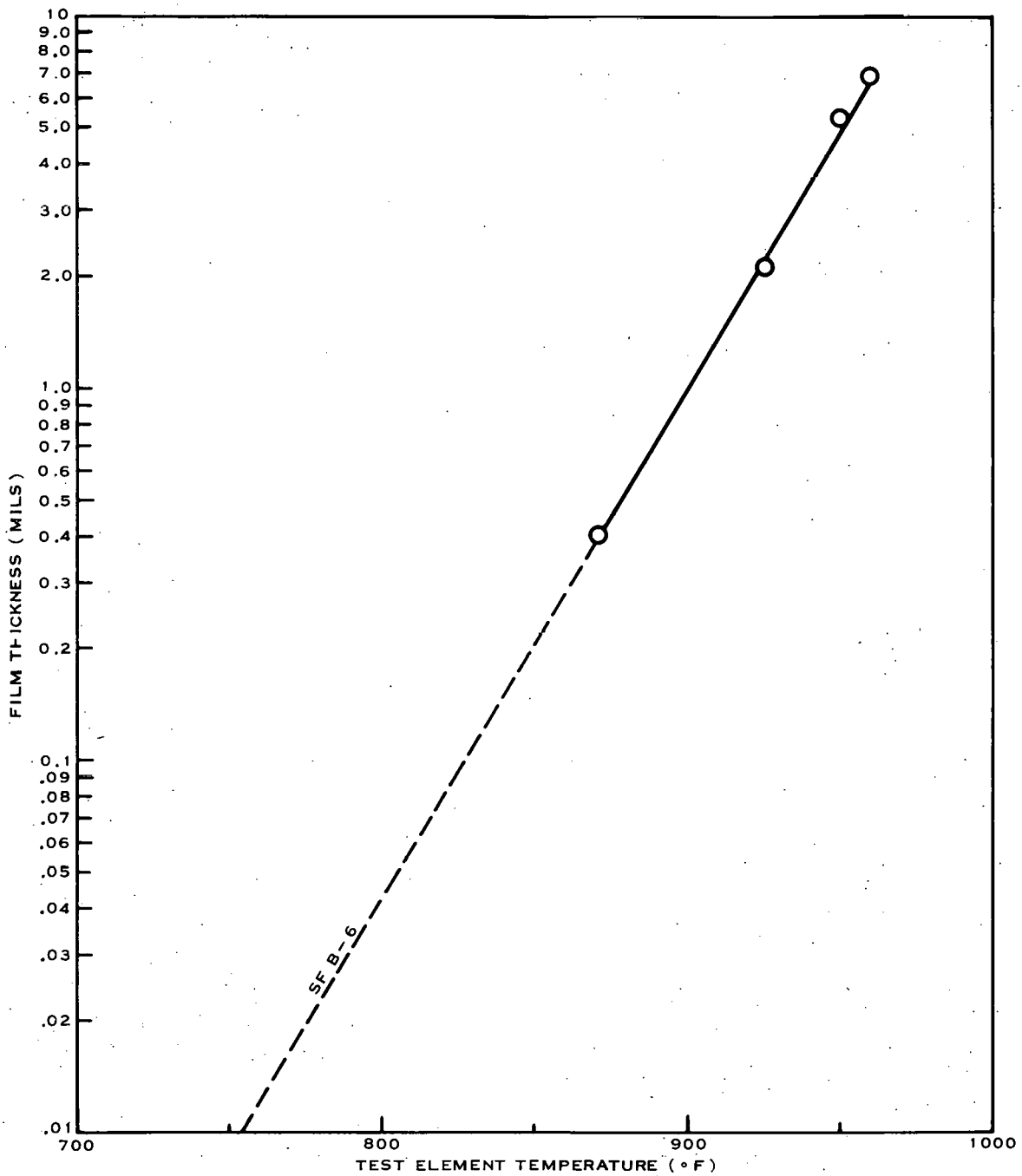

Fig. 6 Effect of test element temperature on film thickness in OMRE Core II coolant (23% HB, 50-ppm total iron).

Less than 0.01 mg/hr and a power loss of zero indicated a minimum amount of film formation. Compared with test SFB-6, which used Core II coolant, this was an excellent spread in results.

Test SFB-8 was conducted on Core II coolant to which 100-ppm iron in the form of magnetite was added. Results showed film formation rate increased to 1.25 mg/hr as compared to 0.80 mg/hr for Core II coolant. Thus, this test procedure was sensitive to iron content in the coolant in a manner similar to the SF test.

In general the SFB test procedure was reproducible and easily distinguished between clean and dirty coolants. In addition, it used only 600 grams of coolant and produced almost three times the film as the SF test.

Tests of Reactor Cleaning Procedures. In test SFB-10, the coolant studied was Santowax OMP which had been refluxed on iron pipe for five hours at 575°F, the pipe having previously been cleaned and treated by the Piqua procedure. Test results (Table X) showed a relatively high film formation

TABLE X

SFB TEST DATA

Test No.	Coolant	Coolant Additive	Total Iron (ppm)	Blanket Gas	Film Weight (mg)	Film Formation Rate (mg/hr)	Power Reduction (%)	C/H	Ash (%) Top Layer	Ash (%) Bottom Layer
SFB-10	OMP	Piqua procedure	3	N_2	2.2	0.09	9	—	—	—
SFB-11	OMP	No treatment	4	N_2	0.3	0.01	—	—	—	—
SFB-12	Core II	—	50	H_2	19.8	0.83	28	0.7	70	62
SFB-15	Core II	Decalin	50	N_2	19.4	0.81	34	1.8	—	53
SFB-16	OMP + 23% high boiler	Fe_3O_4	100	N_2	4.9	0.24	7	—	—	—
SFB-17	OMP	0.25% benzene soluble high boiler	10	N_2	0.5	0.02	0	—	—	—

rate when compared to test SFB-11 using Santowax OMP which had been refluxed for five hours at 575°F on untreated iron pipe. An emission spectrograph of the ash of the SFB-10 coolant before testing showed: 19 percent silicon, 11 percent aluminum, 10 percent iron, and 10 percent calcium. Ash content of this coolant was 25 ppm. The ash of the SFB-11 coolant before testing showed: >10 percent silicon, 10 percent aluminum, 9 percent iron, and 8 percent calcium. The ash content of the coolant was about 30 ppm. Thus, based on the emission spectrogram and total ash determination, there was no significant difference between these coolants. Further testing of coolants which have been refluxed over piping treated by various cleaning procedures will continue.

Effect of Hydrogen Atmosphere. Test SFB-12 was conducted in order to determine if a hydrogen blanket at 700 psig would inhibit film formation and power reduction. Earlier tests with hydrogen blankets at 400 psig using the SF procedure showed an increase in film weight but a reduction in power loss. Test results shown in Table X show a film formation rate of 0.83 mg/hr.

This was no improvement over SFB-6 with a nitrogen blanket which gave 0.80 mg/hr. However, power loss was only 28 percent with hydrogen as compared to 40 percent with nitrogen. Analysis of the film by X-ray diffraction showed the iron to be in the form of cementite and alpha iron in the hydrogen run. With nitrogen blankets magnetite is usually obtained. The bottom layer of film had an ash of 62 percent while the top layer was 70 percent ash. With the exception of better heat transfer no benefit was observed by using a hydrogen blanket under the conditions indicated.

Miscellaneous Tests on Coolant Compositions. Atomics International, using their PCFT procedure, has reported that one percent decalin in OMRE Core II coolant reduces film formation. This was tested in SFB-15. Test results indicated no decrease in film weight but there was a slight improvement in power reduction.

Test SFB-16 was run in order to test the relative film-forming tendency of OMRE Core III high boiler and magnetite as compared to OMRE Core II coolant. The test data shown in Table II indicated less than one-third of the film weight normally obtained with OMRE Core II coolant. Either the 50-ppm iron in Core II coolant was more active than the 100 ppm of magnetite added to Core III high boiler, or the high boiler in Core II coolant contained more film binder or "stickiness" than the Core III high boiler. There was evidence of magnetite dropping out of suspension in test SFB-15. This may be an important factor in the test results.

Test SFB-17 was conducted in order to evaluate a benzene soluble fraction of Core II high boiler. X-ray fluorescence indicated a blend of 0.25 percent of this material in Santowax OMP had an iron content of 10 ppm. Test results indicated a film formation rate of 0.02 mg/hr which was about twice that obtained with clean Santowax OMP. However, due to experimental error it was doubtful if this was significant at these low film formation rates.

Summary of SFB Test Results. Based on SFB test data obtained during this quarter, the following items summarize results and conclusions of the work.

(1) The SFB test procedure is reproducible and uses only 600 grams of coolant.

(2) Increasing the heater temperature from 900 to 950°F increases film weight by a factor of almost three.

(3) Increasing the blanket pressure from 400 to 700 psig has a small effect on film formation.

(4) As heater temperature increases, the ash content of the film decreases.

(5) The use of a hydrogen blanket at 700 psig did not reduce the weight of film formed but did improve heat transfer of the film.

(6) The use of one percent decalin in Core II coolant did not reduce film weight but did improve slightly the heat transfer of the film.

3.12 Role of Soluble Iron in Film Formation. The preceding quarterly report (IDO-16787) presented experimental evidence which strongly suggested that under certain conditions iron exists as a true solution in terphenyls. It was postulated that the iron was held in solution in the form of coordination compounds with oxygen-containing ligands. During the present quarter experimental work has been performed to investigate the possibility that soluble iron compounds are the source of the fouling films that are formed on reactor fuel elements. Evidence has been obtained to support this theory.

The idea that soluble iron is the source of fouling films receives strong support from observations that have been made on mass transport in pressurized water reactors. These will not be reviewed here because they have been well summarized elsewhere [3]. The consensus of that report is that mass transport in carbon steel or mild steel circuits is caused mainly by atomic iron or freshly formed colloidal particles. Although the chemical environment in aqueous systems is different from that in a hydrocarbon fluid, experiments in this laboratory are being designed and performed to test the premise that fouling from organic fluids also proceeds via atomic processes.

Synthesis of Iron Percarbide. An experiment that substantiated this idea was the recent synthesis of Hägg carbide (Fe_2C) under conditions comparable to those in the OMRE. This carbide, which is identical with iron percarbide ($Fe_{20}C_9$), is the only crystalline component that has been reported present in the fouling films that have appeared on the fuel plates during operation of the OMRE. In a previous quarterly report [4] possible modes of its synthesis were discussed, and reasons were presented for believing that in the OMRE carbon monoxide is the reactant involved in the carburization of iron. Hägg carbide was synthesized at the Bartlesville laboratories in the bomb that is used for PCF tests, using a solution of 212-ppm ferric iron (as the chelate of benzoylacetone) in virgin Santowax OMP. The bomb was heated at 620°F for 10 days under 700 psig of Matheson Manufactured Gas B (55% H_2, 18% CO, 24% CH_4, 3% C_2H_6). The stainless steel test heater in the bomb was maintained at 825 to 850°F for eight days but was off for the last two days of the experiment because of a malfunction in the controller. At the conclusion of the test the polyphenyl fluid, when drained from the bomb, contained only 5-ppm iron, indicating that essentially all the iron had been thrown out of solution during the exposure. Most of it had settled to the bottom of the bomb from where it was recovered by rinsing with benzene and cleaned by repeated centrifugation under fresh portions of benzene. XRD analysis of this fraction showed only cementite (Fe_3C). The silvery gray deposit that adhered tenaciously to the test element, comprising about 5 percent of the iron added to the fluid, gave an XRD pattern of pure Hägg carbide.

This is believed to be the first time that this compound has been synthesized under conditions comparable to those obtained in the OMRE, although numerous attempts have been made to do so starting with preformed particles of iron or its compounds. The observations made in this experiment suggest some conclusions that are pertinent to the fouling phenomena. The formation of Fe_2C at the test heater while Fe_3C was formed at the lower bulk temperature of the terphenyls constitutes substantial proof that in this experiment the heater deposit did not come from preformed particles in the fluid. The reported effect of increasing temperature on the known carbides of iron is [5]:

Hexagonal close-packed $Fe_2C \longrightarrow$ Hägg $Fe_2C \longrightarrow Fe_3C \longrightarrow \alpha\text{-Fe} + C$

Thus, the conversion of particulate Fe_3C in the bulk to Fe_2C on the heater is apparently impossible, and presumably the two different carbides were formed independently. A possible explanation of the appearance of these two forms of iron carbide in the same experiment is this: decomposition of the soluble iron coordination compound produces an oxide of iron which is reduced to elemental iron; at the bulk temperature of the fluid this is carburized relatively slowly to Fe_2C, permitting the known reaction $Fe + Fe_2C \longrightarrow Fe_3C$; at the higher temperature of the test element, free iron is carburized as rapidly as it forms, and no excess iron is available to convert Fe_2C to Fe_3C.

Chelation of Iron in Coolants. The selection of benzoylacetone as the chelating agent for ferric iron was based on preliminary experiments in which a number of bidentate ligands were examined. These were salicylaldehyde, salicylic acid, pyrocatechol, benzoylacetone, 1-hydroxy-2-naphthoic acid, and 8-quinolinol. Coordination compounds with iron were made by reacting three moles of ligand per mole of ferric nitrate in absolute methanol. After evaporation of the solvent, qualitative tests were made to determine their solubility in boiling toluene and in molten Santowax. Since all these coordination compounds are intensely colored, this property was used to estimate solubility. The complexes with salicylic acid and pyrocatechol were insoluble in the solvents tested, and that with the naphthoic acid was only sparingly soluble. The other three were quite soluble, but no attempt was made to determine their solubility since they were to be used only in dilute solutions.

Before making the bomb experiment described above, a preliminary experiment was performed to discover the chemical form of iron obtained when different solutes containing it are exposed to elevated temperature for an extended period. Five solutions were prepared in m-terphenyl each containing one weight percent iron as chelates of salicylaldehyde, 8-quinolinol, benzoylacetone, iron stearate, or ferrocene. These were exposed in glass containers at 350°C for 160 hours under 15 psig of Matheson Manufactured Gas B. At the conditions of the experiment nearly all of the ferrocene sublimed to a cooler part of the apparatus and was not altered, although a small quantity of dark, insoluble particles remained in the solvent. Upon completion of the test the mixtures were dissolved in benzene and the insoluble residues were separated and washed by centrifugation. XRD analyses of the residues showed that the quinoline compound yielded amorphous iron-containing material, while the other four yielded magnetite plus alpha-iron. Electron micrographs of the crystalline residues were quite similar, showing particle size distributions from about 0.3 micron maximum down to about 20 millimicrons (the lower limit of detectability at x50,000 magnification). In a previously reported experiment it had been demonstrated that ferric oxide, immersed in terphenyls and maintained for four weeks at the identical conditions used in this experiment, was appreciably converted to cementite, and it was inferred then that the cementite was formed via Fe_2C. Failure to observe iron carbide in this experiment may have been due to insufficient time; however, it may also have been due to the presence of a substantial amount of water produced by the reduction of the iron, since carburization is known to be adversely affected by water.

The chemical and physical nature of the particles prepared in the experiments described above are in accord with the hypothesis that iron enters the organic

coolant of a reactor by some atomic process, in which it is initially soluble, but decomposes by thermal and radiolytic mechanisms.

Mössbauer Effect Tests. The possibility of exploiting the Mössbauer effect to elucidate the chemical form of iron involved in fouling phenomena was discussed with Dr. R. L. Collins of the Physics Branch. He felt that in principal the effect could be used profitably, but the low concentration of iron being considered in the organic medium would not permit direct application. For him to obtain usable spectra, sufficient iron-57 to make ≈ 0.15 mg/cm^2 (or 7 mg/cm^2 of natural iron) is required. This would necessitate working at iron concentrations several orders of magnitude greater than are realistic, or of concentrating the iron from dilute solutions with the concomitant danger of changing the chemical form of iron by the concentration process. The possibility of using enriched iron-57 from ORNL has been considered, but even so the technique would be difficult to use successfully, and no experiments are presently planned.

4. COMPOSITION AND REACTIONS OF COOLANTS
(P. S. Hudson, W. M. Hutchinson, P. W. Solomon, R. C. Doss)

4.1 Characterization of Santowax

4.11 Purification of Terphenyls. Pure terphenyls are needed for precise results in irradiation experiments. O-terphenyl (Eastman White Label) contained 0.5 percent m-terphenyl, 1.3 percent p-terphenyl and 0.2 percent quaterphenyls when analyzed by gas chromatography. The purity was raised to 99.8 percent by three recrystallizations from ethanol and activated charcoal.

M-terphenyl (Eastman White Label) contained 5.2 percent p-terphenyl when analyzed. Since the two isomers form a eutectic near 4.3 percent para, ordinary recrystallization failed to improve the purity greatly. Liquid-solid chromatography using silica gel, alumina, 10X molecular sieves, and Wyex carbon black with cyclohexane solvent failed to improve the purity. Zone refining also failed. Finally, a two-stage process was developed which brought the purity to 99.8 percent.

In this process, one kilogram of impure m-terphenyl was dissolved in 10 liters of boiling cyclohexane. When the solution was cooled to 30°C and filtered, approximately 30 grams of p-terphenyl were removed. By successively cooling to 10°C and concentrating the solution to one liter, 900 grams of 98 percent m-terphenyl were recovered. The combined precipitates were dissolved in 16 liters of boiling methanol-ethanol (3:1). The mixture was allowed to cool without agitation to 40 to 45°C. The m-terphenyl precipitated quickly. At this point platelets of p-terphenyl were observed forming in the solvent. The supernatant liquid was then quickly decanted. The crystals were poured onto a Buchner funnel and sucked dry. About 350 grams of m-terphenyl were recovered and melted at 86.5 to 88.0°C. This represented a 40 percent yield of 99.8 percent pure m-terphenyl.

4.12 Isolation and Characterization of a Yellow Impurity in Santowax OMP. Commercial Santowax OMP has a yellow color which is not present in pure

terphenyls. This color also has been observed in reputedly pure commercial samples of o-terphenyl. Because of the possibility that the colored material may contribute to fouling and therefore may have to be removed from the reactor coolant, it was considered desirable to isolate and identify the source of the color.

The source of the color was easily extractable in acetone or methanol. About 250 grams of Santowax OMP were extracted by one liter of acetone and an equal portion was extracted by one liter of methanol. The resulting extract solutions were combined and concentrated to 500 ml, cooled to 25°C, filtered, and the filtrate concentrated until a brown oil separated at 300 ml. An equal volume of water was added and the mixture cooled to 10°C. Decanting the liquid phase left a yellow paste. The paste was dissolved in cyclohexane and dried with 5A molecular sieves. The solution was put through a silica gel column and a brown band was retained. The eluate was bright yellow. The yellow color could not be removed from the eluate by chromatography on activated charcoal, alumina, magnesia, sucrose or powdered filter paper. Treating the solution with oxidizing agents such as aqua regia and basic permanganate did not discharge the color. The material was extracted from the cyclohexane by sulfuric acid which became purple. The purple color disappeared when water was added to the sulfuric acid but no material could be isolated. Pure terphenyls were only colored a pale yellow when treated with sulfuric acid under similar conditions.

The brown material was removed from the silica gel column with acetone. Evaporation of the solvent left a viscous brown oil (0.06 percent of the original Santowax OMP). The material showed a strong aliphatic carbonyl band, small amounts of aliphatic hydrogen, polyphenyl structure, and no methyl groups in its infrared spectra. A 2,4-dinitrophenylhydrazone derivative melted at 270 to 280°C. Elemental analysis gave 84.4 percent carbon, 5.3 percent hydrogen, and 10.3 percent oxygen (by difference). The number average molecular weight was 270 and nuclear magnetic resonance showed 80 percent aromatic protons and 20 percent aliphatic protons. These analytical results suggest a diphenyl-cyclohexenedione type of structure. This sort of material, particularly the ortho dione, could serve as a chelating agent for metals. This type of compound might account for a mass transfer effect in film formation.

4.13 Separation of Terphenyls by Clathration. Radzitzky and Hanotier [6] described clathrates of $Ni(SCN)_2 \cdot 4C_6H_5CHCH_3NH_2$ which form with many aromatic compounds. The complexes were quite selective for certain isomers. This technique was applied to a 1:1 blend of o-terphenyl and m-terphenyl. The complex formed in a cyclohexane solution of the terphenyls. The complex was decomposed with dilute hydrochloric acid. Only one percent of the clathrate was hydrocarbon material. This material analyzed 61 percent o-terphenyl and 39 percent m-terphenyl. Thus, only a slight enrichment of the ortho occurred.

4.2 Identification of Products of Irradiation of Terphenyls

4.21 Hexaphenyls from Irradiation of m- and p-Terphenyls. In order to verify the predictions made with partial rate factors and to study irradiation mechanisms, the products from the radiolysis of terphenyls were characterized.

The hexaphenyl products from m-terphenyl were examined by gas chromatography. Peaks were identified by adding known hexaphenyls and observing the increase in height. Certain peaks were isolated from the gas chromatograph

prep column and compared directly with known hexaphenyls. Three compounds have been definitely verified: m,p,m-quinquephenyl, m,p,m,m-hexaphenyl and m,p,p,m-hexaphenyl. Verification of other peaks is continuing.

In the radiolysis of p-terphenyl, a number of quaterphenyls, quinquephenyls, and hexaphenyls have been isolated with a prep column on the chromatograph. The materials were recrystallized, examined by infrared analysis, and checked with mixed melting points. Table XI shows the 10 expected hexaphenyl isomers from the radiolysis. Products identified by direct comparison with known compounds are marked with a "k". Products with question marks have not been obtained in pure form but were tentatively identified with infrared and GSC by elution order. Several products besides the hexaphenyls are listed.

TABLE XI

PRODUCTS FROM TERPHENYL IRRADIATION

Isomer	GSC Elution Temperature (°C)(a)	Melting Point (°C)	
		Found	Literal
2,5,2',5'-tetraphenylbiphenyl	375(?)		
p,o,o,p-hexaphenyl	400(?)	oil	189-190
2,5-diphenyl-2'-(4-xenyl)biphenyl			
2,5-diphenyl-3'-(4-xenyl)biphenyl	430	201-204	—
p,o,m,p-hexaphenyl	433	167-170	
p,o,p,p-hexaphenyl	450(k)	228-231	231-232
2,5-diphenyl-4'-(4-xenyl)biphenyl	450(?)	—	—
p,m,m,p-hexaphenyl	465	254-257	247.5
p,m,p,p-hexaphenyl	475(k)	317-320	321-323
p-hexaphenyl	492(k)	439-445	465
p-quaterphenyl	385(k)	307-316	318
p-quinquephenyl	430(k)	383-390	392
p,m,p-quinquephenyl	430(k)	266-268	264-266

(a) Five feet, 0.5 in. ID, 20% lithium chloride on 60- to 80-mesh Chromosorb P; helium flow was 200 cc/min.

Work on further separation is continuing.

4.22 Non-Polyphenyl Products of Irradiation of Biphenyl. As the radiolysis of polyphenyls continues, the molecular weight of the high boiler increases. In addition, chemical species other than pure polyphenyls are formed. These

non-polyphenyl species were examined to learn more about irradiation mechanism and organic types which influence fouling.

A series of biphenyl samples were electron-irradiated in sealed tubes with an air atmosphere at 600°F. Conversions varied from 25 to 40 percent. The samples were combined and sublimed to yield four fractions shown in Table XII.

TABLE XII

FRACTIONS FROM BIPHENYL IRRADIATION

	Sublimation Conditions						% Protons by NMR(a)	
Cut	Temperature (°C)	Press (mm)	Wt%	Molecular Weight	% C	% H	Aromatic	Aliphatic
A	100	1.0	52	158	93.5	6.7	Biphenyl	Biphenyl
B	200	0.1	20	176	93.5	6.6	97	3
C	300	0.1	14	435	93.0	6.4	84	16
D	residue	—	14	1245	92.8	6.6	70	30

(a) Cuts B, C, and D contained paramagnetic species; the amount increased as the aliphatic content increased.

The NMR data show that aliphatic structure increased with increasing molecular weight. Infrared analysis also verified the NMR finding. No carbonyl structure was detected with the infrared even in the last fractions where the carbon-hydrogen analysis total was low.

The non-aromatic material was subjected to mild oxidation and strong oxidation. Strong oxidation consisted of refluxing 0.5 gram of material in 50 ml of nitric acid for five hours. All fractions dissolved in the acid media and increased nitric oxide evolution occurred with increasing amounts of aliphatic structure. After oxidation the products were separated into acidic and nonacidic fractions by basic extraction. Mild oxidation (does not oxidize alkyl groups, only activated methylene groups) with potassium permanganate was accomplished by refluxing one-gram samples in 100 ml of pyridine, with 0.5 ml of water and four grams of permanganate for six hours. The results obtained are shown in Table XIII.

The data show the acids produced by nitric acid increased as the aliphatic structure in the fraction increased. Infrared analysis showed nitro groups in both the acidic and nonacidic portions. All samples showed a trace of aliphatic structure except the residue which contained a considerable amount of carbonyl structure. Permanganate oxidation also increased with increasing aliphatic structure. The amount of acid product was less than the nitric acid samples. These low values still represent a considerable amount of easily oxidized

TABLE XIII

OXIDATION OF BIPHENYL IRRADIATION PRODUCTS

Cut	Milligrams of Product Recovered/Gram Sample		
	Nitric Acid Oxidant		Permangenate Oxidant Acid
	Nonacid	Acid	
A	1460	20	—
B	1500	160	210
C	760	700	490
D (residue)	80	1120	520

groups. Evidently the oxidation was not due to alkyl groups but some sort of saturated or partially saturated cyclic structure. The residue fraction will be hydrogenated and subjected to mild oxidiation to learn more about the oxidizable species.

4.3 Polyphenyl Reactions

4.31 Reaction of Polyphenyls with Hydrogen Atoms. During the radiolysis of polyphenyls, hydrogen radicals probably are formed. To learn the fate of these reactive atoms, hydrogen radicals were generated and allowed to react with various polyphenyls. The products formed could be compared with materials found in irradiated mixtures.

A diagram of the apparatus in shown in Figure 7. Hydrogen atoms were generated by a 2450-megacycle electrodeless discharge powered by a 125-watt Raytheon Microtherm diathermy unit. Moist hydrogen was introduced at 75 cc/min STP. The system pressure was maintained at 1 mm. Estimated hydrogen atom delivery rate to the polyphenyl surface was 0.012 mole per hour.

An attempt was made to use biphenyl as a reactant but it was too volatile to keep in the reaction flask. Therefore, o- and m-terphenyl were reacted under the following conditions:

	O-terphenyl	M-terphenyl
Pot temperature (°C)	67 to 80	82 to 99
Condenser temperature (°C)	60 to 65	75 to 80
Reaction time (hr)	8	8

In both cases, the reactants turned a bright yellow in less than one minute. During the runs, a brown film built up on the hydrogen atom inlet tube. During the m-terphenyl run, about 0.1 gram of liquid was found in the first liquid nitrogen trap. The kettle products in both cases were waxy yellow solids. Sublimation at 150°C and 0.3 to 1.0 mm gave residues which were orange glasses. The analytical results obtained are shown in Table XIV.

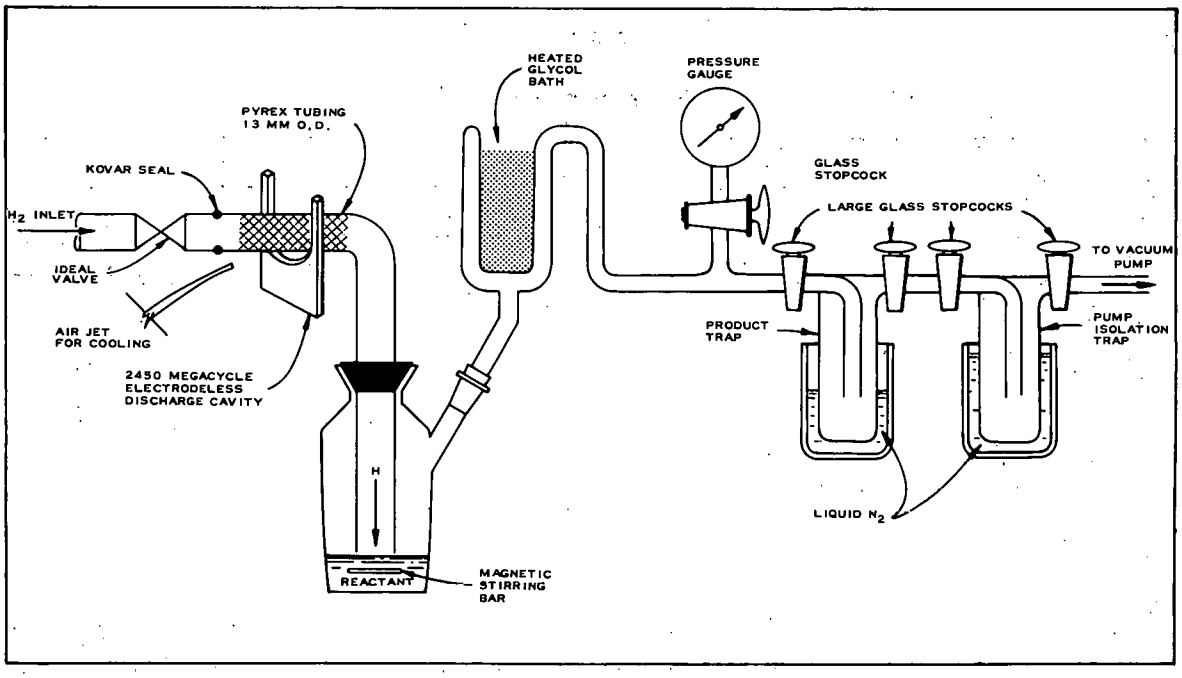

Fig. 7 Hydrogen atom generating system.

TABLE XIV

PRODUCTS OF HYDROGEN ATOM ATTACK

Property	O-terphenyl			M-terphenyl		
	Total	Sublimate	Residue	Total	Sublimate	Residue
Weight percent	100	93	7	100	92	8
Molecular weight	246	237	469	248	235	502
Melting point (°C)	—	—	60-75	68-80	68-80	70-80
Nuclear magnetic resonance(a)						
% Aromatic protons	93	94	57	89	90	49
% Olefinic protons	2	2	9	2	1	8
% Aliphatic protons	5	4	34	9	9	43

(a) Most of the aliphatic and olefinic protons were on cyclic structure. No triphenylene was found in the o-terphenyl products.

Infrared analysis confirmed the aliphatic structure in the residue fractions. No methyl groups were indicated and some terphenyl remained in both residues.

Gas-solid chromatography showed three product groupings: (a) a series eluting prior to the terphenyl starting material, (b) the starting terphenyl, and (c) a broad area of peaks eluting in the hexaphenyl range. A relative yield was

calculated by dividing the terphenyl peak area into the peak area of the products, as shown in Table XV.

TABLE XV

PEAK AREA RATIOS

	O-terphenyl			M-terphenyl		
Ratio: Product Peak Area to Terphenyl Peak Area	Total Product	Sublimate	Residue	Total Product	Sublimate	Residue
Peaks prior to terphenyl	0.04	0.06	0.43	0.07	0.05	0.62
Hexaphenyl range peaks	0.02	0	0.41	trace	0	0.36

At present there is no explanation for the large amount of material eluting prior to the terphneyl from the residue fractions. Peaks eluting prior to terphenyl would be expected to sublime with the terphenyl fraction rather than remaining in the residue. These peaks will be trapped by a prep column and analyzed for structure.

Mass spectra were obtained on the material isolated in the liquid nitrogen trap during the m-terphenyl run. Mass peaks were found at 154 (biphenyl), 158, 160, and 164. Also benzene, toluene, and a six-carbon structure (olefin or cyclic) were indicated.

The brown film found on the hydrogen-atom inlet tube was examined by infrared. The structure was similar to the high molecular weight residues isolated after sublimation except more hydrogenation was indicated. The films were benzene insoluble which indicated a crosslinked polymer.

Some conclusions can be made from the analytical data about the reaction of hydrogen atoms with polyphenyls under mild conditions. The primary reaction was the addition of hydrogen atoms to the double bonds in the aromatic system. The second steps may be disproportionation, dimerization, and polymerization. Very little ring opening occurred and some scission between rings was indicated. The polymer probably was formed from olefinic materials and will be checked for fouling characteristics in film tests.

4.4 Synthesis of Reference Polyphenyls

The synthetic program to produce pure samples of polyphenyls, particularly the more important hexaphenyls, has been continued. It is hoped that these reference compounds will in part identify high boiler fragments formed from the irradiation of terphenyl which in turn may lead to a better understanding of the chemistry of terphenyls.

An earlier report from Phillips Petroleum Co [7] presented calculations whereby the relative yields of hexaphenyls formed from the electron irradiation of m-terphenyl at 500 to 600°F were predicted. Nine were expected to constitute about 85 percent of the total yield of hexaphenyls. To date, seven of these

nine have been made available. In addition, similar calculations have been made for the electron irradiation of p-terphenyl at 500 to 600°F. Ten are expected to constitute 100 percent of the total yield of hexaphenyls. To date, two have been prepared. The major efforts of the synthetic program have therefore been directed towards the preparation of intermediates necessary for the synthesis of these p-terphenyl-derived hexaphenyls.

During the current period, several intermediates were prepared. The first was 1,4-diphenylbut-1-ene-3-one prepared in a 45 percent yield from benzaldehyde and phenyl-2-propanone [8]. This was then treated with the monosodium salt of diethyl malonate to give, in a 30 percent yield, ethvl-2,4-dioxo-3,6-diphenylcyclohexane carboxylate. Hydrolysis and decarboxylation of this ester gave, in a 60 percent yield, 2,6-diphenylcyclohexane-1,3-dione [9]. This dione is to be converted to the monomethyl enol ether, which will then be coupled with a lithio terphenyl to give one of the desired reference hexaphenyls. Etherification of this dione will be carried out with diazomethane [9]. Consequently, diazomethane was prepared via its nitrosomethyl urea precursor. Both materials were prepared according to the method of F. Arndt [10].

The intermediate, 2'-bromo-p-terphenyl, is a precursor thought to be necessary in the preparation of some hexaphenyls. Therefore, this compound is being sought through the following route: 4,4'-dinitrobiphenyl→4-amino-4'-nitrobiphenyl→4-acetamino-4'-nitrobiphenyl→3-bromo-4-amino-4'-nitrobiphenyl→3-bromo-4-phenyl-4'-nitrobiphenyl→2'-bromo-p-terphenyl. The selective reduction of 4,4'-dinitrobiphenyl to 4-amino-4'-nitrobiphenyl was carried out in a 50 percent yield by the use of sodium sulfide and sulfur [11]. Acetylation was made in an 82 percent yield with acetyl chloride. The bromination step was carried out in a 75 percent yield by brominating the substituted acetanilide in acetic acid [12]. The remainder of the synthesis scheme is still in progress. Detailed progress in the synthesis and separation of intermediates is given in the following paragraphs.

1,4-Diphenylbut-1-ene-3-one [8]. Benzaldehyde (30.6 grams, 0.28 mole) was added to a solution which contained 2.25-gram sodium hydroxide dissolved in 1200-ml water. The contents were heated to 60°C with stirring and phenyl-2-propanone (37.5 grams, 0.27 mole) was added. The stirring was continued for 20 hours at 60°C after which time the mixture was cooled and the yellow cake which formed was filtered and air dried. Recrystallization from methanol gave 27 grams (43.5 percent yield) of a light yellow crystalline material; melting point 70 to 73°C.

Ethyl-2,4-dioxo-3,6-diphenylcyclohexane carboxylate [9]. To sodium (2.4 grams, 0.106 mole) dissolved in 50-ml absolute ethanol was added diethyl malonate (16.6 grams, 0.103 mole). The mixture was gently warmed on a steam bath for a few minutes, cooled and 1,4-diphenylbut-1-ene-3-one (23.0 grams, 1.103 mole) dissolved in 200-ml ethanol was added, and the mixture was set aside overnight. The solution was concentrated, diluted with an equal amount of water, and the mixture filtered. Acidification of the filtrate with dilute aqueous hydrochloric acid gave about 21 grams of a semicrystalline material. The aqueous phase was removed and the mass dissolved in benzene and heated on a steam bath to remove additional amounts of water by azeotrope. The benzene solution

was cooled and the crystalline material which was formed was filtered and dried to give 10.2 grams (29.4 percent yield) of a white crystalline material; melting point 173 to 174°C (Literature melting point 174 to 175°C).

2,6-Diphenylcyclohexane-1,3-dione [9]. Ethyl-2,4-dioxo-3,6-diphenyl-cyclohexane carboxylate (55.1 grams, 0.164 mole) was refluxed for 20 hours with anhydrous sodium carbonate (50.0 grams, 0.47 mole) in 450 ml of water. The solution was then acidified with dilute hydrochloric acid and refluxed for one hour. The mixture was cooled and filtered and the residue washed with water and dried. Recrystallization from 2-methoxyethanol gave 25 grams (58 percent yield) of a crystalline material; melting point 245°C.

Nitrosomethyl urea [10]. Concentrated hydrochloric acid (64 mil) was added with cooling to a solution which contained approximately 23 grams, 0.74-mole monomethyl amine in 80 grams of water (100 grams of a 24 percent aqueous monomethyl amine solution). The end point was determined by methyl red indicator. Water was added to bring the total weight to 250 grams. Urea (150 grams, 2.5 moles) was added and the solution boiled gently for 2 hours. The mixture was allowed to stand at room temperature for several days. Sodium nitrite (55 grams, 0.75 mole) was dissolved in it and the whole cooled to 0°C. A mixture of 300 grams of ice and 50 grams of (0.5 mole) concentrated sulfuric acid was placed in a 2-liter beaker and stirred mechanically. The beaker was cooled by means of acetone and dry ice and the bath temperature controlled near -10°C. The cold methylurea-nitrite solution was added dropwise (siphoning action) with stirring at such a rate that the temperature did not rise above 0°C. The nitrosomethylurea raises to the surface as a crystalline foamy precipitate which was quickly filtered, washed with a minimum amount of cold water, and vacuum dried. The desiccator was stored in the refrigerator to prevent decomposition of the product which occurs rapidly above 20°C. There was obtained 56.3 grams (72 percent yield) of light tan colored crystals.

Diazomethane [10]. To a 500-ml round bottom flask which was cooled in a wet ice bath was placed 100 ml ether and 30 ml of a 40% aqueous potassium hydroxide solution. To this was added at 5°C, 10 grams of powdered nitrosomethylurea in small portions over a period of 5 minutes. The deep yellow ether layer was decanted and dried over pellets of potassium hydroxide for 3 hours. (Note: It is reported that this ethereal solution contains about 2.8 grams of diazomethane plus some dissolved impurities which in most cases is sufficient to use as is.)

4-Amino-4'-Nitrobiphenyl [11]. Sodium sulfide nonahydrate (105 grams, 0.4 mole) was melted on a steam bath. Sulfur (14 grams) was added and the mixture heated until all the sulfur dissolved. Upon cooling, a mixture of water (300 ml) and 4,4'-dinitrobiphenyl (70 grams, 0.28 mole) was added and the mixture heated for 5 hours on a steam bath with occasional shaking. The

mixture was cooled and washed with boiling water. The residue was extracted several times with near-boiling 5 percent aqueous perchloric acid. The combined acid extracts were cooled, filtered, and rendered basic with ammonium hydroxide. The precipitate which formed was filtered and twice recrystallized from benzene to give 30 grams (50 percent yield) of a bright orange-red material; melting point 197 to 200°C.

4-Acetamino-4'-nitrobiphenyl. 4-Amino-4'-nitrobiphenyl (21.4 grams, 0.1 mole) in 150 ml of pyridine was cooled to approximately 10°C whereupon acetyl chloride (9.4 grams, 0.12 mole) was slowly added with stirring. The mixture was stirred one hour at room temperature, then poured into 250 ml of concentrated hydrochloric acid and ice, filtered, and dried. Recrystallization from concentrated acetic acid gave 21 grams (82 percent yield) of a material which melted at 235 to 238°C. (Literature values: Willstedder and Cobb, Ber. 39, 3479; melting point 240°C and Schmidt and Schulz, Ann. 207, 347; melting point 264°C.)

3-Bromo-4-acetamino-4'-nitrobiphenyl [12]. 4-Acetamino-4'-nitrobiphenyl (20.6 grams, 0.08 mole) and anhydrous sodium acetate (23.8 grams, 0.03 mole) were dissolved in 500 ml of hot glacial acetic acid and the mixture allowed to cool rapidly. Bromine (10 ml) was added followed by 15-hours heating on a steam bath. The mixture was cooled and diluted threefold with water. The precipitate was filtered and recystallized from glacial acetic acid. There was obtained 20.6 grams (75 percent yield) of a yellow-orange material which had a melting point of 226.5 to 228°C. F. H. Case [12] reports a melting point of 235 to 236°C.

5. NEW ORGANIC COOLANTS FOR NUCLEAR REACTORS

(W. M. Hutchinson, R. C. Doss, L. V. Wilson)

5.1 Ideal Coolants

The ideal coolant program continued in three areas: non-benzenoid, fused ring, and hydrogen-donor coolants. The aim of non-benzenoid coolants is to find ring systems that, when under irradiation, will not form hydroaromatics that are capable of oxygenation or polymerization. This goal is derived from two hypotheses that film on nuclear reactor elements is caused (a) by polymerization of hydroaromatics to p-linked polyphenyls (due to R. O. Bolt), and (b) by transfer of iron from piping to hot surfaces via organic iron compounds soluble in the coolant (due to R. B. Regier).

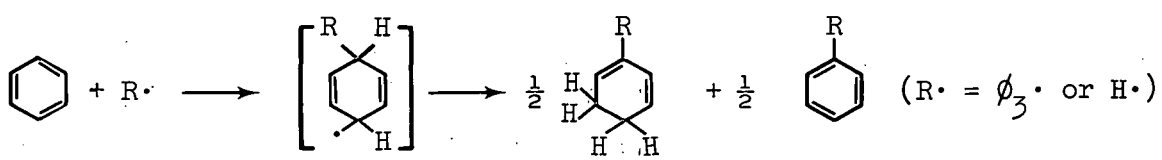

(a) 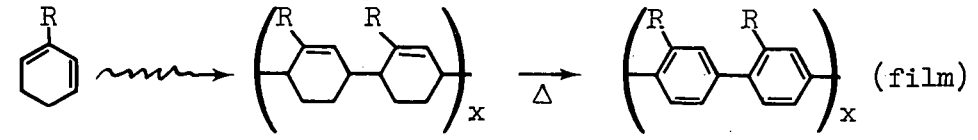

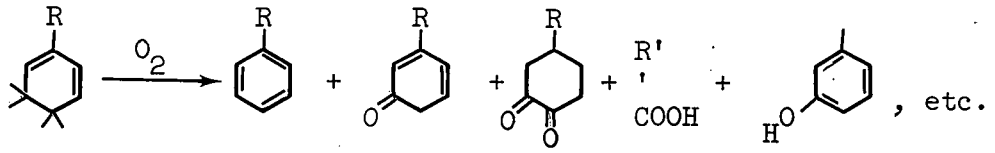

(b) Fe oxides + oxygenated products ⟶ soluble iron compounds⟿film.

Neither mechanism would be operable if the ring system in the coolant did not form reactive hydroaromatics as does benzene. The primary aim of the search for fused ring coolants is to find one more stable than polyphenyls thermally and radiolytically. The aim of the hydrogen-donor coolants is primarily to reduce radiolytic damage.

The tendency of various heterocycles to form dihydro derivatives probably can be tested by irradiation of the monoheterocycles such as pyridine, thiophene, thiazole, imidazole, and s-triazine, and by detection of hydroaromatics by chromatography and infrared spectroscopy (in absence of air). The tendency of the hydroaromatics to polymerize and oxygenate could then be tested. Low $G(H_2)/G(dimer)$ ratios also should be an indication of the ring systems that become partially hydrogenated. This approach will be pursued to find stable heterocyclic coolants that do not form troublesome hydroaromatics.

Meanwhile, synthesis of model compounds has progressed. Trial synthesis of 2,4,6-tri(2-pyridyl)-s-triazine, tri-(3-pyridyl)-s-triazine, tri-(4-pyridyl)-s-triazine, 2-phenylthiazole, and 4-phenylthiazole have been made. These are to be tested for pyrolytic and radiolytic stability that should simultaneously indicate which heterocycles show promise and where they can be advantageously linked together to reduce volatility. One bipyridyl has been screened for radiolytic stability.

The low yield of high boiler (dimer) from irradiation of 9,10-dihydrophenanthrene [13] has been assigned to the formation of a radical (A) that does not substitute aromatic rings:

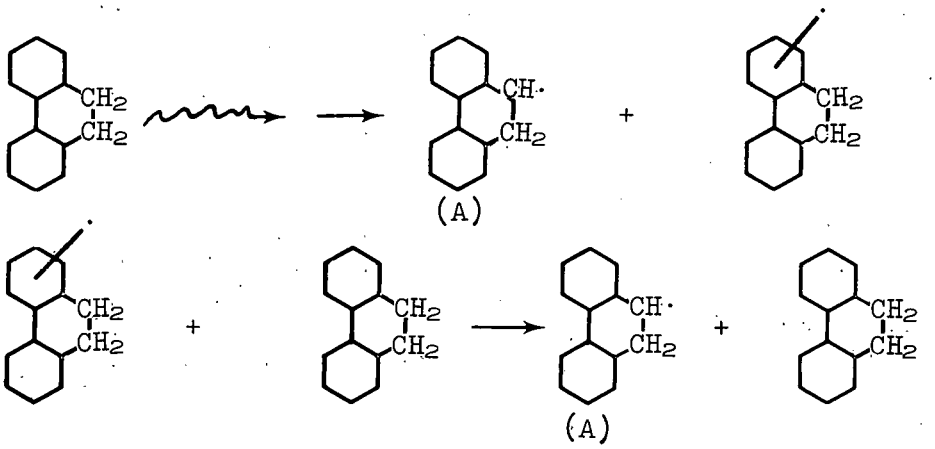

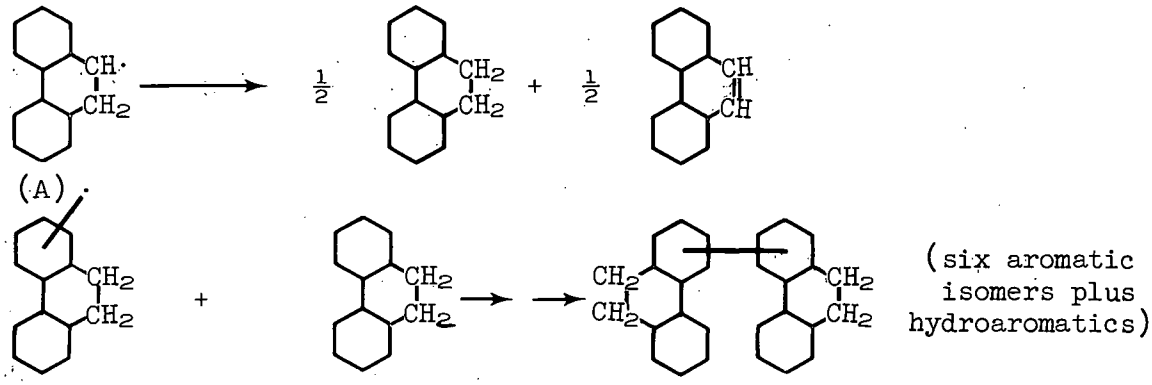

Thus, a lesser amount of phenanthrene is produced at the expense of dimeric high boiler. This mechanism was quantitatively developed and evaluated from data on the radiolysis of toluene to benzyl and tolyl radicals (like first reaction) and data on hydrogen abstraction from toluene and ethylbenzene by phenyl radicals (like second reaction). The model approximated experimental results but predicted a linear dependence of radiolytic yield of total high boiler on concentration of 9,10-dihydrophenanthrene in mixtures of it and terphenyl. The experimental curve was nonlinear (see section on stabiliziers). Validation of the mechanism is too incomplete to allow its quantitative treatment to be reported now.

The thermal stability of 9,10-dihydrophenanthrene is of some concern. When heated at 800°F in a mild steel container for 48 hours it developed only 4.3 percent high boiler but most of the starting material was converted to phenanthrene. The small sample (2 grams) resulted in a large surface-to-volume ratio and the test may not be a reliable measure of the rates of catalytic vs thermal dehydrogenation. Work on radiolysis and pyrolysis of 9,10-dihydrophenanthrene will be pursued.

Examination of a sample of 9,10-dihydrophenanthrene by gas chromatography with a 5-foot, 20 percent lithium chloride column revealed that a considerable amount of impurities appear to be present. Therefore, an attempt was made to separate or at least concentrate these impurities. It was subjected to fractional crystallization whereby a solid phase (Fraction A) was removed at room temperature; another solid phase (Fraction B) was separated at 5°C; and the filtrate (Fraction C) obtained from the separation of Fraction B. These three fractions were subjected to irradiation (Table XVI) and the results indicated no substantial differences in either the amount of gas or polymer formed. No explanation can be made as to why the original sample showed impurities. Later samples of 9,10-dihydrophenanthrene were shown by gas chromatographic analysis to be reasonably pure.

A sample of 1,2,3,4,5,6,7,8-octahydrophenanthrene was irradiated and gave the lowest relative polymer value yet obtained, namely 0.14. However, it also gave one of the highest relative gas values yet obtained, 21.6. It in itself has, perhaps, no commercial value as a coolant but it does point to the apparent need for further study on cyclic materials that are partially or even fully saturated.

TABLE XVI

IRRADIATION OF IDEAL COOLANT CANDIDATES

Conditions: Temperature, 600 to 650°F; time, 8 hr.				
Irradiation No.	Compound	Dosage (rads x 10^8)	Relative Polymer	Relative Gas
D-6	Santowax OMP (control)	6.3	1.00 (20.6%)	1.00 (0.13 cc/watt-hr)
	9,10-Dihydrophenanthrene (Fraction A)		0.17	4.70
	9,10-Dihydrophenanthrene (Fraction B)		0.19	4.16
	9,10-Dihydrophenanthrene (Fraction C)		0.19	4.22
	1,2,3,4,5,6,7,8-Octahydrophenanthrene		0.14	21.60
	2,4,6-Tri-(m-tolyl)-s-triazine		0.95	2.38
	Dibenzothiophene		0.81	1.77
D-7	Santowax OMP (control)	7.6	1.00 (23.9%)	1.00 (0.23 cc/watt-hr)
	2,2'-Bipyridyl		1.34	3.08
	Tetramethylpyrazine		0.99	35.00
	Dihydropyrene		0.37	2.64
D-8	Santowax OMP (control)	13.0	1.00 (34.1%)	1.00 (0.32 cc/watt-hr)
	Phenazine		2.67	6.95
	M-diphenoxybenzene		2.02	5.95
	Quinoxaline		2.10	3.59
	Quinaldine		0.95	3.71
	Fluorene		0.74	2.72
D-9	Santowax OMP (control)	4.9	1.00 (17.1%)	1.00 (0.10 cc/watt-hr)
	Benzoxazole		5.7	25.00
	Benzothiazole		2.3	11.00

Dihydropyrene gave good relative results (0.37 for polymer and 2.64 for gas). Although it is not quite as good as 9,10-dihydrophenanthrene, it is satisfactory and continues to support the premise that the best candidates so far tested are the partially saturated fused ring (hydrogen-donor) compounds.

Two linear compounds which possess an intervening fused five-membered ring, dibenzothiophene and fluorene, were tested. Dibenzothiophene was the better of the two with a relative polymer value of 0.81 and a relative gas value of 1.77.

The study of nitrogen-containing compounds has not to date shown any great improvement over the control, Santowax OMP. Tetramethylpyrazine gave a polymer value the same as Santowax but its relative gas value was the highest found to date, namely 35.0. A relative radiolytic polymer value of 1.34 and a relative gas value of 3.08 were obtained from 2,2'-bipyridyl. Fused ring compounds which contained one or more nitrogen atoms within the structure in general have not possessed radiolytic stability as good as the control, Santowax OMP.

Results from the irradiation of benzothiazole and benzoxazole were so poor (2.3 and 5.7 relative polymer and 11.0 and 25.0 relative gas, respectively) that further consideration of these fused ring structures appears to be useless.

The compound, 2-phenyl-benzo(h)-quinoline, has a low melting point (melting point 68°C) and reportedly a good thermal stability [14] (weight loss after five hours at 700°F, 0.3 percent). It therefore appeared that this material and others like it should be considered as candidate coolants. The intermediate to the desired coolant, 2-phenyl-benzo(h)-quinoline-4-carboxylic acid was prepared in a 30 percent yield from alpha napthylamine, pyruvic acid and benzaldehyde. Separation of this intermediate from the by-product, 1-(benzimido)-napthalene, was successfully carried out by alkaline extraction. Decarboxylation of the acid with copper powder at 290°C was successfully carried out in an 80 percent yield.

Details of syntheses of model compounds and candidate coolants are given in the following paragraphs.

2-Phenyl-benzo(h)-quinoline-4-carboxylic acid [15]. Alpha naphthylamine (35.8 grams, 0.25 mole) benzaldehyde (26.5 grams, 0.25 mole) and 300 ml of methanol were rapidly stirred and pyruvic acid (22.0 grams, 0.25 mole) dissolved in 100 ml of methanol was quickly added. Within 20 minutes a precipitate began to form. The mixture was stirred two hours, filtered, and the residue washed with methanol and air-dried. There were 8.4 grams of a yellow material obtained. The material was treated with aqueous sodium hydroxide, heated on a steam bath, cooled, and filtered. Any low-molecular-weight acids or a Schiff base, ie, 1-(benzimido)-naphthalene, should be soluble and thus removed. The residue was treated with aqueous acetic acid whereupon a yellow product again formed. Recrystallization of this product was accomplished by dissolving it in a minimum amount of acetone and diluting with water. There was obtained 22.5 grams (30 percent yield) of product which melted at 295°C (decreased).

2-Phenyl-benzo(h)-quinoline [14]. Twenty-nine grams (0.1 mole) 2-phenyl-benzo(h)-quinoline-4-carboxylic acid and 1.0 gram of copper powder were intimately mixed. The mix was added portion-wise to a flask which was immersed in a silicone oil bath at 290°C. The addition was made over a period of one hour, after which the flask was cooled and the residue extracted with hot ethanol. The extract was cooled, filtered, and the filtrate evaporated to 19.8 grams (80% yield) of the desired decarboxylated substituted quinoline; melting point 68.5 to 70°C.

Synthesis of 2,4,6-tri-(2-pyridyl)-s-triazine. This compound was synthesized by cyclotrimerization of 2-cyanopyridine on sodium hydride at 160 to 165°C [16]. Six grams of distilled (109°C/20 mm Hg) 2-cyanopyridine (Aldrich Chemical Co) were put in a 50-cc round botton flask fitted with an air-cooled reflux condenser. Air in this assembly was displaced with argon, 0.1 gram of sodium hydride (50 percent in wax, Metal Hydrides, Inc) was added down the condenser, and the top of the condenser was plugged with glass wool. The flask was immersed to its equator in an oil bath which

was heated to 160 to 165°C. When the mixture reached this temperature a dark brown color developed within about 15 minutes. Heating continued for five hours. The reaction mixture was cooled, extracted with hot benzene (40 cc), and filtered. The product extract was evaporated to dryness and the residue crystallized from 50-50 water-isopropyl alcohol (20 cc). The crystals were filtered, washed with a small amount of chilled water-methanol (about 50-50) and recrystallized from this medium. The product (2.0 grams) was in the form of fine, yellow crystals melting at 246.5 to 250°C (literature 244 to 245°C). It formed an intense, dark blue color with ferrous chloride when their aqueous solution was made neutral with sodium hydroxide. This is reported to be characteristic of furoin grouping: -N=C-C=N-. Literature reported a stable trihydrate of this s-triazine, but the product dehydrated in an ordinary oven at 120°C. Analyses vs calculated values on anhydrous basis were: carbon 68.9 weight percent (69.2), hydrogen 3.9 weight percent (3.9), nitrogen 26.6 weight precent (26.9), molecular weight 320 (312).

Synthesis of 2,4,6-tri-(4-pyridyl)-s-triazine. This was similar to the foregoing excepting that 4-cyanopyridine (Reilly Tar and Chemical Corp) was used instead of 2-cyanopyridine and the heating period was six hours. After two hours, crystals formed in the reaction mixture and gradually increased in quantity. The reaction mixture did not discolor as much as previously. It was extracted three times with hot benzene (total volume about 130 cc). The crystals that had formed in the reaction mixture did not dissolve so unconverted 4-cyanopyridine could be cleanly extracted. A subsequent extraction with a hot mixture of isopropyl alcohol and water removed most of the brown (amorphous?) contaminant from the crystals which had a "salt-like" form. No nonacidic solvent was found for the product and it was sublimed at 20-mm mercury and at sufficient temperature to give a sodium flame where the flame hit the pyrex tube. A minor residue was black-brown, but the sublimate was white and weighed 1.0 gram. Melting point of the sublimate was 383°C. It gave a furoin reaction. It was soluble in an alcohol-water solution of HCl and in glacial acetic acid but on dilution formed impure precipitates. Its analyses vs calculated values for 2,4,6-tri-(4-pyridyl)-s-triazine were: carbon 69.3 weight percent (69.2), hydrogen 3.9 weight percent (3.9), and nitrogen 26.8 weight percent (26.9).

Synthesis of 2,4,6-tri-(3-pyridyl)-s-triazine. The cyclotrimerization over sodium hydride was repeated with 3-cyanopyridine (Reilly Tar and Chemical Corp). No product was obtained so the reaction was repeated on a larger scale (100 grams 3-cyanopyridine, 1.0 gram sodium hydride-wax). The reaction mixture was left in a 160°C bath overnight (temperature of reaction mixture was 10°C lower). Unconverted 3-cyanopyridine was distilled from the reaction mixture at 97°C/20 mm Hg. The small, dark brown residue was extracted with hot benzene. The extract was evaporated until crystals began to form. After cooling, the crystals (3 grams) were filtered off. They melted at 308 to 310°C and were contaminated with the brown by-product. No analyses were attempted because

of the impurity. When this procedure was repeated with 4-cyanopyridine an impure sample melting at 382°C and weighing 8.5 grams was obtained. It has not yet been sublimed.

Synthesis of mixed pyridyl-s-triazine. Six grams each of 2-cyano-, 3-cyano-, and 4-cyanopyridine were reacted as before. The unconverted cyanopyridines (9.0 grams) were removed by vacuum distillation (98 to 112°C/20 mm Hg). Pressure was reduced to 1.5-mm mercury and the product distilled and sublimed at 192 to 198°C. The distillate-sublimate mixture melted from 220 to 270°C (first liquid to last solid).

Synthesis of 4-phenylthiazole. This material was synthesized by the Hantzsch Method [17]. Formamide (1.0 gram), α-chloroacetophenone (3.4 grams) and phosphorus pentasulfide (4.0 grams) were mixed by stirring in an evaporating dish and heated on a steam bath. Foaming occurred with formation of a dark, brown-black, viscous mass. After foaming subsides (15 minutes), water (5 cc) was added. On cooling, aqueous hydrochloric acid (10 cc, 3N) was added to extract the thiazole as the hydrochloride. The filtrate was placed in a flask, neutralized to a pH of 6.5 to 7.0 with aqueous sodium hydroxide, and steam distilled. The oil in the distillate crystallized when shaken. The crystals were recrystalized twice from n-hexane and melted at 51.8 to 52.4°C (literature melting point 52°C). Yield was one gram.

Synthesis of 2-phenylthiazole. This was synthesized by the Hantzsch Method [17]. Benzamide (61.5 grams) and phosphorus pentasulfide (158 grams) were mixed in an evaporating dish, 1,2-dichloro-ethyl ethyl ether (71.5 grams) was poured over the mixture, and the mixture stirred into a crumbly mash. The dish was immediately covered with aluminum foil and placed on a steam bath. After 30 minutes, foaming had subsided. The reaction mixture was cooled to about 40°C. Then water (100 cc) was added with stirring. After one hour the bubbling had stopped and hydrochloric acid (200 cc, 6N) was stirred in. Some more bubbling occurred and the mixture sat for three days. The aqueous solution of the thiazole hydrochloride was filtered off. The filtrate was extracted twice with ether (300-cc portions) to remove impurities and the raffinate (water) was transferred to a flask and made neutral (pH 6.8) with aqueous sodium hydroxide. Phase separation occurred and the entire contents was steam-distilled to recover 2-phenylthiazole as a pink oil (15 grams). The color persisted after vacuum distillation.

Synthesis of 1,5-naphthyridine. This was made by the Skraup synthesis [18]. Anhydrous glycerol (60.0 grams), 3-aminopyridine (15.0 grams), arsenic pentoxide (20.0 grams) and concentrated sulfuric acid (30 cc) were mixed in a one-liter, round bottom flask by rotating it. The flask was placed under a reflux condenser and heated in an oil bath at 170°C for two hours. The reaction mixture was poured into 400 cc of ice and water. Sodium hydroxide solution (50 percent excess) was added with stirring. The mixture was

steam-distilled until 2.5 liters of distillate was collected. The first liter and last 1/2 liter were "salted" with 1.1 pound of fused sodium hydroxide. The second liter was "salted" with 0.5 pound of anhydrous potassium carbonate. This seemed better as a larger oil phase separated and then crystallized. All were extracted three times with ethyl ether (the literature calls for continuous extraction). The extracts were combined, dried with anhydrous potassium carbonate, and distilled; 1,5-naphthyridine distilled at 124 to 126°C/20 mm Hg and solidified as it condensed. The solid was pressed between paper to remove traces of liquid. The crystals were white, melted at 68 to 70°C (literature, 72°C), and weighed 3.0 grams (literature, 7.5 grams). It showed three impurity peaks totaling about one percent by gas chromatography. Analyses vs calculated values for anhydrous naphthyridine were: carbon 71.7 weight percent (74.0), hydrogen 5.1 weight percent (4.6), nitrogen 18.8 weight percent (21.4). The analyses were not consistent with naphthyridine nor a hydrate and may have become contaminated with carbon dioxide.

Use of m-nitrobenzene sulfonate instead of arsenic pentoxide as the oxidizing agent is reported to give a superior yield [19].

5.2 Thermal Stability Testing

Testing of industrial stocks and of pure compounds for thermal stability was continued during this quarter. Results of these tests are given in Table XVII.

5.21 Industrial Stocks. The thermal stability tests were carried out at 675, 700, and 725°F for 48 hours for the industrial stocks, which is 25°F higher than tests the previous quarter. The large aluminum blocks for constant temperature and the small steel sample holders (2 grams charge) were described in an earlier report. The samples are carefully degassed and are blanketed with a pressure of one atmosphere of argon for the test.

As can be seen in Table XVII, all of the industrial stocks show poor thermal stability when tested under these conditions. The Humble Nuclear Reactor Coolant fraction, with heavy ends removed by distillation, is fairly stable at lower temperatures but breaks down rapidly at 700°F and above.

A dimethylsulfoxide extract of an SO_2 plant extract, tested during the previous quarter, gave a relative radiolytic polymer of 0.95 when compared with Santowax OMP control, but gave 18.4 percent polymer when held 48 hours at 700°F. This stock was hydrodesulfurized and then tested again for radiolytic and thermal stability. The relative radiolytic polymer was still less than one after desulfurization, and the change in thermal polymer was greatly improved. The increase in polymer was only 5.4 percent after 48 hours at 700°F, and was 15.6 percent after 48 hours at 725°F. The hydrodesulfurized sample was then distilled to remove heavy ends and was again tested for radiolytic and thermal stability. The relative radiolytic polymer yield was 0.86 compared with Santowax OMP control, and the radiolytic gas produced was 1.1 cc/watt-hr, or 7.2 relative to Santowax OMP. This distilled, desulfurized extract gave 8.8 percent polymer after 48 hours at 700°F, and 18.8 percent after 48 hours at 725°F.

TABLE XVII

THERMAL STABILITY

	Gas (cc/g)	Percent High Boiler[a]
Industrial Stocks		
Humble NRC fraction (673 to 836°F boiling point)		0
48 hr at 675°F	1.3	5.6
48 hr at 700°F	19.8	19.9
48 hr at 725°F	27.3	55.7
Desulfurized DMSO extract of SO_2 extract		9.7
48 hr at 675°F	2.7	9.7
48 hr at 700°F	15.3	15.1
48 hr at 725°F	19.8	25.3
Distilled, desulfurized DMSO extract of SO_2 extract		0
48 hr at 675°F	7.0	1.5
48 hr at 700°F	14.0	8.8
48 hr at 725°F	33.0	18.8
Pure Compounds		
2,4,6-s-triphenyl triazine[b]		0
48 hr at 675°F	0	0
48 hr at 700°F	2.4	0.3
48 hr at 725°F	3.5	0.6
2,4,6-tri(m-tolyl)-s-triazine[b]		0
48 hr at 675°F	0.7	2.4
48 hr at 700°F	2.4	4.9
48 hr at 725°F	4.8	10.5
9,10-dihydrophenanthrene		0
48 hr at 675°F	1.7	0.4
48 hr at 700°F	2.6	0.3
48 hr at 725°F	6.6	0.5
48 hr at 750°F	8.2	0.3
48 hr at 775°F	11.7	0.8
48 hr at 800°F	22.0	4.3

(a) Percent residue after sample is placed under 0.1-mm pressure and held for 30 min at 220°C.

(b) High boiler contents run at 290°C due to high boiling point of original material.

Since hydrodesulfurization and also hydrodealkylation have improved thermal stability of industrial stocks, several distillations of extracts, decant oils, cycle oils, and coal tar products have been made to prepare samples for hydrodesulfurization and for hydrodealkylation when equipment becomes available.

5.22 Pure Compunds. Thermal stability tests on 2,4,6-s-triphenyltriazine gave only 0.6 percent polymer after 48 hours at 725°F. Percent polymer was determined at 290°C instead of 220°C due to the higher boiling point of this compound. The radiolytic stability was better than Santowax, but the high melting point would present handling difficulties. A sample of 2,4,6-tri(m-tolyl)-s-triazine gave 10.5 percent polymer after 48 hours at 725°F. These also were sublimed at 290°C due to the higher boiling point.

A sample of 9,10-dihydrophenanthrene which had given a low yield of radiolytic high boiler when tested under the Linac for 8 hours at 650°F was tested for thermal stability for 48 hours at temperatures up to 800°F. Only 0.8 percent polymer was formed at 775°F, and 4.3 percent at 800°F. Gas chromatograms indicated phenanthrene and new compounds forming, possibly aromatics, with more present after treatment at the higher temperatures. After 48 hours at 800°F almost complete dehydrogenation to phenanthrene had occurred. A coolant system could be visualized which would incorporate a plant to hydrogenate a side stream of reactor effluent back to 9,10-dihydrophenanthrene.

6. RADIATION STABILIZERS

(R. B. Regier, H. A. Hartzfeld)

The study of radiation stabilizers has been carried out with the objective of discovering materials which, at reasonable cost, will reduce appreciably the damage to organic moderator-coolants under ionizing irradiation. This investigation has been restricted to the stabilization of terphenyls. The testing of 87 individual additives, as well as a number of combinations of additives, was reported previously [20]. With only a few exceptions the best stabilizers comprised three types of substances: (a) sulfur in an elemental, divalent, or tetravalent state, (b) fused ring compounds structurally related to anthracene, and (c) hydrogenated fused ring compounds not necessarily possessing the skeletal structure of anthracene. The protection provided by such effective stabilizers as anthracene, phenothiazine, and 2-mercaptobenzothiazole was only slightly dependent on concentration over a wide range; in contrast, stabilization by 9,10-dihydroanthracene and by elemental sulfur was greatly influenced by concentration. Combinations of effective stabilizers exhibited no synergism in protective action. Anthracene as an additive disappeared quite rapidly under irradiation, but its beneficial effect remained. Elemental sulfur, too, was consumed rapidly, approximately two-thirds of it being converted to hydrogen sulfide.

The experimental program during this quarter for studying stabilization of Santowax OMP under high temperature electron irradiation has been a continuation of the work described previously. With the exception of irradiation 44 (Table XVIII), irradiations were carried out at 600 to 660°F (316 to 349°C) for 7 hours. Determinations of polymer in the irradiated samples were made by sublimation (in a closed system) at 220°C for 30 minutes at an initial pressure of 0.10 mm; gas analyses were carried out by mass spectrometry.

TABLE XVIII

EFFECT OF ADDITIVES IN RADIOLYSIS OF SANTOWAX OMP

Irradiation No.	Additive	Dosage (rads x 10^8)	Relative Polymer	Relative Gas
44(a)	Control	5.8	1.00 (19.5%)	1.00 (0.145 ml/watt-hr)
	Sa, 0.4 mole %		0.77	1.15
	Sa, 0.7 mole %		0.73	1.82
	Sa, 1.0 mole %		0.75	2.23
	Anthracene, 3 mole %		0.84	0.91
	9,10-Dihydroanthracene, 3 mole %		0.77	0.99
	Phenazine, 3 mole %		0.72	0.63
45	Control	9.0	1.00 (26.8%)	1.00 (0.083 ml/watt-hr)
	Pd/C, 2 wt%		1.16	2.89
	Anthracene, 6 mole %		0.86	1.11
	Anthracene, 6 mole % + Pd/C, 2 wt%		0.99	2.02
	9,10-Dihydroanthracene, 6 mole %		0.73	1.29
	9,10-Dihydroanthracene, 6 mole % + Pd/C, 2 wt%		0.95	2.48
	9,10-Diphenylanthracene, 3 mole %		1.06	1.54
46	Control	9.7	1.00 (28.0%)	1.00 (0.124 ml/watt-hr)
	HB-40 (hydrogenated terphenyls), 100%		0.72	10.1
	1,2,3,4-Tetrahydronaphthalene, 3 mole %		0.95	1.02
	Decahydronaphthalene, 3 mole %		1.00	1.09
	Perhydropyrene, 3 mole %		0.79	1.25
	Tetrahydroacenaphthene, 3 mole %		0.87	0.95
	Acenaphthylene, 3 mole %		0.91	0.87
47	Control	7.6	1.00 (23.9%)	1.00 (0.114 ml/watt-hr)
	9,10-Dihydrophenanthrene, 10 mole %		0.79	1.11
	9,10-Dihydrophenanthrene, 25 mole %		0.60	1.53
	9,10-Dihydrophenanthrene, 50 mole %		0.42	2.12
	9,10-Dihydrophenanthrene, 75 mole %		0.32	2.96
	9,10-Dihydrophenanthrene, 90 mole %		0.27	3.37
	9,10-Dihydrophenanthrene, 100%		0.24	4.22

(a) Irradiation temperature was 650 to 700°F (343 to 371°C).

Irradiation 44 (Table XVIII) was carried out at 650 to 700°F (343 to 371°C) for 6 hours on some of the more promising stabilizers in order to determine temperature effects on protective action. A comparison of relative polymer values with those previously obtained in irradiation 40 (Table XIX) conducted at 460 to 480°F (238 to 249°C) for 10 hours revealed that relative polymer values were influenced by temperature surprisingly little. The greatest difference was the small improvement shown by phenazine at the higher temperature. The optimum concentration of sulfur appeared to decrease with increased temperature. As expected, gas formation from the control sample was much greater at the higher temperature, thus contributing to the rather low relative gas values from the sulfur blends at this high temperature.

The primary purpose of irradiation 45 was to study the effect of a hydrogenation catalyst (10 percent palladium on powdered charcoal) on stabilized

TABLE XIX

STABILIZATION OF SANTOWAX OMP UNDER IRRADIATION (5.4×10^9 RADS) AT 460 to 480°F (238 to 249°C)

Sample	Relative Polymer	Relative Gas
Control	1.00 (18.2%)	1.00 (0.062 ml/watt-hr)
S_8, 0.4 mole %	0.81	3.36
S_8, 0.7 mole %	0.76	4.74
S_8, 1.0 mole %	0.74	5.76
Anthracene, 3 mole %	0.87	0.94
9,10-Dihydroanthracene, 3 mole %	0.79	1.07
Phenazine, 3 mole %	0.78	0.86

and non-stabilized Santowax. Relatively high concentrations of anthracene and 9,10-dihydroanthracene were used in order that differences in their stabilizing action would be easily observed. It was conceivable that the presence of a hydrogenation catalyst might permit an interconversion of anthracene and dihydroanthracene, thus imparting to anthracene a stabilizing effect approaching that of its dihydro derivative. However, the hydrogenation catalyst was found to be universally harmful with respect to both polymer and gas formation in the presence of either anthracene or dihydroanthracene, or in Santowax alone. The large increase in hydrogen formation was responsible for the much higher relative gas values observed in the presence of palladium on charcoal. The ineffectiveness of 9,10-diphenylanthracne indicated the importance of having hydrogen atoms in the 9,10-positions of hydrocarbons of the anthracene structure.

Irradiation 46 demonstrated further that hydrogenation of fused ring systems improves the stabilizing action of such substances used as additives. Tetrahydroacenaphthene was slightly superior to acenaphthene, studied previously, and perhydropyrene was more effective than pyrene or the partially hydrogenated pyrenes investigated earlier. On the other hand, tetrahydronaphthalene was slightly beneficial in contrast with naphthalene and decahydronaphthalene, both ineffective. The protective action of acenaphthylene was equal to that of its dihydro derivative, acenaphthene. HB-40 (terphenyls hydrogenated to 40 percent of complete saturation) was considerably superior to Santowax OMP with respect to polymer formation; however, gas production was greater by an order of magnitude.

Irradiation 47 was designed to study the effects of irradiation on mixtures of Santowax OMP and 9,10-dihydrophenanthrene over the complete concentration range. As expected, relative gas formation increased with increasing concentration of dihydrophenanthrene, primarily due to the larger amount of hydrogen formed. However, radiation stability with respect to the more important criterion of polymer formation progressively improved with increasing concentration of dihydrophenanthrene. It appears that at low concentrations the

phenanthrene derivative provided true protective action to the Santowax, whereas at higher concentrations the improved stability was primarily an effect of dilution of the less stable terphenyls. This irradiation, together with earlier studies, demonstrated that at concentrations up to at least 50 mole percent, 9,10-dihydroanthracene provides more protection than does 9,10-dihydrophenanthrene; however, at higher concentrations the phenanthrene derivative is superior. The molecular weights of polymer from the irradiation of samples containing 0-, 10-, 25-, 50-, 75-, 90-, and 100-mole-percent 9,10-dihydrophenanthrene were 483, 456, 446, 420, 423, 417, and 406, respectively. In a brief study of the products from the irradiation of the dihydrophenanthrene alone, gas chromatographic analysis of the sublimate from the polymer determination revealed the major components to be 9,10-dihydrophenanthrene and phenanthrene in concentrations of 57 and 34 percent, respectively. Six major components in amounts of 0.8 to 2.4 percent accounted for the remainder of the sublimate; each of these minor substances eluted at a temperature lower than those of the major constituents. The formation of phenanthrene in rather large amount should permit regeneration of the dihydro derivative by hydrogenation in a recycle process.

As an aid in obtaining information relative to the mechanism of stabilization of terphenyls by additives of the anthracene-like structure, 9,10-dihydroanthracene-9,10-d_2 was prepared in 35 percent yield (48 percent crude yield) by the reaction of 16.1 grams (0.70 grams-atom) of sodium with 53.5 grams (0.30 mole) of anthracene in 300 ml of refluxing 1,2-dimethoxyethane for three hours, followed by hydrolysis of the disodio adduct with 20 grams (1.0 mole) of heavy water. A nuclear magnetic resonance study of the deuterated product indicated it to be of 94 percent isotopic purity, if one makes the questionable assumption that no mono-deuteration occurred. The presence of mono-deuterated product should not greatly detract from the usefulness of this material in mechanism studies as the total approximate amount of deuterium in the equivalent 9- and 10-positions is known.

In an attempt to prepare perhydroanthracene for study as a stabilizer, anthracene was hydrogenated at about 750 psig and 180°C for three hours in the presence of a nickel-on-alumina catalyst. However, the only product isolated was 1,2,3,4,5,6,7,8-octahydroanthracene (71 percent yield). Phenanthrene under more severe conditions (1000 psig, 4-1/3 hours, 180 to 260°C) underwent reaction much more poorly.

7. RECLAMATION OF RADIOLYZED ORGANIC NUCLEAR REACTOR COOLANT

(W. M. Hutchinson, L. E. Gardner, L. V. Wilson)

7.1 Introduction

The objective of this phase of the organic moderator studies has been to find an economical method for conversion of damaged terphenyl coolant to usable coolant. The major portion of research has been in conversion by catalytic hydrocracking. The goal this quarter was to complete some phases of the work for termination of this program. Experimental work on hydrocracking high boiler was essentially completed with a series of six-hour runs on OMRE Core II high boiler. However, initial tests on hydrocracking the total coolant had revealed that a more efficient operation might be developed. This involved

selectively hydrocracking the high boiler present in the coolant with minimum destruction of the terphenyls. Thus, at the usual high boiler levels, the preliminary low vacuum distillation would not be required. Should a reactor be operated with very low high boiler in the coolant, this distillation could be replaced by a much cheaper vacuum flash drum which would return a fraction of the terphenyls to the coolant loop. A valuable asset of treating coolant would be aromatization of hydroaromatics generated by radiolysis. These possibilities appeared promising enough to extend the total coolant reclamation program into this quarter with emphasis on optimizing yields, studying high boiler types and concentrations, and investigating solvent-free charge stocks which closer simulates plant-scale operation. During the quarter further evaluations of reclaimed coolants were made on radiolytic stability as compared to Santowax OMP. Using the available information from bench scale hydrocracking tests, economic evaluations were made on both the low conversion, recycle process of straight high boiler and on a once-through coolant hydrocracking process.

7.2 Catalytic Hydrocracking

7.21 High Boiler Conversion. A series of six-hour hydrocracking runs on OMRE Core II high boiler was carried out at the same reaction conditions of 1000 psig, 900°F, 1.0 liquid hourly space velocity, 40 weight percent high boiler in p-xylene, and 30 moles hydrogen per mole high boiler. The purpose of this series was to compare the most promising catalysts at conditions which approach "steady state" activity. Also some of the less efficient catalysts were included for comparative purposes. All catalysts tested were samples which had been coked in previous high boiler hydrocracking runs and air-regenerated at least two times. A list of the catalysts tested in this series is shown in Table XX along with

TABLE XX

CATALYSTS(a) USED IN HIGH BOILER AND COOLANT HYDROCRACKING TESTS

Catalyst	Composition (wt%)	Surface Area (m^2/g)
$CoMoO_4$-Al_2O_3	1.4 Co, 8.9 Mo	60
NiO-Al_2O_3	1.3 Ni	79
Pt-Al_2O_3	1.0 Pt	75
CoO-V_2O_5-Al_2O_3	1.7 Co, 5.8 V	70
Pt-$CoMoO_4$-Al_2O_3	1.1 Pt, 3.4 Co, 5.1 Mo	192
$CoMoO_4$-B_2O_3-Al_2O_3	3.4 Co, 4.7 Mo, 2.2 B	110
Pt-$CoMoO_4$-B_2O_3-Al_2O_3	0.9 Pt, 3.1 Co, 4.0 Mo, 2.4 B	153
HF-Pt-Al_2O_3	0.6 F, 0.6 Pt	200
$CoMoO_4$-Al_2O_3 (girdler)	9.0 Co, 18.5 Mo	26
Gamma-alumina		80

(a) All catalyst samples were crushed and sized to 10-20-mesh particles. Catalyst volume in the bench scale hydrocracker was 80 cc.

compositions and surface areas. The test procedure involved removal of the second-, third-, or fourth- and the sixth-hour products from the high pressure product separator with subsequent analysis of the samples. Coke deposition on the catalyst was determined for each run by air regeneration at 900 to 1050°F with measurement of the carbon dioxide formed. Complete activity and analytical data from these tests are summarized in Table XXI, and the sixth-hour products are compared for yields and compositions.

TABLE XXI

SIX-HOUR HYDROCRACKING TESTS ON OMRE CORE II HIGH BOILER

Reaction Conditions: 900°F, 1000 psig, 1.0 LHSV, 40 wt% high boiler in xylene, 20-30 moles H_2 per mole high boiler, data obtained on sixth hour product sample.

	Core II High Boiler	Catalyst(a)									
		G-67	G-71	G-66	R-2023	G-58	G-55	G-57	G-61	G-72	α-Al_2O_3
High boiler conversion (wt%)(b)		38	29	32	21	35	28	30	34	44	20
Product recovery (wt%)(c)		87	93	92	96	92	89	89	85	78	94
Reclaimed coolant yield (wt%)(d)		29	25	29	23	32	22	25	20	26	19
Selectivity (%)(e)		66	73	70	88	73	58	63	49	44	60
Coke yield (wt% of high boiler charged)(f)		6.0	6.4	5.7	2.9	8.5	8.5	10.4	7.9	5.9	4.2
Coke yield (wt% of catalyst)		14.5	14.2	12.9	5.2	20.2	20.2	25.7	18.4	13.3	10.5
Yields (wt% of high boiler chargcd)											
Low boilers(g)		11.6	7.2	8.2	4.2	8.3	10.7	10.5	15.2	22.0	6.5(h)
Reclaimed coolant	8.7	31.6	28.1	29.3	24.0	32.2	23.5	26.0	24.1	26.5	20.0(h)
Unconverted high boiler	91.3	56.8	64.7	62.5	71.8	59.5	65.8	63.5	60.7	51.5	73.5(h)
Total product analysis											
Sublimate (wt%)(i)		34	27	31	24	35	25	28	23	33	20
Average molecular weight	545	325	367	350	343	348	370	369	366	328	400
C/H atomic ratio	1.42	1.30	1.33	1.28	1.36	1.28	1.31	1.30	1.30	1.24	1.36
Reclaimed coolant analysis(j)											
Alkylbiphenyls		13	12	13	9	17	13	10	26	6	11
Alkylterphenyls		15	7	19	10	14	11	11	14	6	5
Biphenyl		18	23	11	21	16	18	12	26	17	19
Phenanthrene		4	3	4	1	6	3	5	0	0	0
O-terphenyl		12	12	5	11	5	10	5	5	12	10
M-terphenyl		20	26	25	29	23	25	30	14	31	32
P-terphenyl		12	12	12	14	12	14	17	10	15	15
Triphenylene		2	4	9	4	5	5	6	4	3	6
Quaterphenyls		4	1	2	1	2	1	4	1	10	2

(a) Catalysts: G-67, $CoMoO_4$-Al_2O_3; G-71, NiO-Al_2O_3; G-66, Pt-Al_2O_3; R-2023, $CoMoO_4$-Al_2O_3 (girdler); G-58, Pt-$CoMoO_4$-Al_2O_3; G-55, $CoMoO_4$-B_2O_3-Al_2O_3; G-57, Pt-$CoMoO_4$-B_2O_3-Al_2O_3; G-61, HF-Pt-Al_2O_3; G-72, V_2O_5-CoO-Al_2O_3.

(b) Dissappearance of high boiler.

(c) Includes biphenyl and heavier.

(d) Represents reclaimable coolant yield per pass and is calculated here by multiplying product recovery by sublimate.

(e) Selectivity to material boiling between (and including) biphenyl and triphenylene.

(f) Calculated on the complete 6 hours.

(g) Product boiling below biphenyl.

(h) Yield data for sixth hour product do not include coke in the calculation.

(i) Sublimable product at 240°C, 0.20 mm, and 30 min.

(j) Chromatographic analysis of the sublimate.

The same trends were found as described in previous reports on shorter runs. In general, the acidic type catalysts and samples with surface areas above 100 square meters per gram gave extremely high coke yields and poor selectivities. Conversions were quite similar for all the catalysts tested. Some conversion (20 percent) was obtained over unpromoted gamma-alumina. Any

conversion over this material might be considered thermal cracking in the presence of hydrogen since no hydrogen-active component was present. The sublimable product * (reclaimable coolant) contained the same alkylpolyphenyls found in catalytic hydrocracking but in smaller yields. This was additional evidence that alkylated and partially saturated ring structures (enes and dienes) are present in high boiler and that cracking possibly occurred between saturated carbon-carbon bonds in these rings.

The two acid-type catalysts included in this series were the most efficient dual-function catalysts found in previous tests on both model polyphenyls and OMRE high boiler. These were Pt-$CoMoO_4$ on boria-alumina and $CoMoO_4$ on boria-alumina. Conversions and selectivities for these two catalysts in the six-hour tests were similar to those found using the nonacidic catalysts. However, coke yields were excessive (8 to 10 weight percent of high boiler charged). Also, Pt-$CoMoO_4$-Al_2O_3 gave high coke yields (8.5 weight percent) although no acidity was present in the preparation. Thus, the surface area of 192 square meters per gram probably contributed to the high coke yield. The surface area effect was first described in an earlier quarterly report [14]. A plot of coke yields against high boiler conversions (Figure 8) shows the differences between the two types of catalysts. The low-surface-area catalysts (less than 100 square meters per gram) gave coke yields of 5 to 10 weight percent of high boiler charged through a wide range of conversion (20 to 98 percent). It was found that in runs of six hours and longer the coke yield was reduced to about 1.0 (or less) weight percent of high boiler charged after the initial rapid buildup in the first few hours. This low coke rate was approached after at least one volume of high boiler per volume of catalyst had passed through the hydrocracker.

A possible explanation of the surface area effect on coke yield might be a combination of catalyst pore size and hydrogen diffusion to active catalyst sites. A study of surface areas of aluminum [21] indicated a fair correlation between average pore diameter and surface area. A semilog plot is shown in Figure 9, and it can be seen that for surface areas above 100 square meters per gram the average pore diameter is 35 angstroms. Thus, it appears possible that adsorption of polyphenyls higher than hexaphenyls could block these pores and prevent enough hydrogen from diffusing in for saturation of fragments from cracking. Thus, cracked products in a hydrogen-deficient atmosphere may tend to polymerize or condense in the pores, and as an end result would form higher molecular weight material which would block the pores and eventually be analyzed as coke. Coke has been defined as material which did not dissolve in xylene solvent and

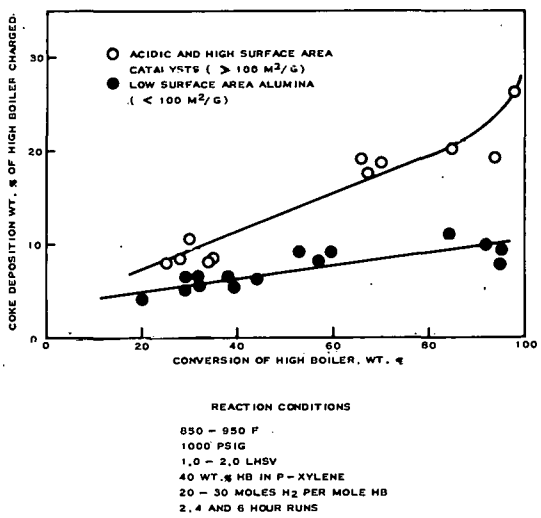

Fig. 8 Effect of catalyst type on coke yield from hydrocracking OMRE Core II high boiler.

* Sublimation at 240°C, 0.2 mm, and 30 min.

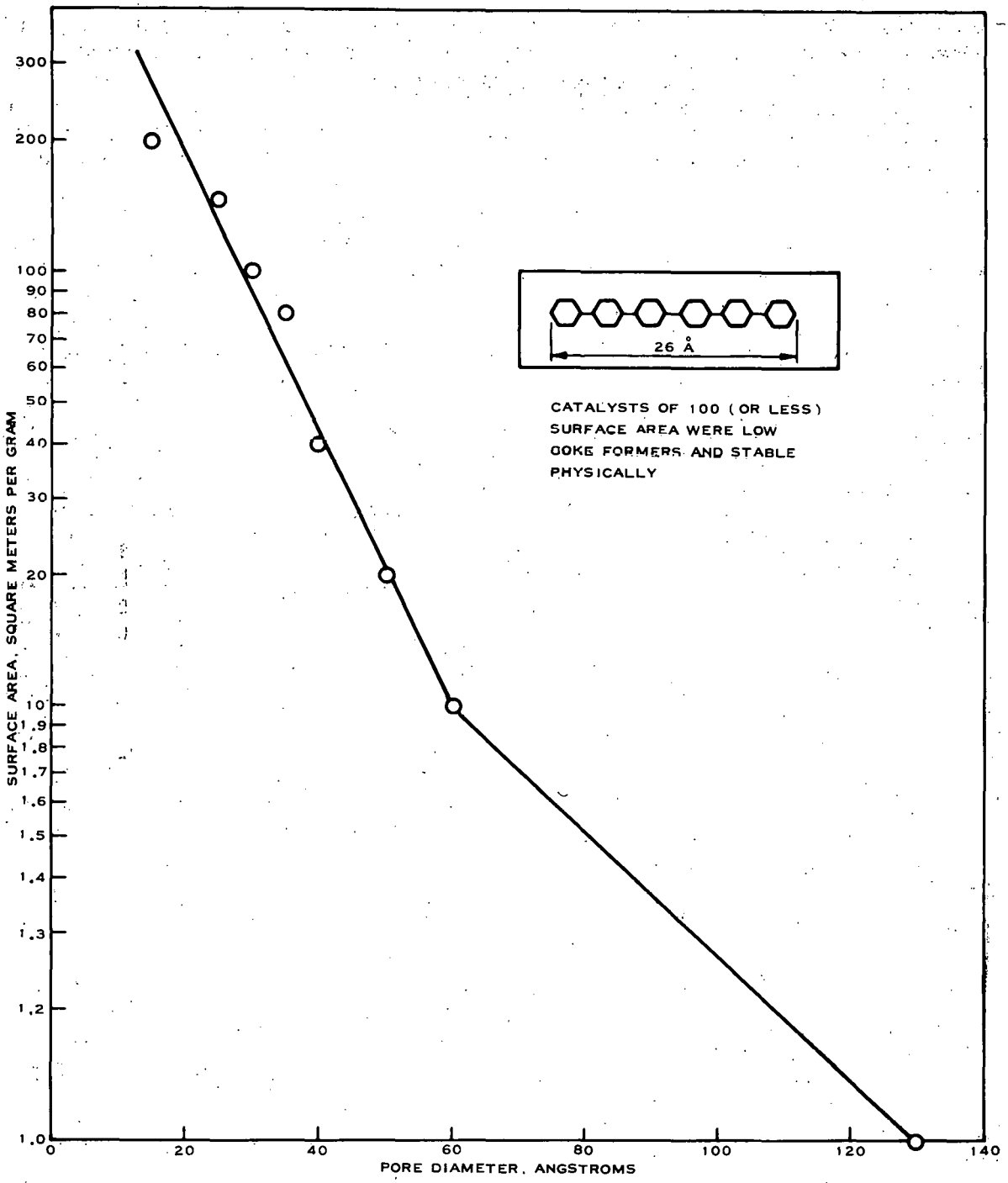

Fig. 9 Surface area - pore size correlation for alumina.

was determined by air burn-off of the catalyst. An alternate explanation of inferior results with high-surface catalysts is a low rate of desorption. These hypotheses may also explain the disintegration observed in several of the $NiO-Al_2O_3$ preparations since nickel is known to be a polymerization catalyst under proper conditions. The low-surface, low-nickel-content catalyst has been found to be quite stable physically and quite effective in high boiler conversion.

Hydrocracking data on OMRE Core II high boiler (Table XXI) indicated that the following catalysts were effective and quite similar in activity, selectivity, and yield:

$CoMoO_4$-Al_2O_3

NiO-Al_2O_3

Pt-Al_2O_3

CoO-V_2O_5-$CoMoO_4$

Upon examination of product compositions (biphenyl - terphenyl range material) it was seen that the NiO-Al_2O_3 catalyst gave more selective hydrocracking of the carbon-carbon bond between phenyl rings. At similar conversions (30 to 40 percent range) reclaimed coolant from runs over NiO-Al_2O_3 contained 73 weight percent biphenyl plus terphenyl while Pt-Al_2O_3 and $CoMoO_4$-Al_2O_3 runs indicated 53 and 60 weight percent, respectively.

In order to differentiate further between these catalysts, runs of approximately 100 hours should be made along with studying the effects of adding recycle stock (unconverted high boiler). Low conversions (20 to 30 percent) should result in high ultimate yields of reclaimed coolant. Higher conversions (above 50 percent) usually have given low yields due to high coke yields and "over cracking" to product lighter than biphenyl.

Experimental work on hydrocracking straight high boiler was concluded with the series of six-hour tests discussed above and summarized in Table XXI.

7.22 Total Coolant Hydrocracking. This method of coolant reclamation was introduced in the last quarterly report [22] and appeared quite attractive. A feature of this method is the elimination of a low vacuum distillation to remove high boiler. In place of the vacuum still only a flash drum would be required when operating with very low high-boiler content. This would partially separate terphenyls, and the remaining terphenyl range material would act as solvent for the high boiler. Experimental data have indicated that the high molecular weight polyphenyls hydrocrack at a much faster rate than the terphenyls. A proposed flow diagram of such a process is shown in Figure 10. An added benefit of this method would be removal of particulate matter, soluble iron contaminants, and hydroaromatics from the coolant stream. These are the precursors of film on nuclear elements proposed by various hypotheses.

Hydrocracking runs have been made on OMRE Core II coolant (23 weight percent high boiler) and synthetic coolant prepared by adding OMRE Core II high boiler to terphenyls. Both NiO-Al_2O_3 and $CoMoO_4$-Al_2O_3 catalysts have been used at conditions of 850 to 950°F, 1000 psig, 0.8 to 2.5 liquid hourly space rate, 40 to 50 weight percent coolant in p-xylene, 25 moles hydrogen per mole high boiler, and run lengths of 2, 4, 6, 12, and 24 hours. Data using $CoMoO_4$-Al_2O_3 were presented in the last quarterly report [22]. Some additional runs have been made on this catalyst in an attempt to optimize yields and determine how catalyst activity declines with time on stream. A 12-hour run indicated no decline in activity during the run, and products actually improved in color, going from brown in the first few hours to light yellow in the last

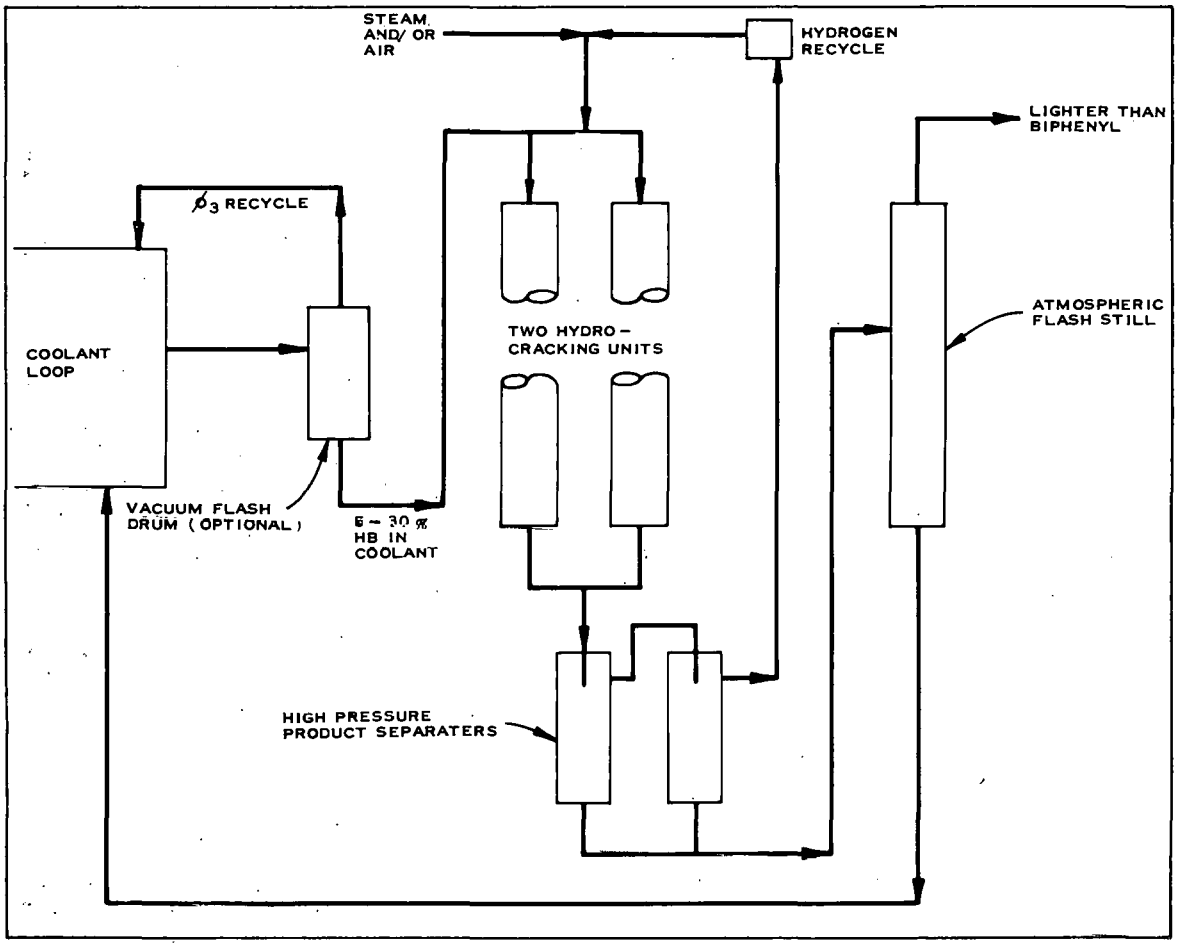

Fig. 10 Simplified flow diagram for total coolant hydrocracking.

part of the run. Coolant yield was 87 percent. Conversion of high boiler was 100 percent throughout the run, but there was a net loss of terphenyls (73 percent in the coolant compared to 67 percent in the total product). The additional 20 percent product yield was accounted for by biphenyl, alkylpolyphenyls, and phenanthrene. However, electron irradiation tests on this product indicated excellent stability. Reaction conditions of 1000 psig, and 0.8 LHSV were possibly too severe, and larger yields would be expected at shorter contact times. The charge rate was held at this value since activity was expected to drop off during the run as found in high boiler hydrocracking tests. The charge contained 50 weight percent p-xylene solvent which gave an actual high boiler throughput of 0.1 LHSV. Molecular weight was reduced from 270 to 225 for the total product, and the sample had the composition as shown in Table XXII.

The analyses of Table XXII were made by micro-sublimation of the biphenyl and heavier products at 240°C, 0.2 mm, and 30 minutes followed by chromatographic analysis of the sublimates. This was carried out using an F and M Model 500 Chromatograph with a lithium chloride (20 percent) on Chromosorb-P packing (5-ft column) programmed from 150 to 350°C at 15°C per minute. All products from coolant hydrocracking runs were analyzed in this manner. The best data obtained in the series of tests on $CoMoO_4$-Al_2O_3 are summarized in Table XXIII.

TABLE XXII

COMPOSITION OF HYDROCRACKED COOLANT

Component	Composition (wt%)	
	Reclaimed Coolant	Core II Coolant
Alkylbiphenyls	3.0	0.2
Alkylterphenyls	9.5	1.2
Biphenyl	8.0	0.5
O-terphenyl	20.7	20.5
M-terphenyl	39.5	37.3
P-terphenyl	13.5	15.0
Triphenylene	2.8	2.6
Quaterphenyls	1.4	0.2
High boiler	0.0	22.5

Several tests were made on $NiO-Al_2O_3$ at high conversion. Most of these were made on a synthetic coolant since the original supply of OMRE Core II (containing 23 weight percent high boiler) was nearly exhausted. The blend was made by mixing the terphenyl isomers with Core II high boiler to give a sample which was similar to that used in tests of $CoMoO_4-Al_2O_3$. Properties of these samples are listed in Table XXIV along with results from runs over $NiO-Al_2O_3$. Data from four runs are shown. The catalyst was air-regenerated between each run, and the last run was made in several segments with the reactor shut in overnight at run conditions between each segment. In general, $NiO-Al_2O_3$ catalyst gave lower product yields than did $CoMoO_4-Al_2O_3$. Inspection data on the products indicated that this was possibly due to higher activity for cracking the carbon-carbon bonds between rings, and more benzene was found in the total product. However, this resulted in higher selectivity for terphenyl yields, and alkylpolyphenyl yields were extremely low when compared to products from hydrocracking over $CoMoO_4-Al_2O_3$. Yield data from these two catalysts are compared in Table XXV which show these differences in selectivities. The products were from the sixth hour of operation at 100 percent high boiler conversion.

Other runs made using $NiO-Al_2O_3$ were with the synthetic coolant rather than the actual Core II coolant and may not be directly comparable to runs over $CoMoO_4-Al_2O_3$. Three runs of 6, 12, and 15 hours are summarized in detail in Table XXIV. The data indicate some loss in activity with increasing on-stream time. There was very little change in conversion when the charge rate was altered in the 1.0 to 2.1 LHSV range. In the 12-hour run (Run 11434-20) it was of interest to follow the changes in product composition by comparison of chromatograms of total reactor effluents. Figures 11, 12, 13, and 14 show these changes for the 0 to 2-, 4 to 6-, 7 to 8-, and 11 to 12-hour products. The

TABLE XXIII

CATALYTIC HYDROCRACKING OF TOTAL COOLANT

Conditions: $CoMoO_4$-Al_2O_3, 1000 psig, 900°F, 1.0 LHSV, 20 mole hydrogen per mole coolant, six-hour run.

	OMRE Core II Coolant	
	Before Hydrocracking	After Hydrocracking
Conversion of high boiler (wt%)		96
Coolant yield (wt%)		95
Yields (wt% of coolant charged)		
Lighter than biphenyl		3
Biphenyl	< 1	5
Alkylpolyphenyls	2	9
O-terphenyl	20	22
M-terphenyl	36	39
P-terphenyl	15	13
Triphenylene	3	3
Quaterphenyls	< 1	3
High boilers	23	1
Coke		2
Coolant molecular weight (average)	270	223
Radiolytic stability(a)		
Polymer (wt%)	24	21
Gas (cc/watt-hr)	0.9	2.8

(a) Relative to Santowax OMP total dosage of 8×10^9 rads at 650°F under the Linac.

major changes were in biphenyl and an unidentified component (probably an alkylterphenyl).

Data from five segments of the extended 15-hour run (Run 11434-23) are shown in Table XXIV. Since the oil-saturated catalyst bed was shut in under reaction conditions overnight between each segment, a higher than normal coke yield value was obtained. However, the run demonstrated that good catalyst activity was maintained even after 25 weight percent coke was deposited on the catalyst (weight percent of catalyst). The last hour on stream still gave 90 percent conversion of high boiler and a product with an average molecular

TABLE XXIV

COOLANT HYDROCRACKING RUNS USING $NiO-Al_2O_3$ CATALYST

Reaction Conditions: 900°F, 1000 psig, 40 wt% coolant in p-xylene, 25 moles hydrogen per mole coolant.

	Core II Coolant	Run 11434-16	Synthetic Coolant	Run 11434-17		Run 11434-20	Run 11434-23				
LHSV		1.0		1.0		1.0	2.0	1.8	2.1	2.4	1.0
Run length (hr)		5		6		12	(——— 15[a] ———)				
Hours sampled		4-5		2-4	5-6	11-12	3-4	5-6	6-7	9-10	14-15
High boiler conversion (wt%)[b]		100		100	95	95	92	100	100	87	90
Reclaimed coolant yield (wt%)[c]		83		82	87	84	91	87	88	94	91
Product analysis											
Sublimate (wt%)[d]		100		100	99	100	89	100	100	97	98
Average molecular weight	270	237		221	232	227	224	221	229	229	231
C/H atomic ratio	1.32	1.26		1.19	1.28	1.24	1.22	1.21	1.22	1.22	1.23
Yields (wt% of coolant charged)											
Low boilers[e]		14.7		15.3	10.1	14.7	6.9	10.9	9.9	4.4	6.6
Alkylbiphenyls	0.2	0.5			0.3	0.3	0.4	0.4		0.3	1.0
Alkylterphenyls	1.2	0.5			0.5	1.6	1.2	1.1		0.5	0.9
Biphenyl	0.5	3.5			3.4	2.1	2.0	2.2		1.5	2.0
O-terphenyl	20.5	25.0	21.5		23.9	23.0	25.0	24.5		26.6	25.9
M-terphenyl	37.3	38.2	39.1	(82.2)[f]	40.4	44.0	41.7	41.3	(88.0)[f]	41.4	42.1
P-terphenyl	15.0	14.3	15.8		17.0	11.3	17.3	14.4		18.6	16.0
Triphenylene	2.6	0.2			0.7	0.2	0.3	0.3		0.3	0.3
Quaterphenyls	0.2	0.6			0.0	1.1	1.3	1.1		1.3	0.9
High boiler	22.5	0.0	23.6	0.0	1.2	0.0	1.8	1.7	0.0	3.0	2.2
Coke		2.5		2.5	2.5	1.8	2.1	2.1	2.1	2.1	2.1

(a) Fifteen-hour run was not continuous.
(b) Disappearance of high boiler.
(c) Total product yield including unconverted high boiler.
(d) Sublimable product at 240°C, 0.2 mm, and 30 min.
(e) Product boiling lower than biphenyl.
(f) Complete analysis was not run.

TABLE XXV

HYDROCRACKING CORE II COOLANT

	Wt% of Coolant Charged	
Yields	$CoMoO_4-Al_2O_3$	$NiO-Al_2O_3$
Lighter than biphenyl	9.3	14.7
Alkylbiphenyls	2.7	0.5
Alkylterphenyls	6.0	0.5
Biphenyl	5.5	3.5
O-terphenyl	20.3	25.0
M-terphenyl	37.5	38.2
P-terphenyl	13.0	14.3
Triphenylene	2.6	0.2
Quaterphenyls	0.6	0.6
High boiler	0.0	0.0
Coke	2.5	2.5

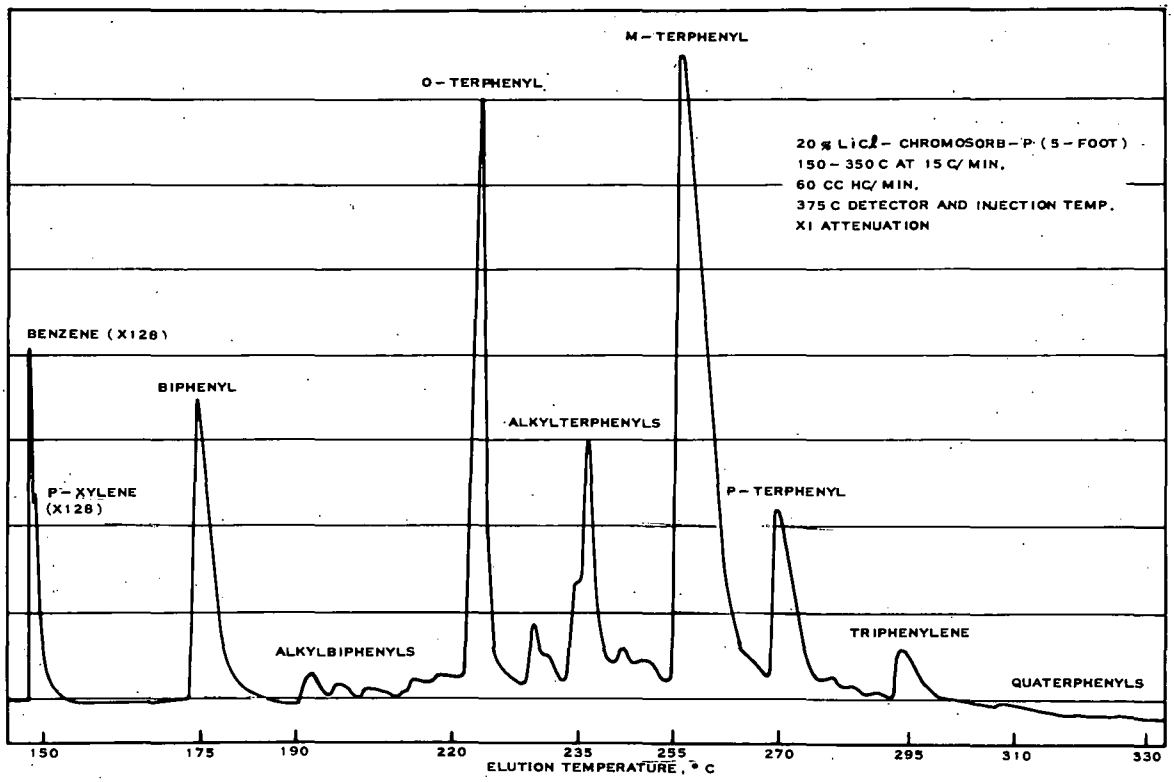

Fig. 11 Product from hydrocracking used coolant over NiO - Al_2O_3 catalyst (0 to 2 hr).

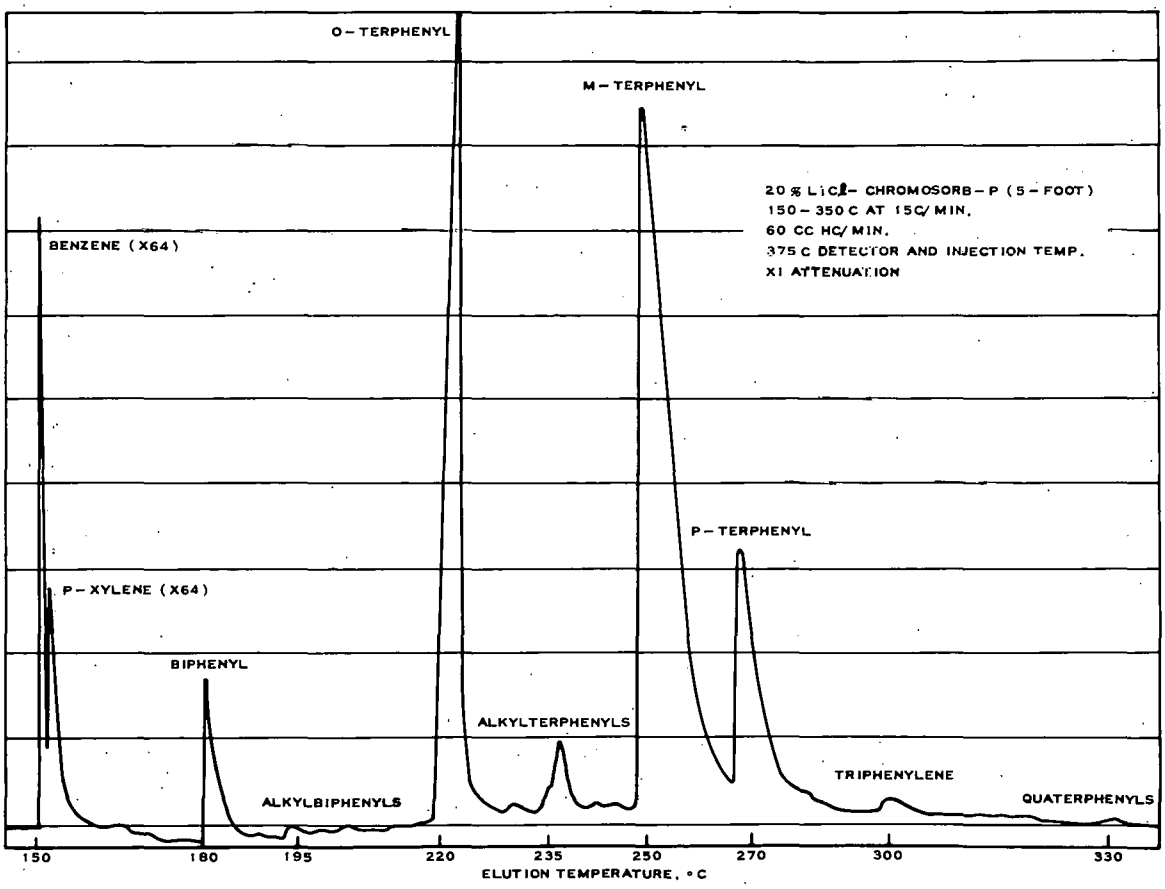

Fig. 12 Product from hydrocracking used coolant over NiO - Al_2O_3 catalyst (4 to 6 hr).

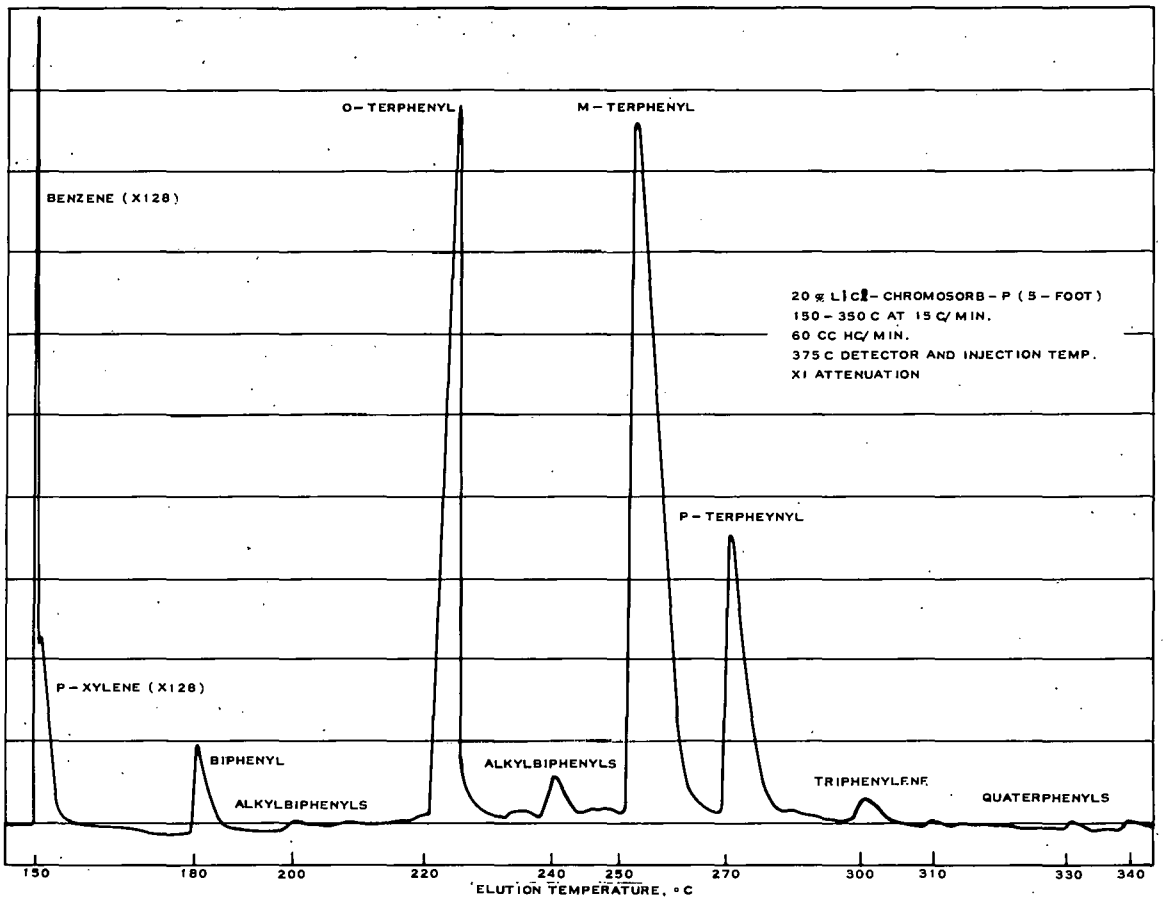

Fig. 13 Product from hydrocracking used coolant over NiO - Al_2O_3 catalyst (7 to 8 hr).

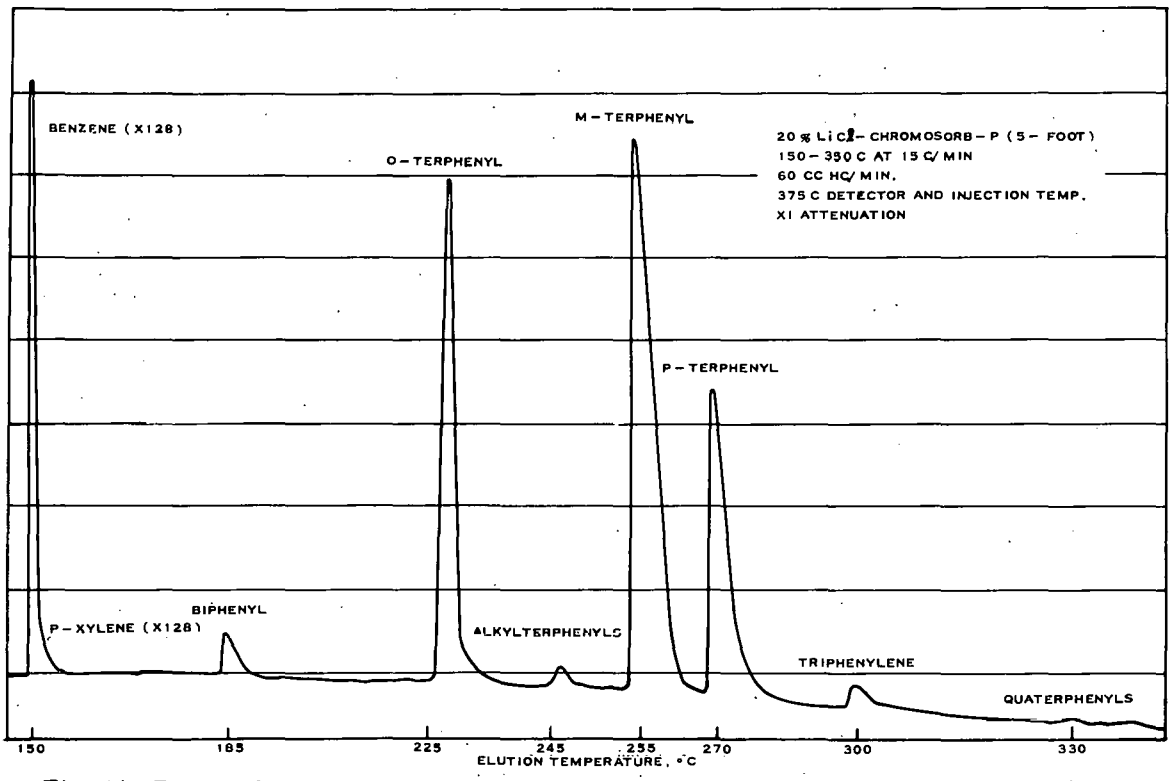

Fig. 14 Product from hydrocracking used coolant over NiO - Al_2O_3 catalyst (11 to 12 hr).

weight of 231. An increase in total charge rate from 1.0 to 2.4 LHSV had very little effect on conversion or product yields. Conversions were in the range 87 to 100 percent, and coolant yields were 87 to 94 percent.

Experimental work on hydrocracking coolant has been very encouraging in that high conversion of high boiler can be obtained selectively with very little destruction of the terphenyls in the coolant. Catalyst activity declined only slightly up to a total charge of 25 volumes per volume of catalyst. Yields were disappointing but were still higher than the ultimate yields predicted for the low conversion with recycle process for hydrocracking straight high boiler. Higher yields could be predicted for higher charge rates of possibly 2.0 to 5.0 LHSV, but conversion would be decreased. This could be tolerated if the end product had good stability towards thermal and radiolytic effects and had low film-forming tendencies.

7.23 Solvent-Free Hydrocracking. In all the laboratory-scale hydrocracking studies there has been concern as to the role of solvent. It has been necessary to employ solvent in all tests on high boiler and coolant since pumping rates were quite low (0.5 to 3.0 milliliters per minute), and the charge would not otherwise remain fluid. Admittedly, there are numerous arguments against studying the process with solvent present because a plant scale hydrocracking unit would undoubtedly operate without solvent. However, by using solvent the bench scale hydrocracker has been in service continuously which made possible a broad survey of catalysts, operating conditions, and feedstocks in a minimum amount of time.

In an attempt to determine the differences between charge stock diluted with solvent (xylene) and solvent-free charge stock, a series of tests has been initiated using a synthetic coolant blend of high boiler dissolved in Monsanto DOM* which is fluid at room temperature. Preliminary results indicate improvements in product yields and greatly decreased coke yields. The lower coke yields may be attributed to the higher partial pressure of hydrogen inside the hydrocracker as compared to a charge stock with 50 to 60 percent solvent. The present study includes the study of both Core II and Core III-A high boilers with varied concentrations in DOM.

7.24 Radiolytic Stability Experiments. Two additional electron irradiations were made on reclaimed coolant samples under the Linac (electron accelerator). In each irradiation three coolant samples were run simultaneously with Santowax OMP as the control. Relative polymer and gas yields were determined, and some chromatographic data, molecular weights, and carbon-hydrogen ratios were obtained. A complete summary is given in Table XXVI. A description of the samples tested is as follows:

Sample F - Hydrocracked OMRE Core II coolant (12-hour run)

Sample G - Distilled product from hydrocracking Core II high boiler in a 24-hour run

Sample H - Hydrocracked OMRE Core II coolant (6-hour run)

Sample I - Distilled product from 30 to 40 percent conversion of Core II high boiler.

---

* Biphenyl-o-terphenyl-m-terphenyl eutectic.

TABLE XXVI

RADIOLYTIC STABILITY OF RECLAIMED COOLANTS FROM HYDROCRACKING(a)

	Santowax OMP		Sample F		Sample G		Sample I		Santowax OMP		Sample F		Sample G		Sample H	
Dosage (rads x 10^8)	7.6		7.6		7.6		7.6		4.8		4.8		4.8		4.8	
Radiolytic polymer (wt%)(b)		23.8		21.0		15.9		16.7		17.1		15.5		10.6		14.6
Radiolytic gas (cc/watt-hr)		0.85		2.81		2.81		2.51		0.10		0.40		0.40		0.25
Relative polymer formation(c)		1.0		0.88		0.67		0.70		1.0		0.91		0.62		0.85
Relative gas yield(c)		1.0		3.3		3.3		3.0		1.0		4.0		4.0		2.5
Analytical Data																
Average molecular weight	230	262	224	251	218	241	220	245	230	252	224	246	218	230	223	246
C/H atomic ratio	1.29	1.30	1.14	1.24	1.20	1.22	1.22	1.28	1.29	1.30	1.19	1.22	1.20	1.21	1.22	1.24
Composition (wt%)(d)																
Alkylbiphenyls		0.0	3.0	2.8	8.3	7.6	6.5	6.0		(e)	3.0	2.0	8.3	(e)	2.7	1.5
Alkylterphenyls		0.3	9.5	6.3	13.7	12.7	10.1	9.1			9.5	5.7	13.7		6.0	4.9
Biphenyl	0.4	0.2	8.0	5.4	10.1	8.1	9.5	5.6			8.0	5.8	10.1		5.6	3.7
Phenanthrene		0.0	0.0	0.0	1.4	1.8	3.3	1.8			0.0	0.0	1.4		0.0	0.0
O-terphenyl	11.9	6.2	21.3	15.2	8.0	4.4	5.9	5.3			21.3	20.1	8.0		24.7	21.5
M-terphenyl	55.0	41.7	39.5	31.6	28.7	23.9	23.2	19.4			39.5	36.3	28.7		41.5	37.7
P-terphenyl	32.5	27.2	13.5	11.5	15.7	13.5	14.9	12.7			13.5	11.2	15.7		13.7	12.0
Triphenylene	0.2	0.5	2.8	3.6	4.6	8.7	10.9	9.5			2.8	2.2	9.6		3.2	2.6
Quaterphenyls		0.4	1.4	1.1	4.5	3.4	15.7	13.9			1.4	1.2	4.5		2.6	1.5
Residue	0.0	23.8	0.0	21.0	0.0	15.9	0.0	16.7			0.0	15.5	0.0		1.0	14.6

(a) Data in right hand columns are after irradiation.

(b) Polymer determined by micro-sublimation technique.

(c) Relative to Santowax OMP data.

(d) Chromatographic analysis of sublimates using LiCl on Chromosorb-P column, programmed 150 to 350°C at 15°C per min.

(e) Data not available.

An observation from recent electron irradiations was that the samples containing the high concentration of alkylpolyphenyls gave lower relative polymer yields. Run conditions have all been 625 to 650°F for 7 to 8 hours with total dosages on the order of 10^9 rads. Polymer values varied from 0.67 to 0.91 relative to the Santowax OMP control. To illustrate this trend a plot of recent data on various reclaimed coolant samples is shown in Figure 15. In all, 18 samples of reclaimed coolant and total hydrocracked product have been irradiated, and all gave less polymer formation than the control. Samples which initially contained material boiling above quaterphenyls were not included in the correlation of Figure 15. Further stability tests are intended to be performed on reclaimed coolant samples in both PCFT and rocking cell experiments.

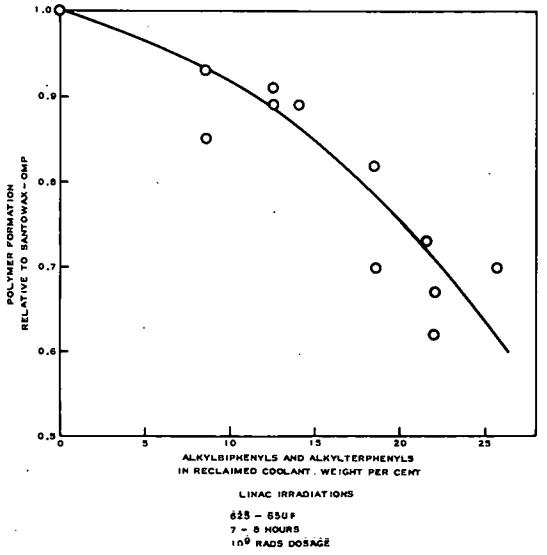

Fig. 15 Effect of alkyl content in reclaimed coolant on relative radiolytic stability.

7.3 Economic Evaluation of Reclamation of High Boiler

A preliminary process design and economic analysis has been completed for plants to produce usable coolant by hydrocracking high boiling polymers from damaged coolant, and by hydrocracking the high boilers in used coolant without separation by distillation. Data for the plant hydrocracking high boiler are taken from the 24-hour run described in the previous quarterly [23]. Data for the plant hydrocracking used coolant are taken as an average of several runs described earlier in this report. These data are summarized in Table XXVII.

Case I - 50,000 lb/Catalyst Day of High Boiler

As a basis for this evaluation, it was assumed that the hydrocracking plant would be built large enough to convert 50,000 pounds per day of high boiler. This amount of high boiler would be produced in a 1000-megawatt thermal reactor if high boiler is formed at a rate of 50 pounds per megawatt-day.

The total investment for the hydrocracking plant is estimated to be $1,700,000. This is for a battery-limits plant, and includes the cost of the initial charge of catalyst. Amortization was assumed to be seven years, straight line. Labor rates and utility rates were based on a midwestern location, but would not vary greatly for other locations.

On this basis the direct manufacturing costs are estimated to be $458,000 per year, which is 3.1 cents per pound of reclaimed coolant. The indirect manufacturing costs including amortization are estimated to be $327,000 per year, or 2.2 cents per pound of reclaimed coolant. This gives a total manufacturing cost of 5.3 cents per pound of reclaimed usable coolant.

If the price of fresh terphenyls is reduced to 10 cents per pound, this reclamation plant would show a gross income of $686,000 per year, or a

TABLE XXVII

PREMISES FOR ECONOMIC EVALUATION

	Feedstock	
	High Boiler(a)	Coolant (30% high boiler)(b)
Catalyst used	$CoMoO_4$-Al_2O_3	$CoMoO_4$-Al_2O_3
Reactor pressure (psig)	1000	1000
Reactor temperature (°F)	900	900
Charge rate (volume high boiler/volume catalyst/hr	0.40	0.15
Conversion of high boiler (%)	20	99
Reclaimed coolant yield from high boiler (%)	80	82
Hydrogen consumption (standard cubic ft/barrel)	150	200
Hydrogen charge rate (mole H_2/mole high boiler)	25	100

(a) Data for high boiler hydrocracking taken from 24-hr run described in a previous report [23].

(b) Data for used coolant hydrocracking taken as average of several runs described earlier in this report.

net income of $343,000 assuming a 50 percent income tax. Adding the amortization credit of $243,000 per year gives an amount applicable to plant payout of $586,000 per year. This would return the $1,700,000 investment in 2.9 years.

Case II - 25,000 lb/Catalyst Day of High Boiler

If coolant damage is reduced to 25 pounds of high boiler per megawatt day, the hydrocracking plant associated with a 1000-metawatt thermal reactor would have a conversion rate of 25,000 lb/catalyst day of high boiler. The investment for this case is estimated to be $1,125,000, and other assumptions were the same as Case I. On this basis, the direct manufacturing costs are estimated to be $385,000 per year, or 5.3 cents per pound of reclaimed coolant. The indirect manufacturing costs including amortization are estimated to be $218,000 per year, or 3.0 cents per pound. This gives a total manufacturing cost of 8.3 cents per pound of reclaimed usable coolant.

With fresh coolant at 10 cents per pound, this plant would show a gross income of $124,000 per year, or $62,000 per year after the 50 percent income tax. With the $161,000 per year amortization credit, the amount applicable to payout is $223,000 per year, which will pay out the $1,125,000 plant investment in 5.0 years.

Case III - Hydrocracking 25,000 lb/Catalyst Day High Boiler in Used Coolant

Recent hydrocracking work has been directed toward hydrocracking the high boiler in used coolant without distillation. This process has demonstrated several advantages over hydrocracking neat high boiler, including the elimination of a distillation step, improved yields, lower investment, lower operating

costs, and less catalyst required. For this plant, the investment is estimated to be $885,000; amortization rate, labor, utilities were the same as previous cases. On this basis, the direct manufacturing costs are estimated to be $354,000 per year, or 4.7 cents per pound of reclaimed coolant. The indirect costs including amortization are estimated to be $172,000 per year, or 2.3 cents per pound. This gives a total manufacturing cost of 7.0 cents per pound of reclaimed usable coolant.

With fresh coolant at 10 cents per pound, this plant would show a gross income of $224,000 per year, or $112,000 per year after taxes. With the $126,000 amortization credit, the amount applicable to payout is $238,000 per year, which will pay out the $885,000 plant investment in 3.7 years.

For all three cases presented, no credit was taken for eliminating the cost of high boiler disposal. For Case III no credit was taken for reduced investment or reduced operating cost with the elimination of the distillation step. The economics of the three cases are summarized in Table XXVIII.

TABLE XXVIII

ECONOMICS OF HYDROCRACKING

	Investment ($)	Operating Costs (¢/lb Reclaimed Coolant)		Ultimate Yield (%)	Payout (yr)
		Total	Direct		
Case I					
50,000 lb/CD high boiler	1,700,000	5.3	3.1	80	2.9
Case II					
25,000 lb/CD high boiler	1,125,000	8.3	5.3	80	5.0
Case III					
25,000 lb/CD high boiler in used coolant	885,000	7.0	4.7	82	3.7

As a full size commercial power reactor comes closer to realization, the hydrocracking process should be developed further by pilot plant operation. Possible process simplifications could reduce the cost of a full-scale plant if shown to be operable on a pilot plant scale. Such factors as catalyst life and hydrogen consumption would need to be more definite before a firm plant design could be prepared.

II. EOCR EXPERIMENTAL PROJECTS

1. LOOPS

1.1 Coolant Technology Loop and Fuel Technology Loop (R. S. Kern, F. K. Clements, L. L. Porter)

Close liaison with AEC-IDO and Fluor Corp on the design of the Coolant Technology Loop (CTL) and Fuel Technology Loop (FTL) continued. The review of the Title II design of the FTL and CTL was essentially completed, and the review of the Title II design of the loop handling equipment was nearing completion. Loop construction progressed to about 13 percent completion.

1.11 Design Liaison. Phillips Petroleum Co was represented at one EOCR loop design review conference with AEC-IDO and Fluor Corp during the quarter. During this meeting, which was held May 9-11, 1962, discussion centered around the following major items:

(a) Loop handling procedures and equipment

(b) FTL and CTL instrumentation leadout

(c) FTL and CTL in-pile tube test specifications

Prior to this meeting, a Fluor representative had spent a week at the NRTS discussing Phillips' handling equipment comments and rewriting portions of the loop handling procedures.

1.12 Construction. During this quarter, the construction schedule for the loops was revised. The loop construction is to be completed February 28, 1963. At the end of the quarter, the construction was considered to be 13 percent completed. Major construction efforts during the quarter were centered around the following:

(a) Tank storage annex

(b) Cooling tower

(c) Dowtherm area

(d) CTL and FTL cubicle walls and floors

(e) Routing of utilities

1.2 Component Development Test Loop (E. R. Oetken, R. G. Young)

During the present quarter the construction of the Component Development Test Loop (CDTL) was completed with the installation of the primary circulation pump and automatic fire protection system. Deficiencies noted in the last quarterly report were corrected. The high loop pressure drop across the turbine flowmeter section of the loop was found to be caused by a nonstandard globe valve containing small ports before and after the valve seat. The turbine

flowmeter continued to function erratically after being cleaned and will be returned to the manufacturer for check-out and recalibration. The failure of the surge tank heaters, as suspected, was found to be caused by shorted leads.

The single-stage Chempump (Model CFGH 1-1/2 - 3/4S) has been modified by the manufacturer and reinstalled in the CDTL, which has been operated exclusively for the pump test during this quarter. Operation of the pump indicates that the high flow of the pumped fluid through the motor portion of the pump has been corrected. Additional reliability testing is scheduled.

The maximum organic temperature achieved in the pump tests was 600°F. No further difficulties in loop operation have been experienced. The eutectic mixture of biphenyl and terphenyl that freezes at approximately 50°F is still being used in the primary system to prevent loop freeze-up during this initial period of loop operation. This material has been analyzed chromatographically as follows:

Light ends	2.4%	M-terphenyl	20.0%
Biphenyl	26.0%	P-terphenyl	0.8%
O-terphenyl	49.0%	Others	1.8%

Viscosity of the eutectic was found to range between 18.7 centistokes at 100°F and 0.59 centistokes at 400°F.

2. EXPERIMENTS

2.1 Initial Core Instrumentation (D. R. Conkling, R. G. Young)

2.11 Thermocouple Locations. The Fuel Technology Loop of the EOCR will be used initially to establish upper power limits for the EOCR. The initial approach-to-power and operation test utilizes a standard EOCR control rod fuel follower in the FTL in-pile tube as part of the initial core loading.

The test is divided into two phases. Phase I is essentially a short-duration experiment to establish a maximum operating power level for the EOCR based on the maximum fuel plate temperature. Phase II is an experiment to monitor film formation on the fuel plates. The FTL sample and eight core driver elements, instrumented with thermocouples, have been selected to provide data necessary to accomplish the objectives of the test.

Selection of the driver elements to be instrumented with thermocouples was based on: (a) monitoring one element for each of the six driver flow patterns, (b) monitoring each quadrant of the core, (c) obtaining temperature for a complete range of flux-flow combinations, (d) instrumenting the hottest element, and (e) control rod programming. Figure 16, a plan view of the core, shows the location of the instrumented elements.

Because of the significance of the maximum fuel plate temperature in the initial approach-to-power and operation test, the core has been instrumented heavily in the areas of calculated maximum temperatures. The axial distribution of heat generation in an EOCR fuel element is approximated by a chopped cosine

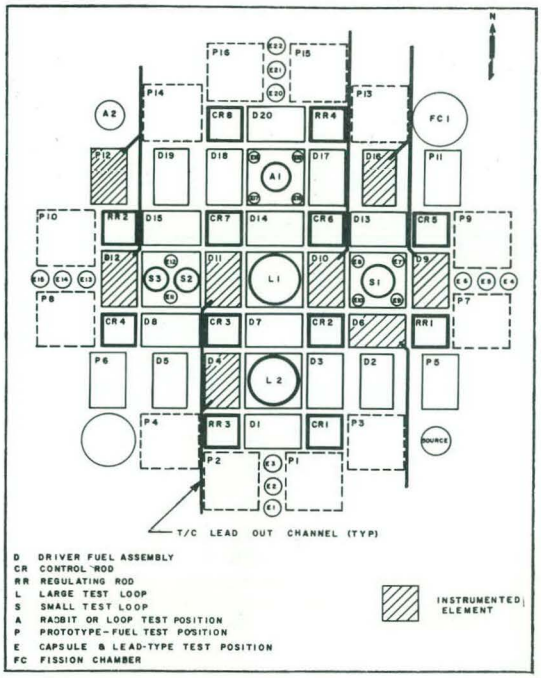

Fig. 16 Location of instrumented elements showing spider leadout pattern.

with a peak-to-average ratio of 1.4. Figure 17 is a set of normalized curves of fuel plate temperature based on this approximation. The curves show that the rise of coolant temperature through the channel has an appreciable effect on the maximum plate temperature. The "flatness" of the curves in the area

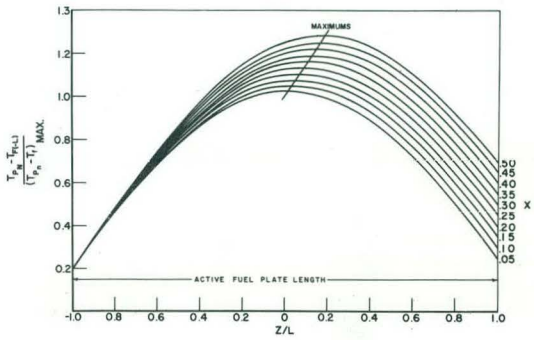

Fig. 17 Normalized fuel plate temperature profile.

of the maximum temperature indicates that axial thermocouple location is not critical, and thermocouples in the vicinity of the maximum should read near the maximum plate temperature.

Thermocouples on both the FTL sample and the core driver elements will be located on the outer plates in order that the leads may be brought outside of the element box as near the point of attachment as possible. This will minimize the hydraulic and thermal disturbance that thermocouple leads would cause in the channel.

The maximum plate temperature for the FTL sample, based on the predicted power distribution, is expected to occur near the corners of the outer plates. The leadout problem associated with the driver elements limits the thermocouple location to the inner corners of their outer plates. Calculations show that thermocouples should be positioned 0.25 inch from the edge of the meat for both the FTL sample and the driver elements. Figures 18 and 19 show the proposed thermocouple locations for the FTL sample and driver elements.

2.12 Calculated Temperature of the Hot Thermocouple for Initial Reactor Operation. The calculated temperature for the hot thermocouple on the instrumented elements is shown in Figure 20. This calculation is intended only to predict the approximate range of temperatures to be expected during initial reactor operation and is based on: (a) calculated core power densities, (b) design flow in the elements, (c) accepted heat transfer coefficients, (d) the nominal dimensions of the channel and fuel plates, and (e) the axial distribution of heat flux given by a chopped cosine with a peak-to-average ratio of 1.4.

The calculation for a driver element in location D-11 is illustrated on page 66.

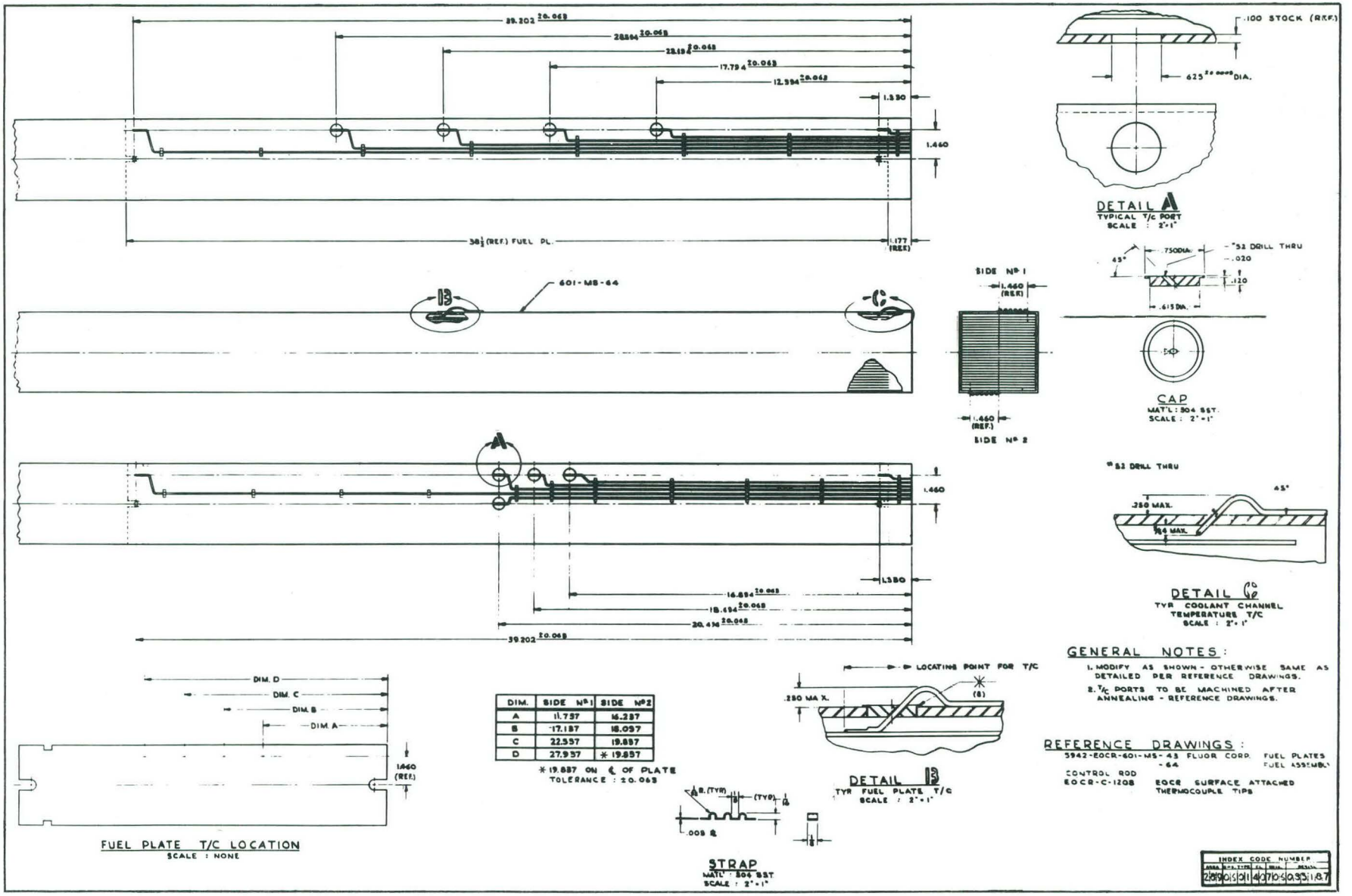

DIM.	SIDE No. 1	SIDE No. 2
A	11.737	16.237
B	17.187	18.037
C	22.537	19.887
D	27.937	* 19.857

* 19.887 ON ℄ OF PLATE
TOLERANCE : ±0.063

Fig. 18 FTL sample thermocouple locations.

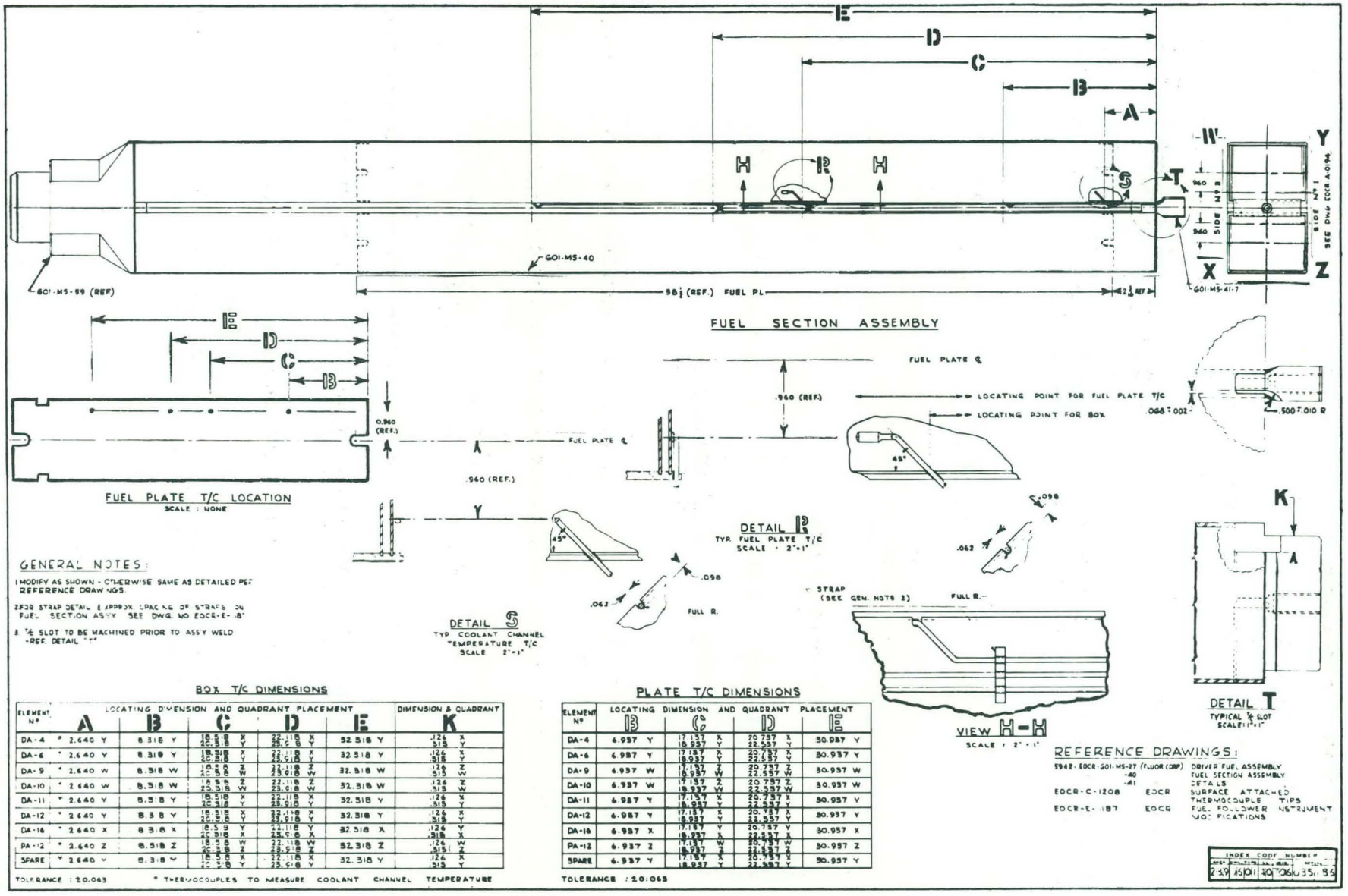

BOX T/C DIMENSIONS

ELEMENT Nº	LOCATING DIMENSION AND QUADRANT PLACEMENT A	B	C	D	E	DIMENSION & QUADRANT K
DA-4	* 2.640 Y	8.318 Y	18.518 X 20.318 Y	22.118 X 25.918 Y	32.318 Y	.126 X .318 Y
DA-6	* 2.640 Y	8.318 Y	18.518 X 20.318 Y	22.118 X 25.918 Y	32.318 Y	.126 X .318 Y
DA-9	* 2.640 W	8.318 W	18.518 Z 20.318 W	22.118 Z 25.918 W	32.318 W	.126 Z .318 W
DA-10	* 2.640 W	8.318 W	18.518 Z 20.318 W	22.118 Z 25.918 W	32.318 W	.126 Z .318 W
DA-11	* 2.640 Y	8.318 Y	18.518 X 20.318 Y	22.118 X 25.918 Y	32.318 Y	.126 X .318 Y
DA-12	* 2.640 Y	8.318 Y	18.518 X 20.318 Y	22.118 X 25.918 Y	32.318 Y	.126 X .318 Y
DA-16	* 2.640 X	8.318 X	18.518 Y 20.318 X	22.118 Y 25.918 X	32.318 X	.126 Y .318 X
PA-12	* 2.640 Z	8.318 Z	18.518 W 20.318 Z	22.118 W 25.918 Z	32.318 Z	.126 W .318 Z
SPARE	* 2.640 Y	8.318 Y	18.518 X 20.318 Y	22.118 X 25.918 Y	32.318 Y	.126 X .318 Y

TOLERANCE : ±0.063 * THERMOCOUPLES TO MEASURE COOLANT CHANNEL TEMPERATURE

PLATE T/C DIMENSIONS

ELEMENT Nº	LOCATING DIMENSION AND QUADRANT PLACEMENT B	C	D	E
DA-4	6.937 Y	17.137 X 18.937 Y	20.737 X 22.537 Y	30.937 Y
DA-6	6.937 Y	17.137 X 18.937 Y	20.737 X 22.537 Y	30.937 Y
DA-9	6.937 W	17.137 Z 18.937 W	20.737 Z 22.537 W	30.937 W
DA-10	6.937 W	17.137 Z 18.937 W	20.737 Z 22.537 W	30.937 W
DA-11	6.937 Y	17.137 X 18.937 Y	20.737 X 22.537 Y	30.937 Y
DA-12	6.937 Y	17.137 X 18.937 Y	20.737 X 22.537 Y	30.937 Y
DA-16	6.937 X	17.137 Y 18.937 X	20.737 Y 22.537 X	30.937 X
PA-12	6.937 Z	17.137 W 18.937 Z	20.737 W 22.537 Z	30.937 Z
SPARE	6.937 Y	17.137 X 18.937 Y	20.737 X 22.537 Y	30.937 Y

TOLERANCE : ±0.063

REFERENCE DRAWINGS:

5942-EOCR-S01-MS-27 (FLUOR CORP)		DRIVER FUEL ASSEMBLY
-40		FUEL SECTION ASSEMBLY
-41		DETAILS
EOCR-C-1208	EOCR	SURFACE ATTACHED THERMOCOUPLE TIPS
EOCR-E-187	EOCR	FUEL FOLLOWER INSTRUMENT MODIFICATIONS

INDEX CODE NUMBER

239	05001	307060	35.85		

Fig. 19 Driver element thermocouple locations.

Element power for core power of 1 Mw

$$= 6.14 \left| \frac{\text{watts}}{\text{cc}} \right. \times 10290 \left| \text{cc} \right. \times 3.413 \left| \frac{\text{Btu}}{\text{hr-watt}} \right.$$

$$= 215{,}633 \text{ Btu/hr}$$

Average heat flux based on 67.7 ft^2 of heat transfer surface per element

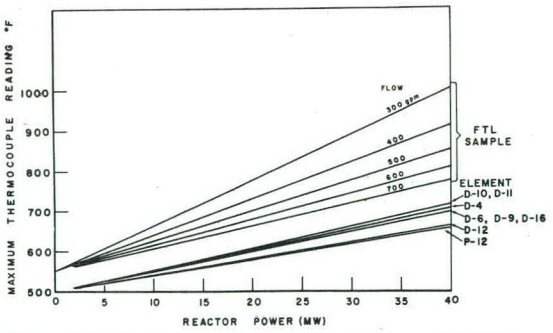

Fig. 20 Maximum thermocouple temperature - instrumented elements.

$$= 215{,}633 \left| \frac{\text{Btu}}{\text{hr}} \right. \times 1/67.7 \left| \frac{1}{ft^2} \right. = 3185 \text{ Btu/hr-ft}^2$$

Heat flux at the hot thermocouple

$$= 3185 \left| \frac{\text{Btu}}{\text{hr-ft}^2} \right. \times 2.24 \left| \frac{\text{Peak heat flux}}{\text{Average heat flux}} \right. = 7134 \text{ Btu/hr-ft}^2$$

The film heat transfer coefficient, based on 970-gpm flow (v_z = 18.96 ft/sec), is h = 1430 Btu/hr-ft^2 °F.

From Newton's Law of Cooling the maximum temperature difference between fluid and plate is

$$(T_p - T_f)_{max} = \frac{q'' \text{ max}}{h} = \frac{7134}{1430} = 5°F$$

A simple expression for the temperature along the fuel plate is shown below.

Plate temperature = inlet coolant temperature + film temperature difference + temperature rise of coolant.

From this relationship the following equation may be obtained:

$$\frac{T_p - T_{f(-L)}}{(T_p - T_f)_{max}} = \frac{T_p - T_f}{(T_p - T_f)_{max}} + X \frac{T_f - T_{f(-L)}}{T_{f(L)} - T_{f(-L)}} \qquad (1)$$

Where,

T_p = Temperature of the plate (°F)

T_f = Temperature of the fluid (°F)

$X = \frac{2h\ (1 + N)}{a\ s\ \rho\ v_z\ c} \sin aL$ (dimensionless)

h = Film heat transfer coefficient (Btu/hr-ft^2 °F)

a = Constant for EOCR driver (= 1.37/1.5 ft^{-1})

s = Channel thickness (= 0.100/12 ft)

ρ = Channel density (= 57 lb/ft^3)

v_z = Coolant velocity (= 18.96 x 3600 ft/hr)

c = Coolant specific heat (= 0.52 Btu/lb °F)

N = Ratio of maximum heat flux of opposite plates

L = One-half active fuel plate length (1.5 ft)

Figure 17 is a plot of Equation (1) for several values of X. For the outside channel of element D-11, a value of X is

$$X = \frac{2h\ (1 + N)}{a\ s\ \rho\ v_z\ c} \sin aL = \frac{2(1430)(1 + 0)\ \sin\ (\frac{1.37}{1.5})(1.5)}{(\frac{1.37}{1.5})(\frac{0.100}{12})(57)(18.96\ x\ 3600)(0.52)} = 0.182 \qquad (2)$$

From the curves of Figure 17 for X = 0.182, the maximum value of

$$\frac{T_p - T_{f(-L)}}{(T_p - T_f)_{max}} \text{ is } 1.09 \qquad (3)$$

$$\therefore\ T_p - T_{f(-L)} = 1.09\ (T_p - T_f)_{max}$$

The value of $(T_p - T_f)_{max}$ was determined above to be 5°F.

$$\therefore\ T_p - T_{f(-L)} = (1.09)(5) = 5.45°F$$

Assuming heat flux is proportional to power, the temperature curve for the element in position D-11 is determined as shown in Figure 20.

2.13 Thermocouple Attachment (E. R. Oetken). It was reported in the last quarterly progress report [24] that two methods are under investigation for the attachment of thermocouples to EOCR fuel plates, resistance spot welding, and high temperature furnace brazing.

The resistance welding program during the present quarter has concentrated on developing a reproducibly strong thermocouple plate attachment without penetrating the plate cladding. Results to date have shown that a resistance weld can be made without penetrating the cladding on EOCR fuel plates, but the strength of the weld attachment has been too erratic to be acceptable.

Figures 21 and 22 illustrate the penetration of a weld spot with 0.062- and 0.040-inch-OD spade end thermocouples. Weld energies between 18 and 80 watt-seconds, weld forces between 2-1/2 and 20 pounds, and conical, wedge, and horseshoe-shaped electrode tip designs have been evaluated. Acceptable weld strength has been obtained on a number of welds. No significant difference has been found between welds made with a hand-held probe and welds made with a weld head. The use of a purge gas resulted in cleaner-looking, but not stronger, welds. Results to date indicate that the strength of the attachment comes from the first one to three weld spots. It is suspected that additional welding does not cause fusion of the metal surfaces because the welding current short-circuits through prior weld spots. Figure 23 shows a 0.062-inch spade end thermocouple welded to a 0.030-inch-thick stainless steel plate.

Because there will be several locations in the test loops where thermocouples are required, but cannot be applied by the high temperature furnace brazing technique, efforts will continue to develop an acceptable and uniform spot weld

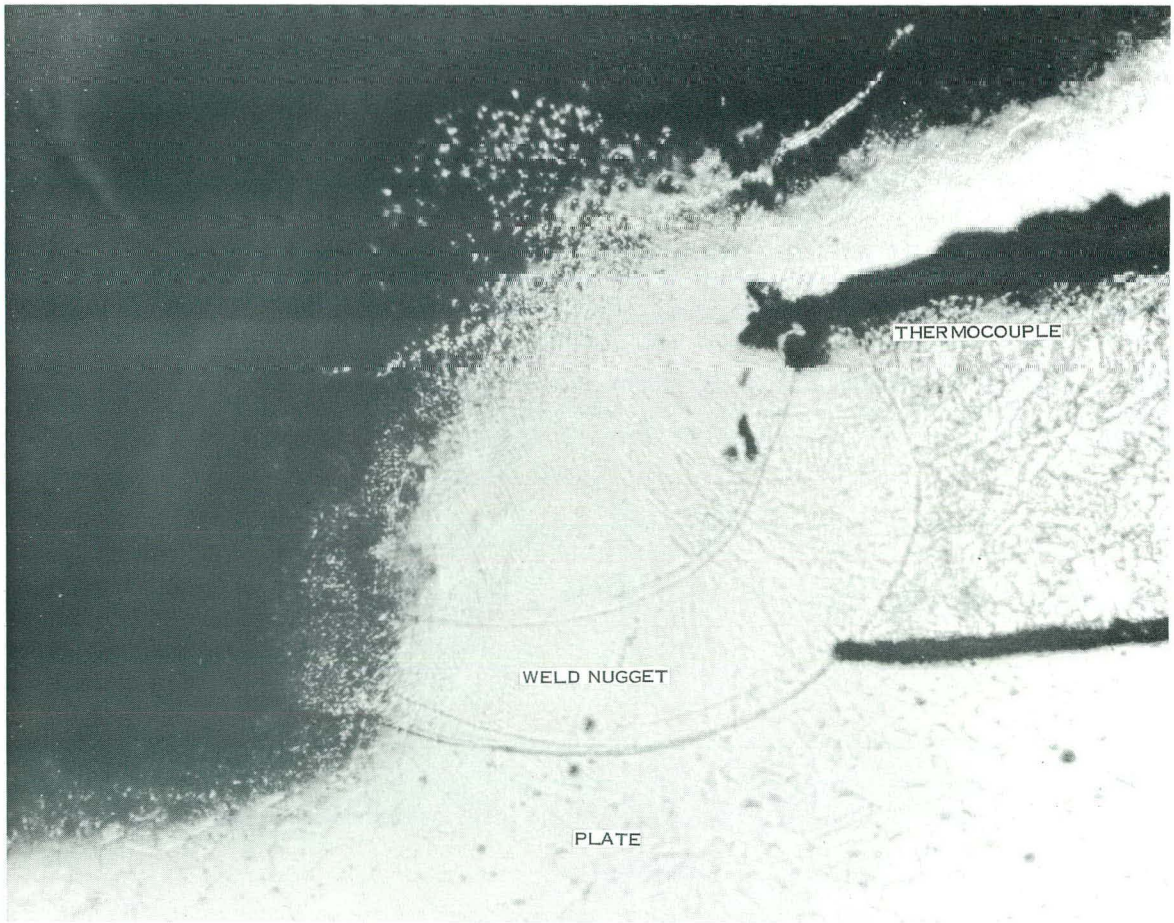

Fig. 21 Weld penetration of 0.062-inch thermocouple resistance-welded to 0.030-inch plate.

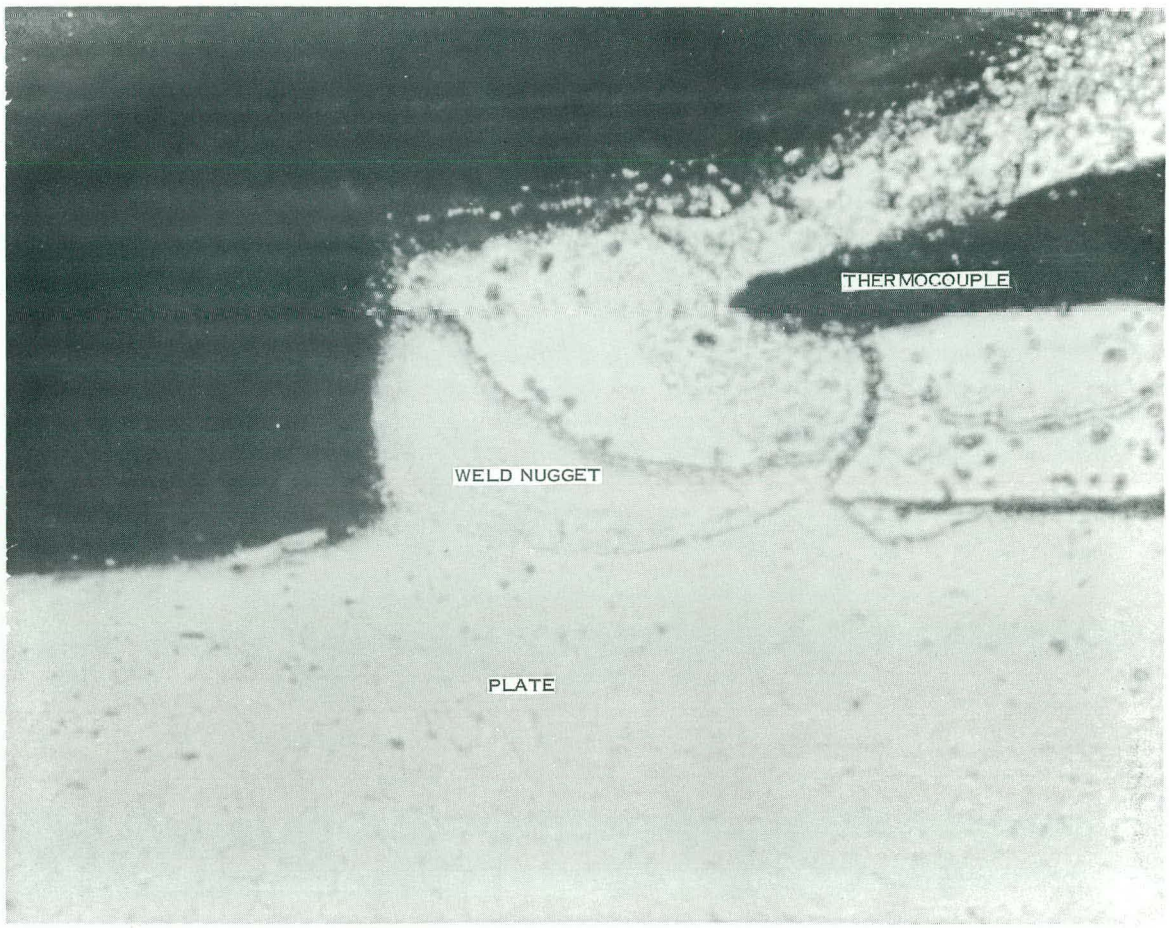

Fig. 22 Weld penetration of 0.040-inch thermocouple resistance-welded to 0.030-inch plate.

strength. In the meantime, efforts are being concentrated on evaluation of the brazing technique, and sample (simulated fuel) plates with brazed thermocouples have been obtained for testing.

The type of thermocouple to be used is a chromel-alumel, 0.062 $\pm$ 0.002-inch-diameter, Type 304 stainless steel sheath, MgO-insulated, with grounded junction. The surface-attached thermocouples will have two tip types, as shown in Figure 24. The spade-offset design tip, T-5288M/T-5302M, will be used on the driver assemblies; the standard-spade tip, T-5287M, will be used on the fuel follower. A standard sealed-in junction tip will be used on all coolant channel thermocouples.

A test section with thermocouples furnace-brazed to a five-mil-thick type 304 stainless steel strip is shown in Figure 25; a close-up of one of the thermocouples is shown in Figure 26. The test section of Figure 25 was made with "Nichrobraz 30" at a brazing temperature of 2175°F in a hydrogen atmosphere with a dew point of -50°F. This

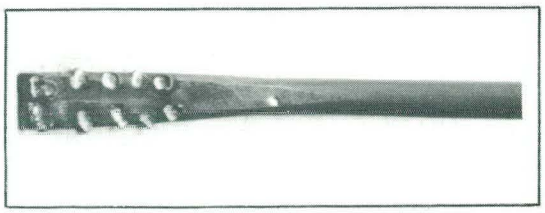

Fig. 23 A 0.062-inch thermocouple resistance-welded to a 0.030-inch plate.

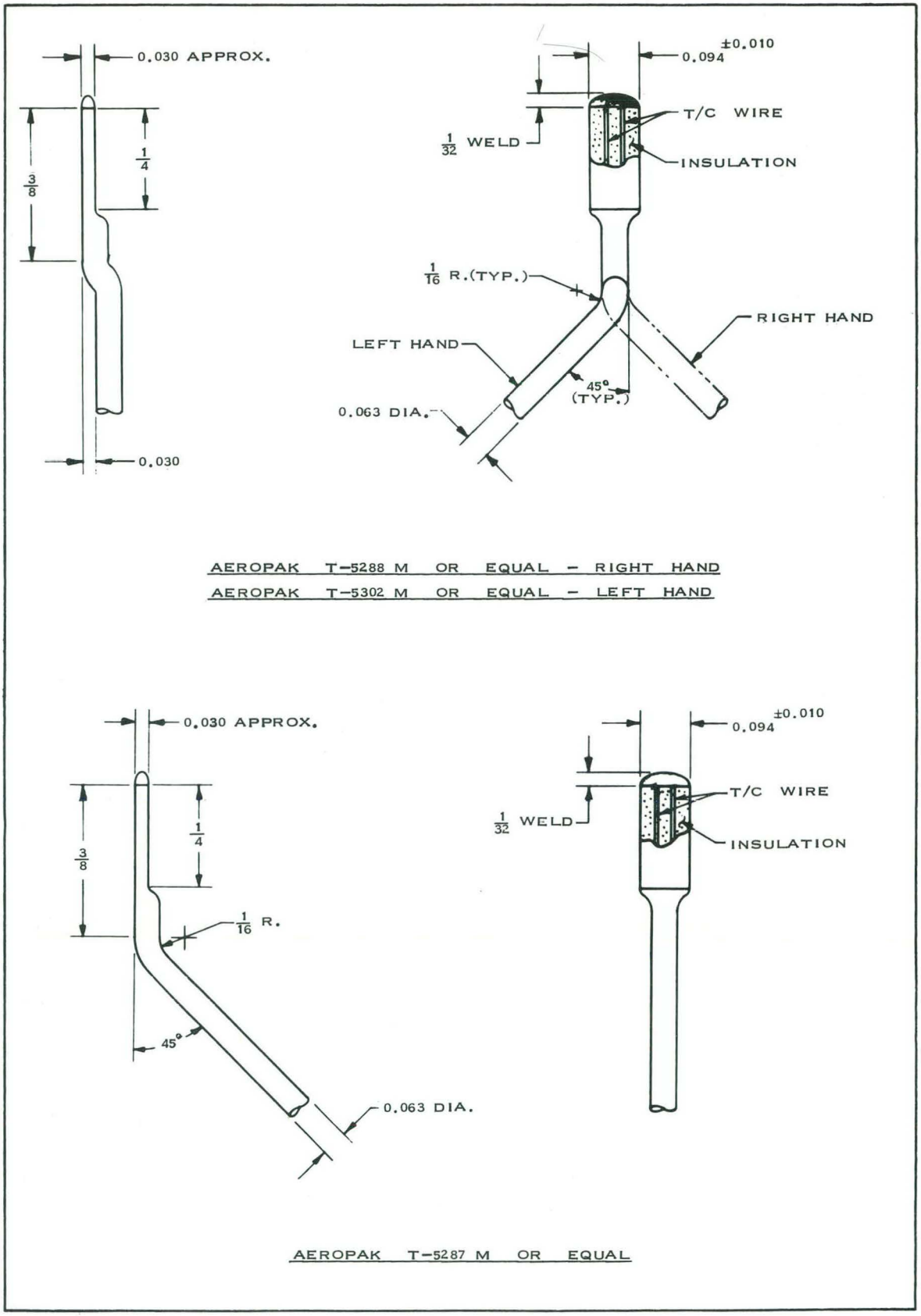

Fig. 24 Thermocouple tip designs.

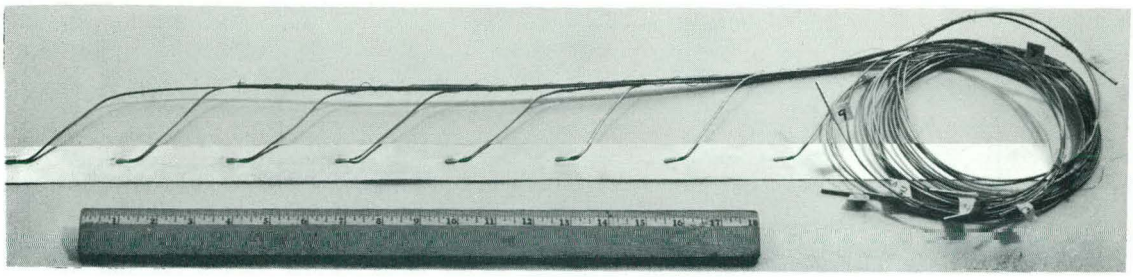

Fig. 25 CDTL heat transfer plate - brazed thermocouples.

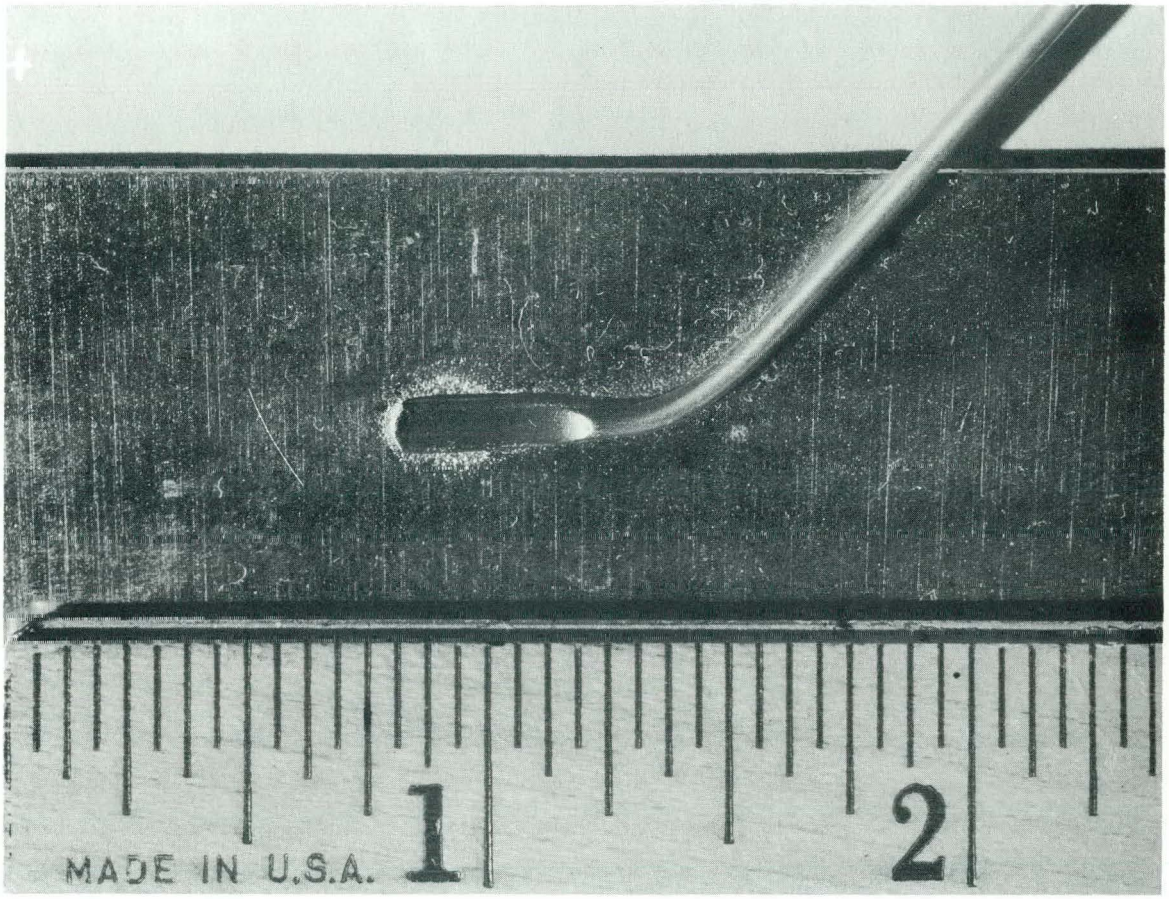

Fig. 26 CDTL heat transfer plate - brazed thermocouple.

operation was performed by the element manufacturer, Metals and Controls, Inc, in Attleboro, Mass. In several preliminary tests the best results were obtained by coating the bottom of the thermocouple with the braze alloy powder and applying pressure while brazing.

The composition of the braze alloy is: Cr - 13.0%, Si - 10.0%, C - 0.15% maximum; the balance is nickel. Joints made with the braze on Type 304 stainless steel have been previously proved satisfactory in NaK and high-temperature water reactors.

2.14 Thermocouple Leadout. It is desirable to get the thermocouple lead away from the plate as soon as possible. In the case of the driver assemblies, the thermocouple will leave the 3- x 4-inch box near the corner and pass into the 0.5-inch space between the boxes (shown in Figure 19). The leads will be attached to the outside of the box by spot-welded straps. The leads will reenter the assembly through a slot machined in the upper support. In the case of the fuel follower, Figure 18, they will leave the 4- x 4-inch box on the side and continue up the outside.

The coolant channel thermocouples will not make contact with the fuel plates. Their tips will lie in mid-channel about 1/2 inch above and 1/2 inch below the meat, and in line with the surface-attached thermocouples.

Figure 16 shows the leadout pattern of the thermocouples in Spider No. 1 from the instrumented driver elements. It should be noted that this pattern uses straight runs that would eliminate the necessity of preforming the thermocouple leads.

2.2 Fuel Element Wash System Development (E Burroughs)

It has been successfully demonstrated that a simulated fuel element immersed in a liquid terphneyl mixture can be cleaned by displacing the terphenyl mixture with a high-boiling organic, such as ethylene glycol. This technique is a melt-displacement process and does not depend upon the solubility of the terphenyl mixture in the displacing liquid. Operation procedure of the loop, designed to demonstrate this process, was published in a previous quarterly report.

After each demonstration run, the fuel element test section was removed and visually inspected. Each inspection indicated complete removal of the wax. There was no waxy feel to the surface of the test element, and all channels between the simulated fuel plates were completely clear. Progression photographs were made during one run and are shown in Figures 27 through 37.

For one demonstration, the fuel element test section was precoated with a terphenyl mixture. The terphenyl mixture had been used previously in a drop latch test and had a heavy concentration of particulates present. The progress photographs of this run are Figures 38 through 43.

Loop tests showed that it was necessary to heat the ethylene glycol to at least 320°F for efficient displacement of Santowax. The results indicate that a higher-boiling organic, such as triethylene glycol, would work better than the ethylene glycol.

No further displacement tests are scheduled at this time; however, fractionation data for terphenyl-glycol and glycol-water systems will be obtained. This information is needed for engineering studies of organic and solvent (displacement liquid) cleanup systems, as related to the EOCR cleanup system. When this work is completed, a report will be issued.

2.3 Chemical Cleaning (E Burroughs)

As reported in the previous quarterly [25], the surface of carbon steel pipe after being chemically cleaned has a lightly adhering passivation film which can be removed easily by the circulation of hot terphenyl mixtures.

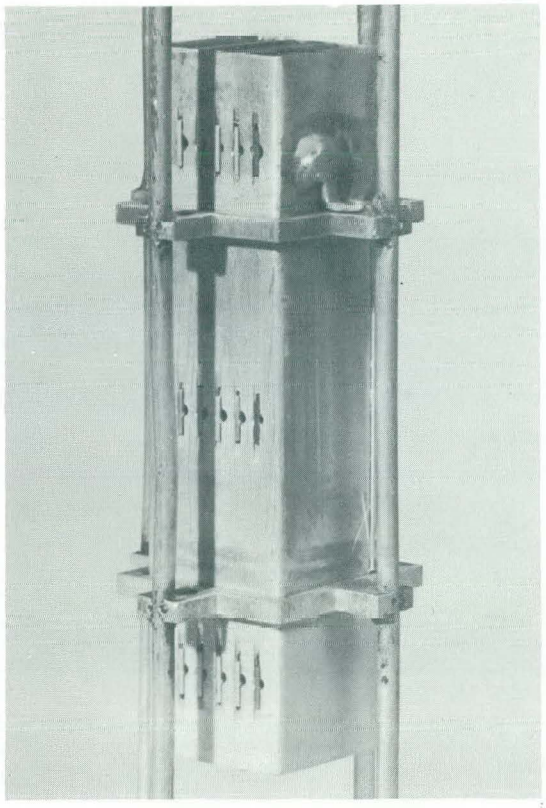

Fig. 27 Test section before installation in loop.

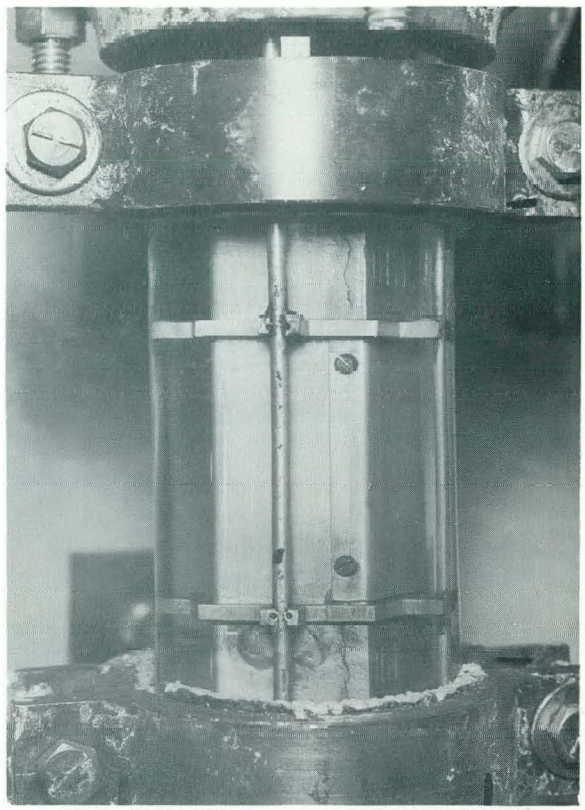

Fig. 28 Test section after installation in loop with ethylene glycol.

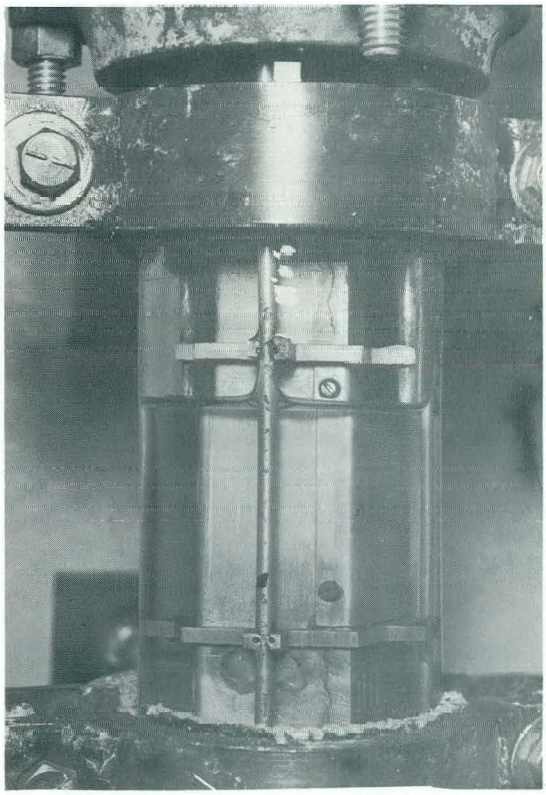

Fig. 29 Ethylene glycol draining from test section.

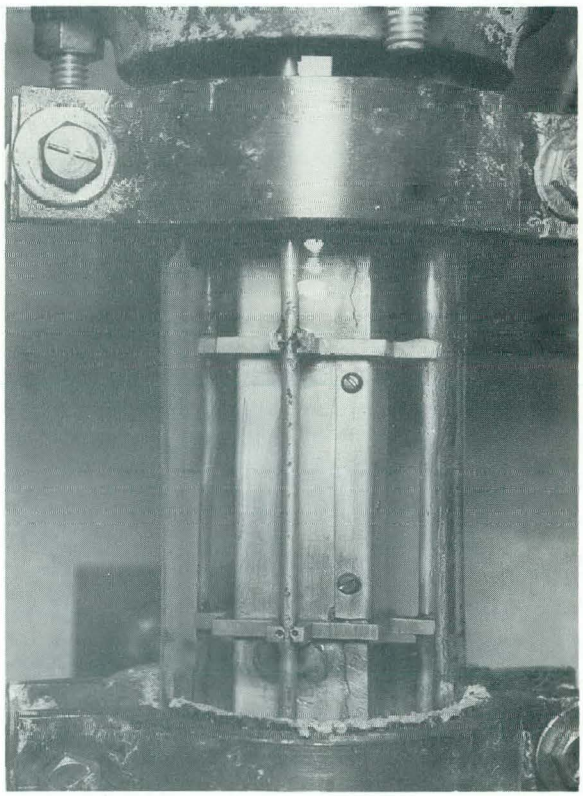

Fig. 30 Ethylene glycol drained from test section.

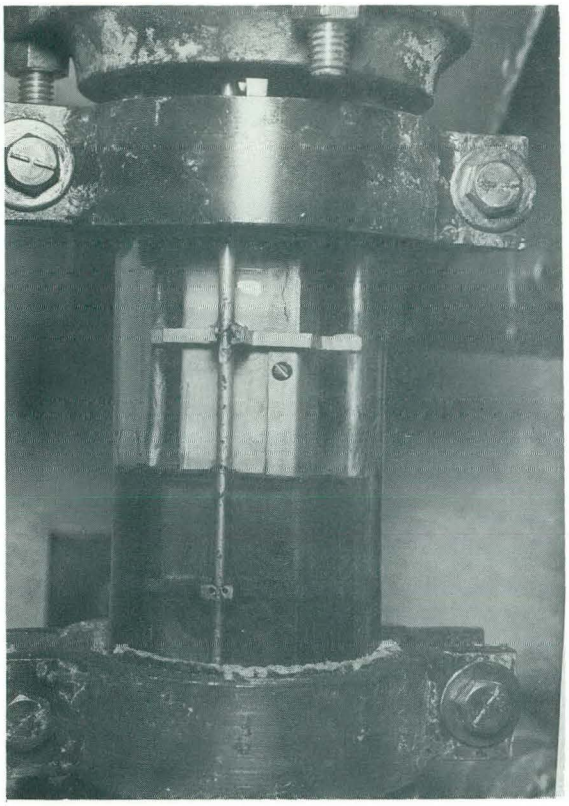

Fig. 31 Introduction of liquid terphenyl to test section.

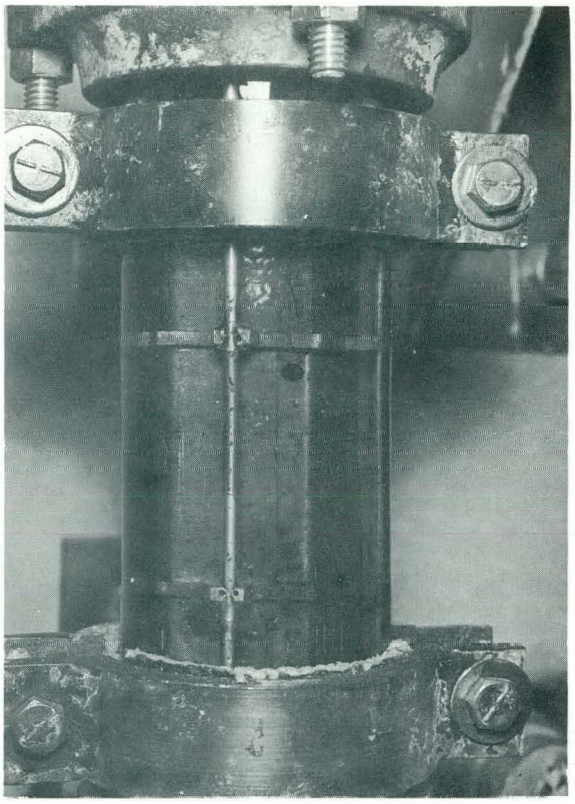

Fig. 32 Sample completely immersed in test section.

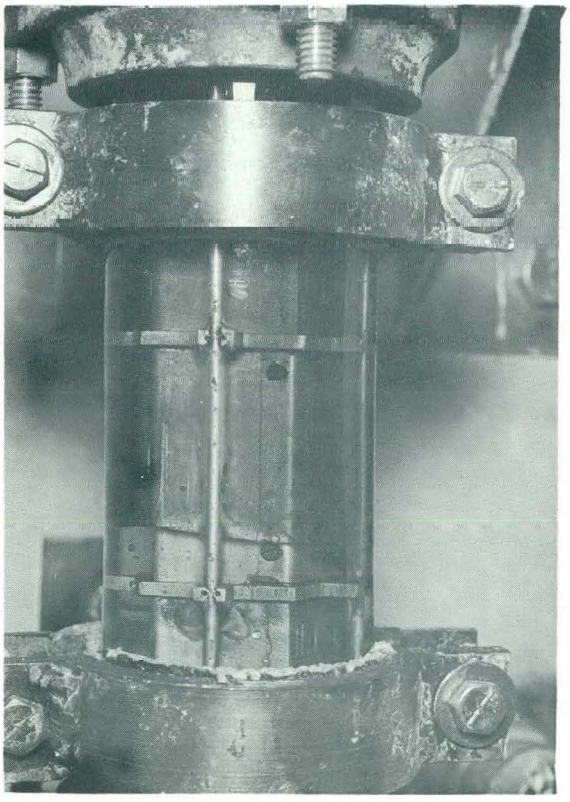

Fig. 33 Displacement of wax by ethylene glycol - view 1.

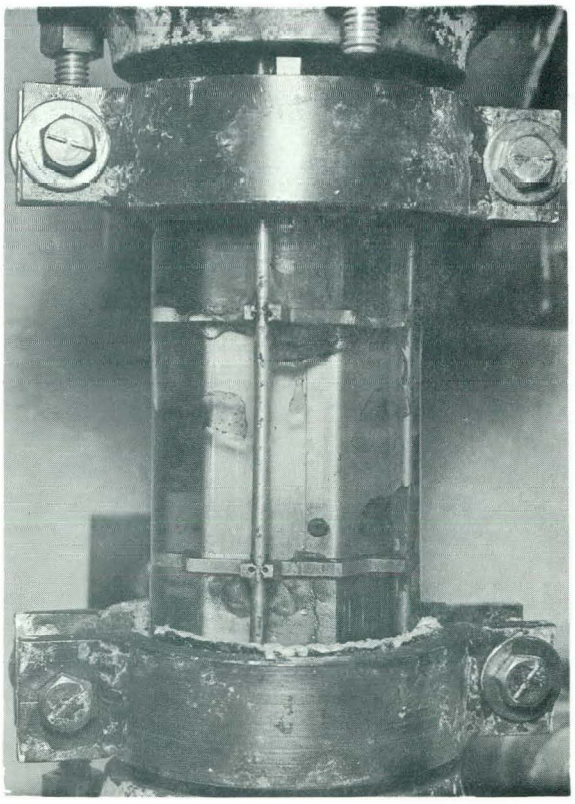

Fig. 34 Displacement of wax by ethylene glycol - view 2.

Fig. 35 Ethylene glycol and terphenyl in terphenyl receiver.

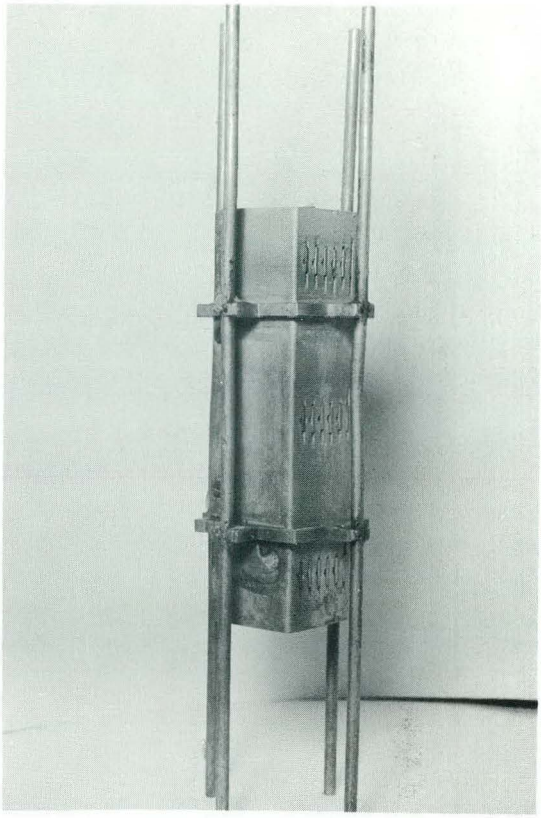

Fig. 36 Test section after processing - view 1.

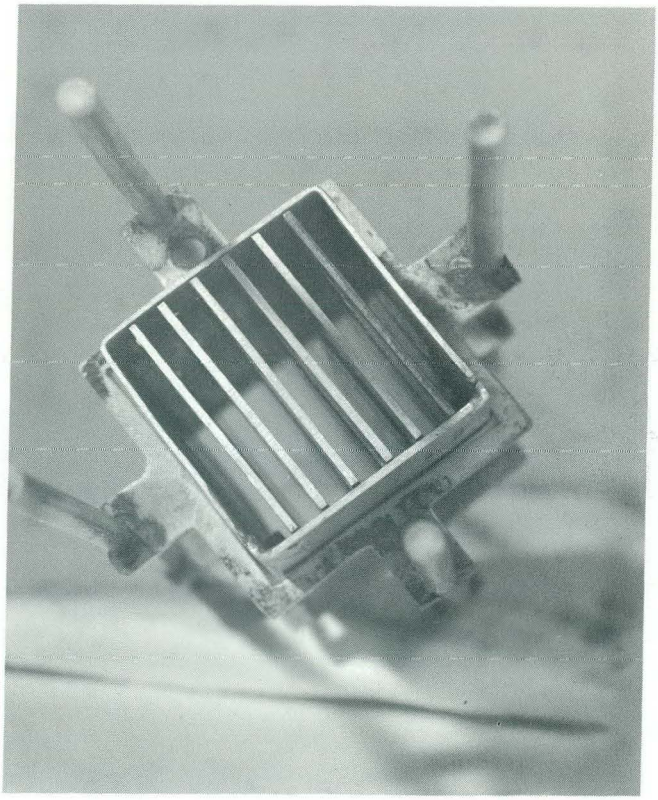

Fig. 37 Test section after processing - view 2.

Fig. 38 Test section precoated with terphenyl.

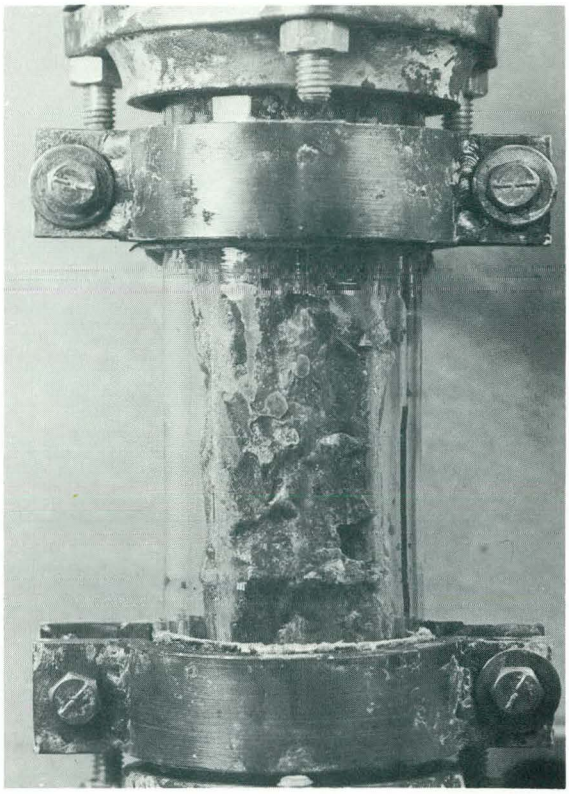

Fig. 39 Installed test section precoated with terphenyl.

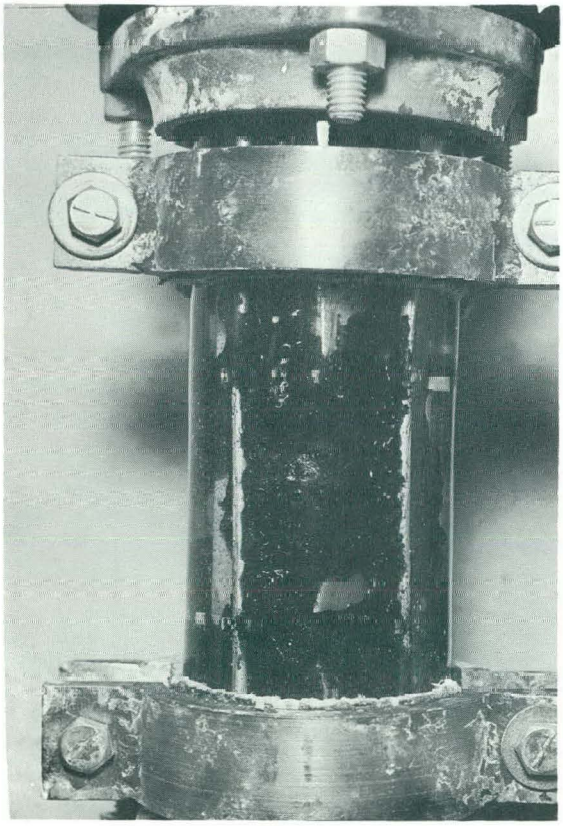

Fig. 40 Hot ethylene glycol displacing wax - view 1.

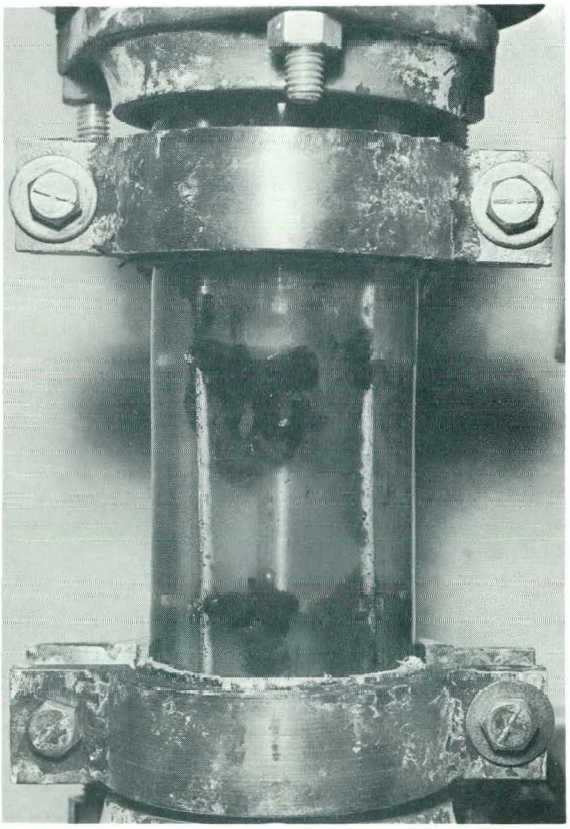

Fig. 41 Hot ethylene glycol displacing wax - view 2.

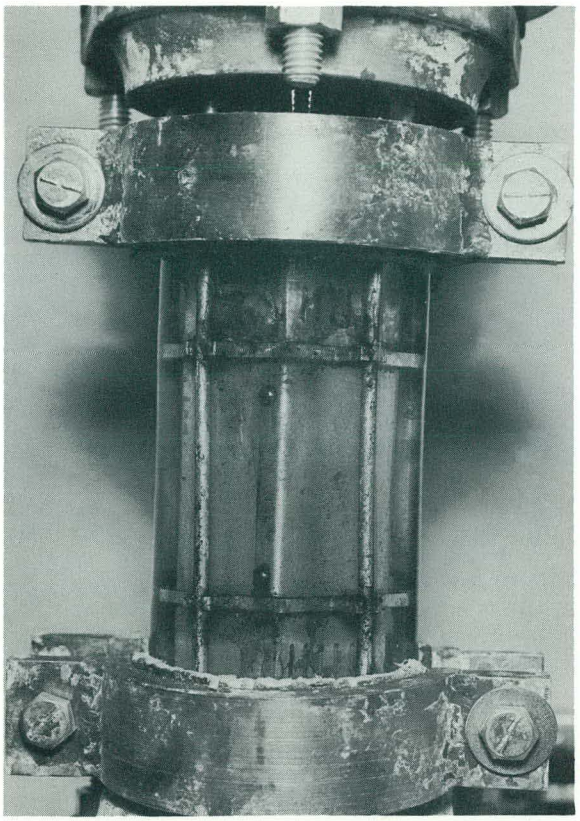

Fig. 42 Test section after water wash.

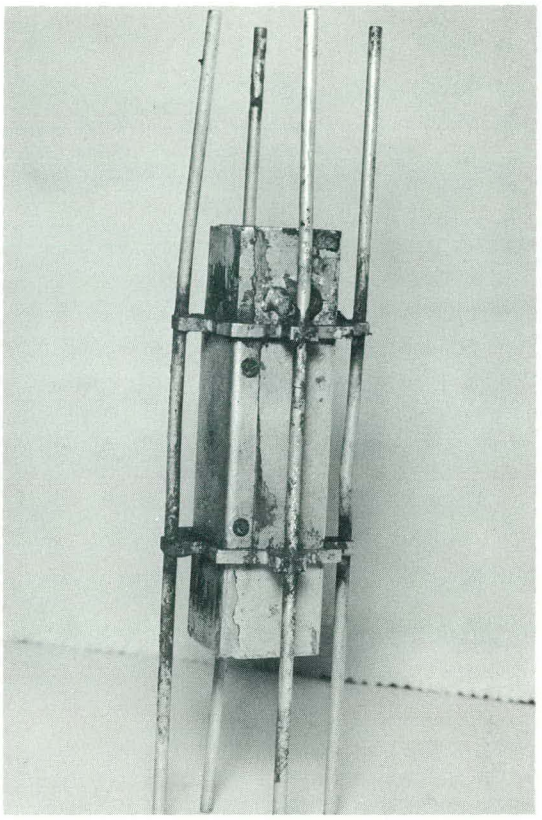

Fig. 43 Test section after processing.

Since the passivation film is removed as particulate matter in the hot organic, it was considered possible that the fouling tendency of the organic might increase. Samples of fresh Santowax OMP, Santowax OMP with pipe passivation particulates, and Santowax OMP with non-chemically cleaned pipe particulates were sent to Phillips' Bartlesville laboratories for fouling tendency tests. The results of these tests are shown in Table XXIX.

The high film formation rate for the sample with passivation particulates was disturbing, particularly with the power reduction of nine percent, as this showed the film was definitely reducing the heat transfer coefficient. Subsequent analysis showed silica in the ash content of the Santowax OMP of this run (caused by a crushed shipping glass container), which tended to invalidate the above results. However, the difference in film formation rate between the wax with passivation film particulates and uncleaned pipe particulates was great enough to show the need for further testing.

Additional runs were made by Plant Engineering, using the chemical cleaning loop to prepare pipe samples cleaned by the Dow Industrial Services procedure and the Charles Pfizer Co procedure (referred to previously as the Piqua method). No difficulty was experienced in reproducing results of previous cleaning runs.

Pipe samples from both cleaning procedures and samples of uncleaned pipe were refluxed in 600 grams of Santowax OMP for six hours at 582°F. The chemically cleaned pipe samples were run in duplicate. All the terphenyl

TABLE XXIX

RESULTS OF FOULING TENDENCY TESTS

Pipe Treatment (6-in. Lengths)		
Treatment	Pipe A	Pipe B
Chemically cleaned, Pfizer procedure	yes	no treatment
Refluxed in 1200 g Santowax OMP for six hours at 575°F	yes	no
Make PCFT on refluxed Santowax	yes	no

PCFT[a] Results			
	Pipe A	Pipe B	Control (Fresh Santowax OMP)
Film weight (Mg)	2.2	0.3	0.2
Film formation rate (Mg/hr)	0.092	0.013	0.008
Power reduction (%)	9	0	0

(a) PCFT run at 700 psig N_2 blanket pressure, heater temperature 950°F, bulk coolant temperature 605°F.

samples were shipped to Bartlesville for film fouling tendency analysis. Fouling tests have not been completed, but preliminary results indicate that the passivation particulates from the Pfizer cleaning method have the highest rate of film formation, the Dow method second highest, and the particulates from uncleaned pipe the least film-formation tendency.

2.4 Film Formation (J. R. McGeachin)

The program to investigate various parameters associated with film formation under reactor conditions is proceeding at an accelerated rate. The first series of 11 capsules to be irradiated in the MTR hydraulic facility are for the purposes of: (a) measuring the gamma flux, (b) determining the overall heat transfer coefficient across an organic-filled annulus, (c) determining the overall heat transfer coefficient for an organic-filled tube, and (d) determining high-boiler formation rate. The construction of this series of capsules has been completed, and a document fully describing the proposed experiments has been prepared and is now being reviewed for approval to place the capsules in the MTR.

The first three capsules in the series have helium-filled annuli, each of different thickness, to determine the gamma flux. A machine program was used to calculate capsule temperature as a function of gamma heating. Each capsule contains a probe located in the center of the inner cylinder. The probe, seen in Figure 44, contains seven different metals to indicate temperature. The temperatures obtained in the capsule during irradiation can be bracketed

during post-irradiation examination by noting which metals reach their melting points. The following is a list of metals used for indicators:

Pb-Sn eutectic	- 361°F mp
Sn-Zn eutectic	- 390°F mp
Sn pure	- 450°F mp
Cd-Zn eutectic	- 509°F mp
Cd pure	- 600°F mp
Pb pure	- 636°F mp
Al-Zn eutectic	- 720°F mp
Zn pure	- 787°F mp

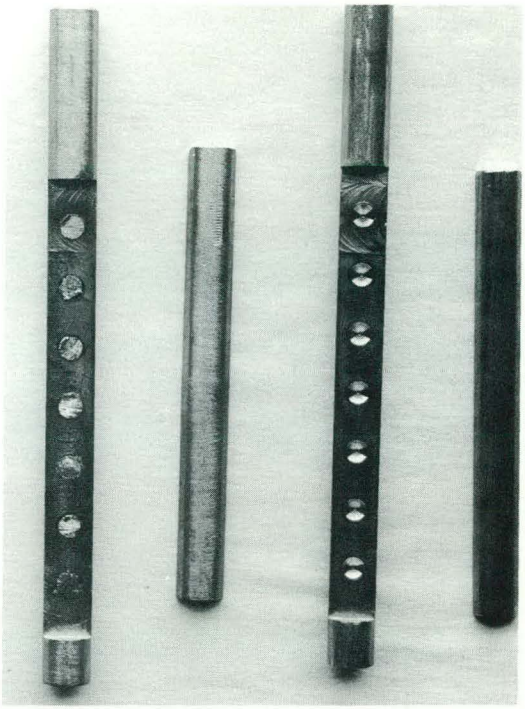

Fig. 44 Capsule temperature indicator.

Six capsules, using organic as the heat transfer medium, are similar to the first three. The annulus for each capsule is different. The organic liquid consists of a eutectic mixture of biphenyl and o-terphenyl (73°F melting point). Figures 45 and 46 show a disassembled and assembled typical capsule. A heat transfer computer program will be used to determine the overall heat transfer coefficient for natural convection.

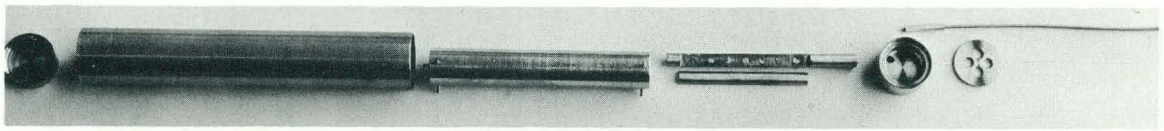

Fig. 45 Disassembled capsule.

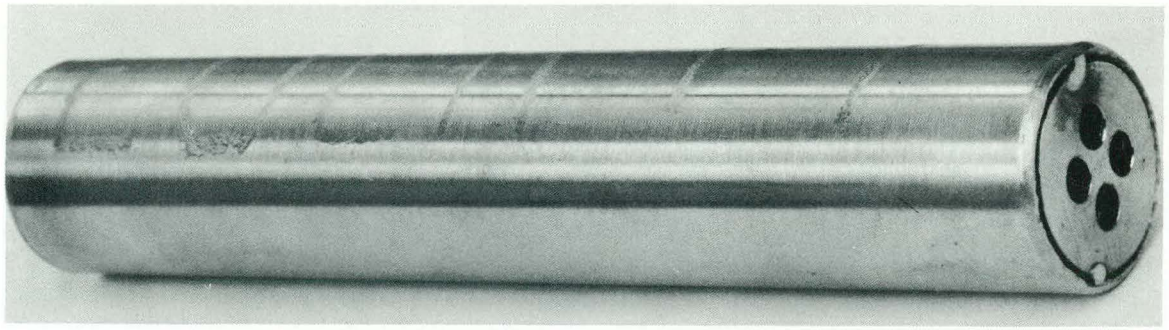

Fig. 46 Assembled capsule.

The remaining two capsules, Figure 47, are designed to provide irradiation of organics at a temperature of 176°F ± 18°F. Because of the heat transfer uncertainties, two sizes of tubes were chosen. Estimates based on two watts/gram gamma heating indicate the above temperature range will be realized when

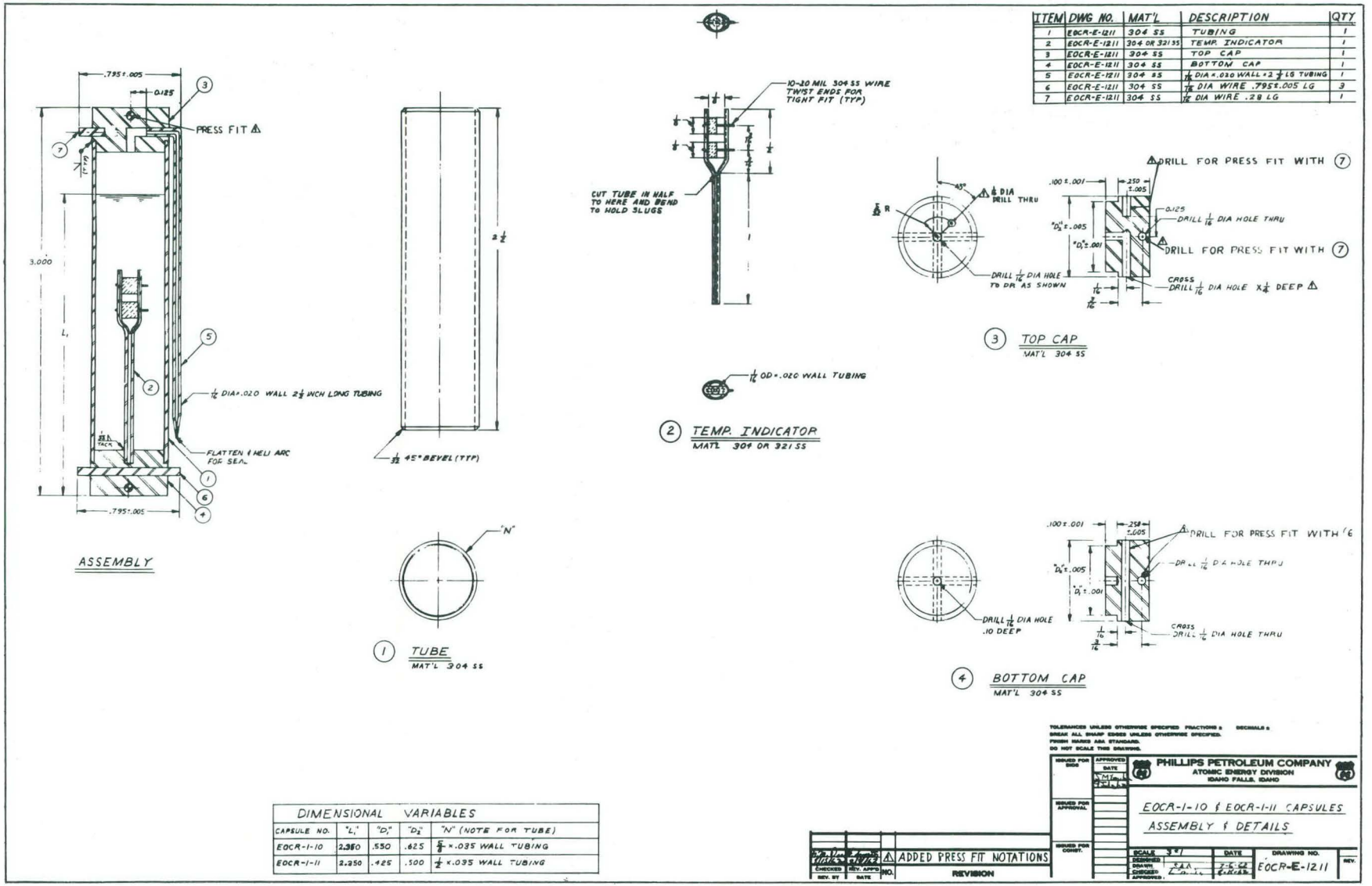

Fig. 47 Capsule design.

using either 1/2- or 5/8-inch-diameter tubing. A 50-mol-percent benzene-biphenyl mixture will be used. Two temperature indicators are used in these capsules to bracket the temperature range obtained during irradiation. They are $Al(NO_3)_3 \cdot 9H_2O$, mp 163°F and $CoCl_2 \cdot 6H_2O$, mp 187°F. These compounds are ground to a fine powder and pelletized under approximately 60,000 to 80,000 psi pressure. They are supported in the center of the capsules as shown in Figure 48.

The organic research program being conducted at Bartlesville has included extensive studies of radiolytic damage mechanisms. The source of radiation used in these studies is an electron beam. The capsule shown in Figure 46 is for the purpose of irradiating organics in a gamma and neutron flux at similar conditions. The irradiated material will be furnished to Bartlesville for investigation of neutron contribution to radiolytic damage.

2.5 Pyrolytic Capsule Fouling Test Under Irradiation (E Burroughs)

The testing of the designed pyrolytic glass capsule and auxiliary power and measurement circuitry has been started. The initial data indicate the platinum heater plate temperature can be measured accurately by resistance thermometry procedures.

Some difficulties were encountered in the construction of the glass test capsule. The silver solder used to attach the platinum to the tungsten rods could not withstand the glass-blowing temperatures. The platinum strips are now brazed to the tungsten rods. The initial resistance leads were too weak; improvement in the technique of attachment corrected this problem.

The measurement circuit was constructed and basically has performed as designed, with a few minor modifications. Due to the different sizes of platinum heater strips being used, it was necessary to build several different-size external resistors to balance the circuit. The heat generation from the external resistors is high, and the resistors must be operated in a constant temperature heat sink.

The power to the heater strip is from a regulated dc power supply. The sensitivity of the measurement circuitry

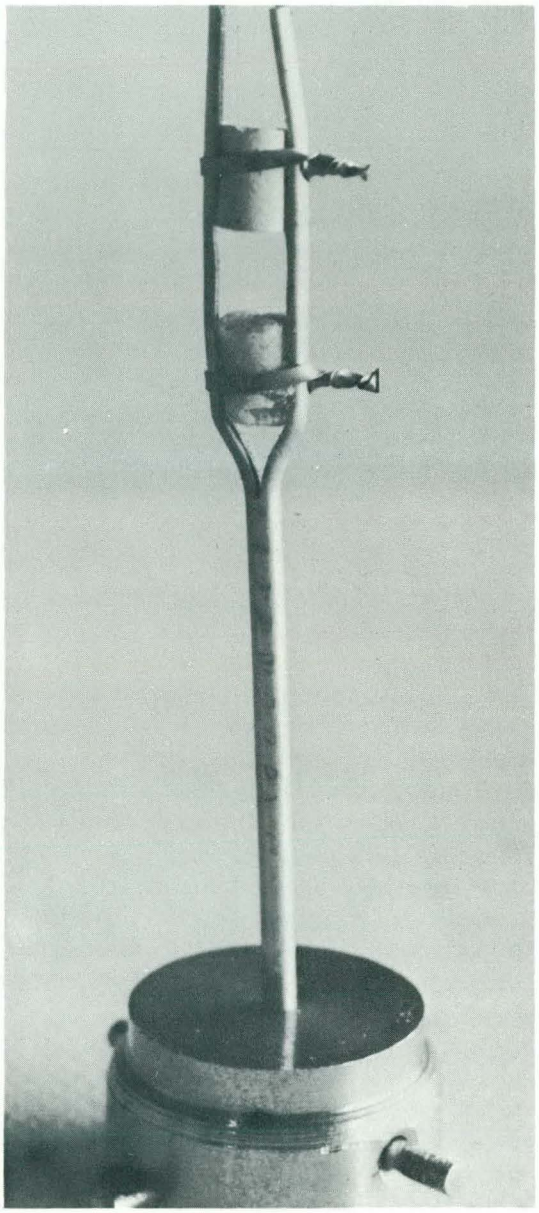

Fig. 48 Low temperature capsule indicator.

to changes in line power required an ac regulator backing up the dc power supply. The bulk temperature of the organic is maintained by means of an electronic temperature controller.

The pyrolytic capsule used for initial check-out work has a platinum heater strip, 6 inch long, 0.125 inch wide, and 0.006 inch thick. The leads to the potential measurement circuitry are attached four inches apart on the heater strip. Santowax OMP is the bulk fluid heated by the external glass heater tape.

Figure 49a is a picture of a capsule before the terphenyl has been charged. Figure 49b shows the first capsule as used for initial circuitry check-out. The terphenyl that was exposed to air turned black after several weeks of operation. Figure 50 is a plot relating temperatures to resistance of the platinum heater strip. The relationship, as expected, is linear. Figure 51, a plot of power (to the strip) vs resistance, clearly indicates nucleate boiling heat transfer was attained.

2.6 Characterization of Unknown Impurities in Monsanto O-Terphenyl (D. G. Kuper)

Two unknown impurities are detected in commercial grade o-terphenyl by gas chromatographic analysis. The first appears as a leading shoulder to the o-terphenyl peak, and the second elutes subsequent to p-terphenyl. These peaks are shown in Figure 52. Each of these impurities concentrates in the light ends upon fractionating o-terphenyl. Separation of the above impurities by absorption chromatography permitted identifying the second peak as the color body responsible for the yellow color of the commercial product. The color body contains carbonyl functional groups. The component that elutes as a shoulder to o-terphenyl is a hydrocarbon with aliphatic groups present.

A fractionating unit, shown in Figure 53, was built to facilitate separation of impurities from terphenyl wax. Approximately 470 grams of material were distilled overhead in this column from a 705-gram charge of o-terphenyl, at a pressure of 23 mm Hg and reflux ratio of 6:1. Initially, a yellow material concentrated in the distillate. This colored material was removed with the first 190 grams of distillate, the subsequent overhead product being water-white. This "white distillate" was chromatographically pure o-terphenyl.

Gas chromatographic analysis of the yellow distillate that was collected first (85-gram cut) shows that two unknown impurities were concentrated while m- and p-terphenyl were removed. These concentrated impurities are pointed out on the chromatogram pictured in Figure 54. The concentrated impurities can be compared to the original charge given in Figure 52. The fact that the component that elutes subsequent to p-terphenyl is concentrated in the light-end cut suggests that it probably forms an azeotrope.

The impurities in the initial light-end cut shown in Figure 54 were further concentrated by eluting a 24-gram aliquot through an activated alumina column using n-hexane as solvent. The yellow color body, which is non-fluorescent, was retained on the column. The colorless fraction, which was fluorescent, was dispersed down the column in an apparent continuous band as viewed under an ultraviolet light.

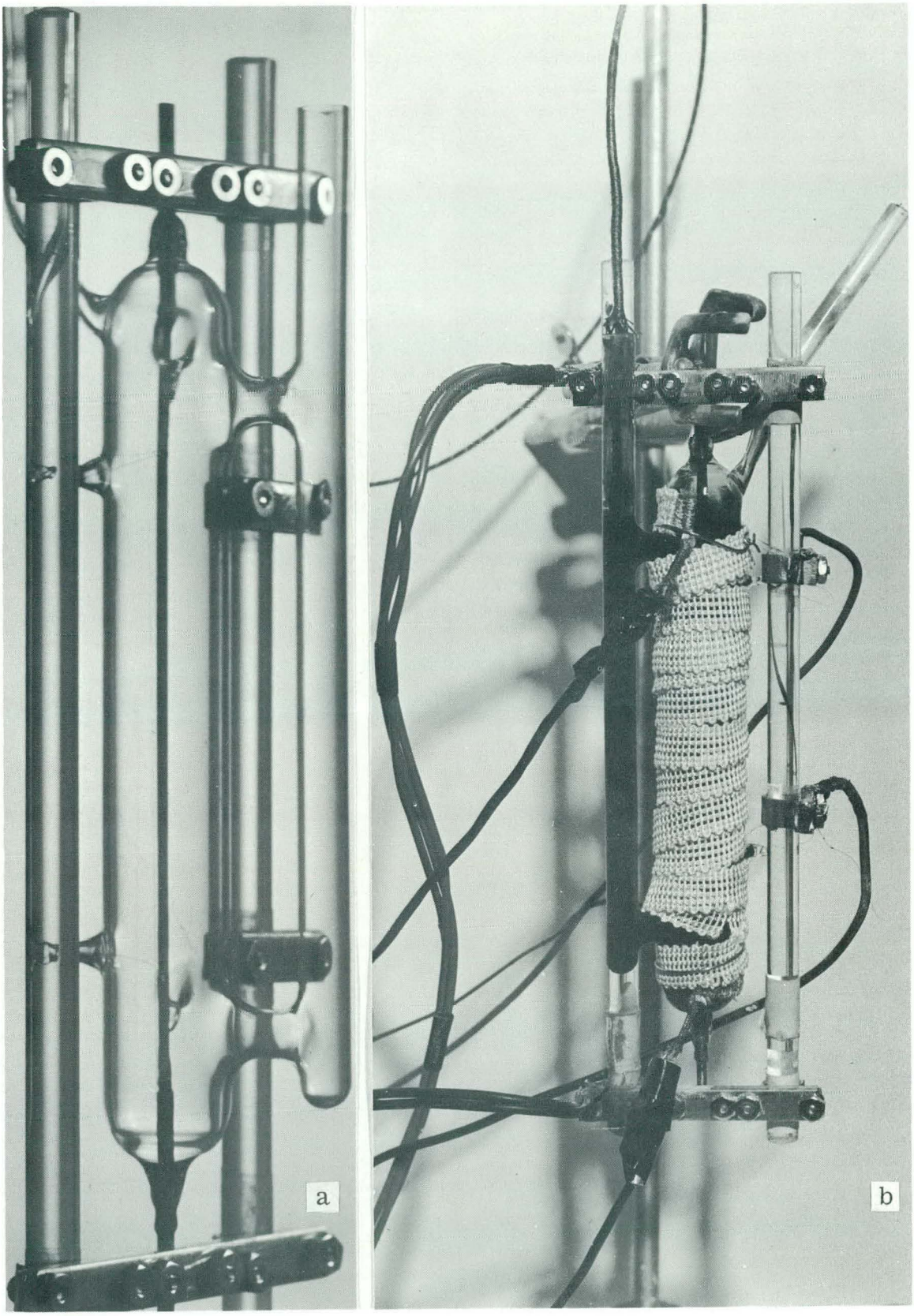

Fig. 49 Pyrolytic capsule (a) prior to charging, and (b) ready for test.

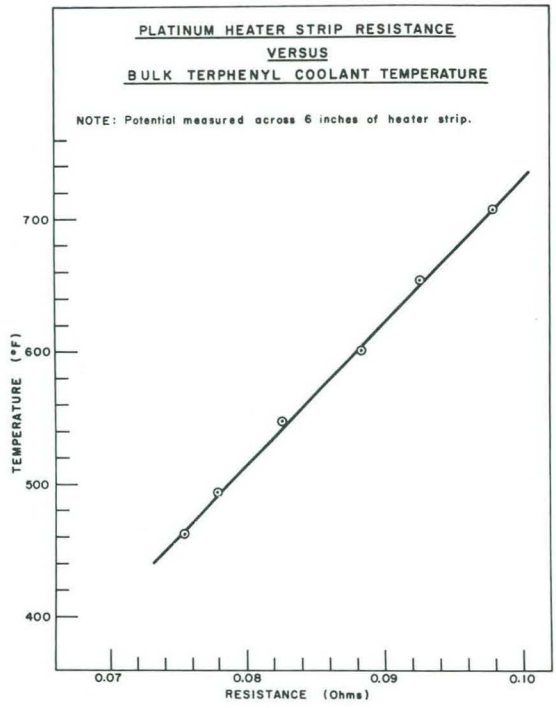

Fig. 50 Temperature vs strip resistance.

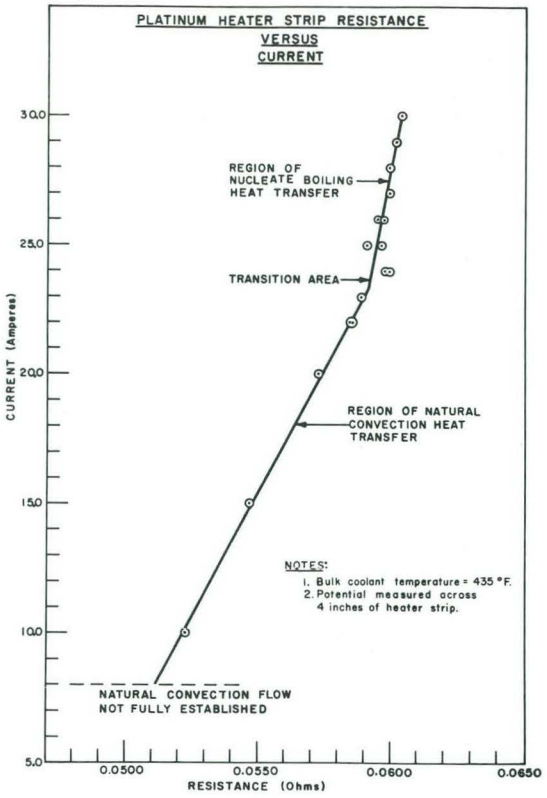

Fig. 51 Power vs strip resistance.

The colorless portion of the sample was eluted with about 3-1/2 liters of n-hexane and was collected as 22 separate fractions. The yellow portion was eluted with about 1200 milliliters of $CHCl_3$ and was collected as a single fraction.

The fractions collected from the adsorption column were analyzed by gas chromatography using an F & M, Model 500 instrument. Conditions were those listed in Figures 52 and 54 through 59. Analysis of the colorless fractions shows that the unknown component that is resolved as a leading shoulder edge on the o-terphenyl peak (impurity No. 1, Figure 52) is made up of three separate components. The presence of these three are verified by the chromatogram contained in Figure 55. The component that peaks closest to o-terphenyl (peak C, Figure 55) was removed by continued elution, while the second shoulder peak (peak B, Figure 55) was enhanced. Additional elution preferentially rejected o-terphenyl until the ortho isomer represented only a minor impurity, as is shown in Figure 56. Material eluted in subsequent fractions, which logically should be the pure shoulder component, was unstable to conditions for gas chromatographic analysis. The breakdown of the material during analysis is shown in Figure 57. It is interesting to note that the material is relatively stable as an impurity in o-terphenyl, but becomes unstable upon isolation. Infrared analysis of the "pure" component shows the presence of aliphatic groups.

The color body eluted as a single fraction also was unstable to gas chromatographic analysis. This can be seen in Figure 58. When diluted with o-terphenyl, stability to analysis resulted, showing that the unknown impurity

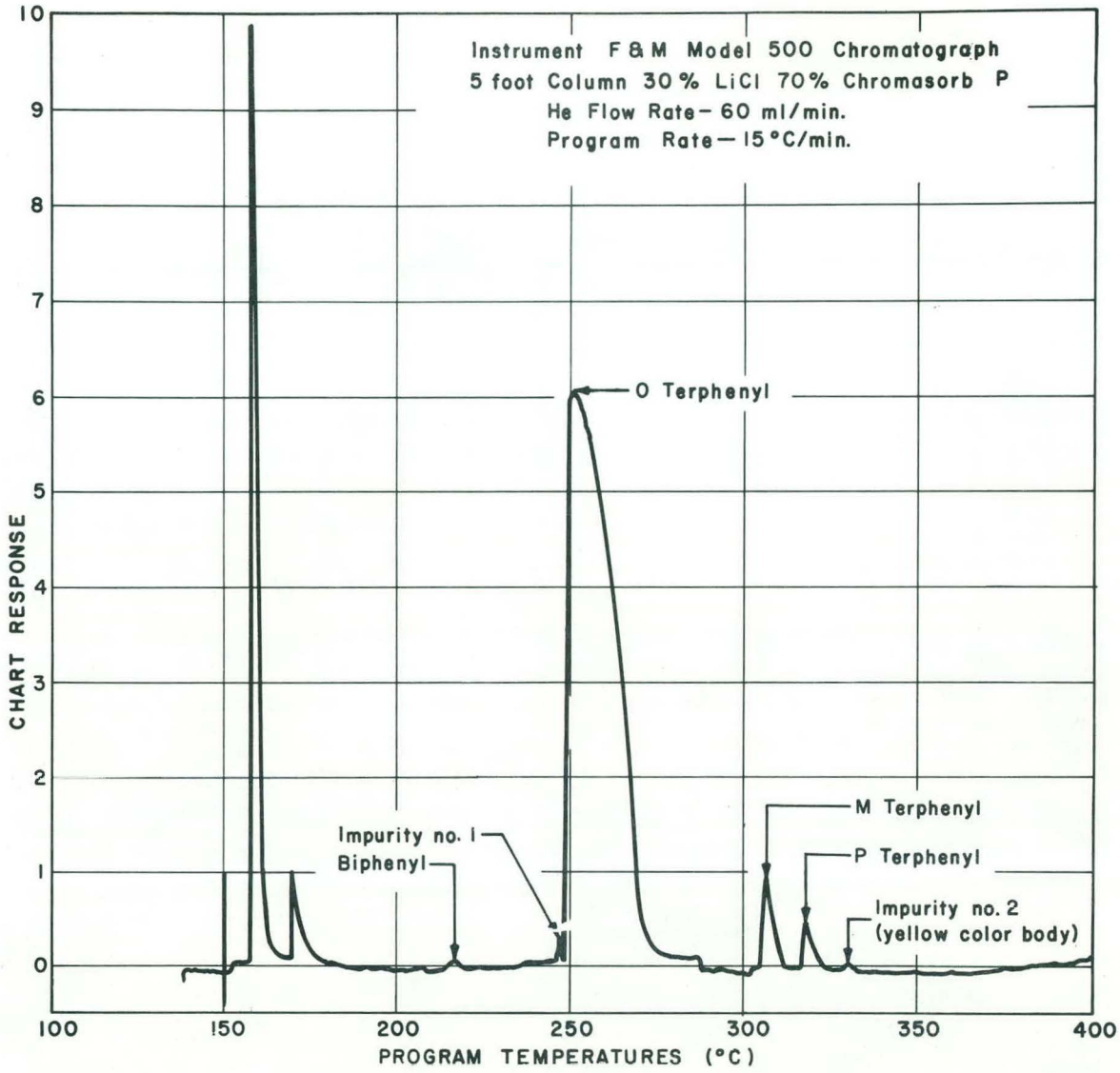

Fig. 52 Chromatogram of Santowax O.

that elutes subsequent to p-terphenyl (impurity No. 2, Figure 52) is the component responsible for the yellow color of the o-terphenyl. Removal of solvent revealed that the color body is an orange oil easily soluble in n-hexane or benzene. A molecular weight of about 370 was indicated by ismometer measurement. Infrared analysis indicated the presence of carbonyl groups. Upon standing exposed to air, the orange oil forms a solid material that is insoluble in hot benzene. This solid decomposes at about 215°C to yield a black tar.

Further characterization tests of the isolated impurities have not yet been made.

Figure 59 relates these impurities to the EOCR reactor coolant, Santowax OMP. The coolant is yellow, and the presence of the yellow color body described

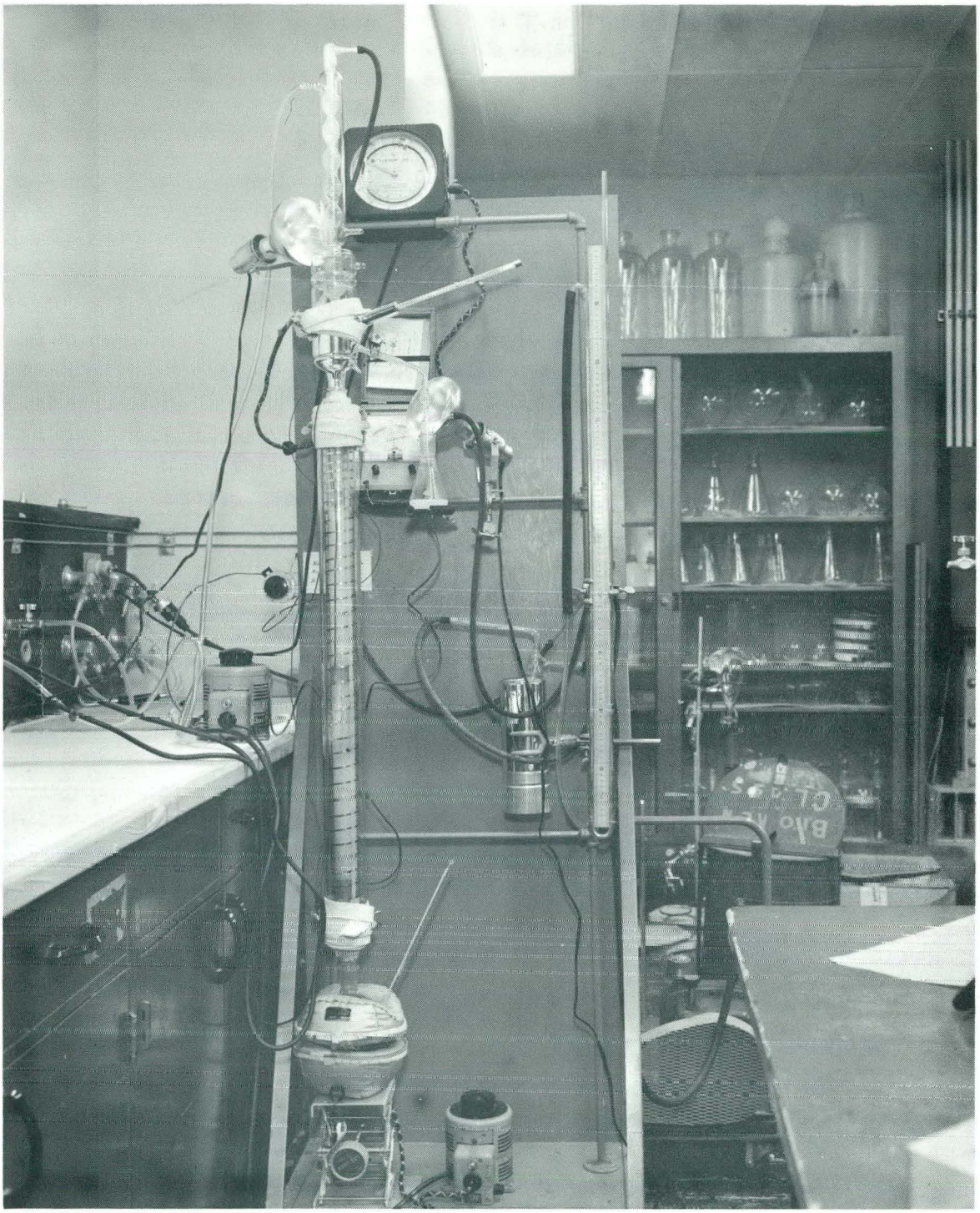

Fig. 53 Fractionating unit.

above is suggested by peak No. 2, shown in Figure 59. The shoulder peak concomitant with o-terphenyl is not seen in this analysis of the Santowax OMP.

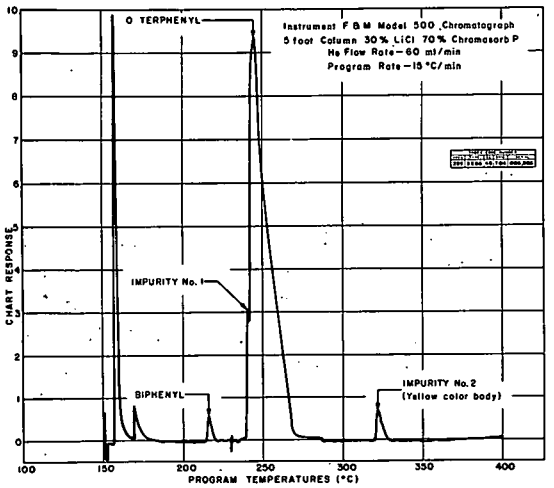

Fig. 54 Chromatogram of light-end fraction obtained from distillation of Santowax O.

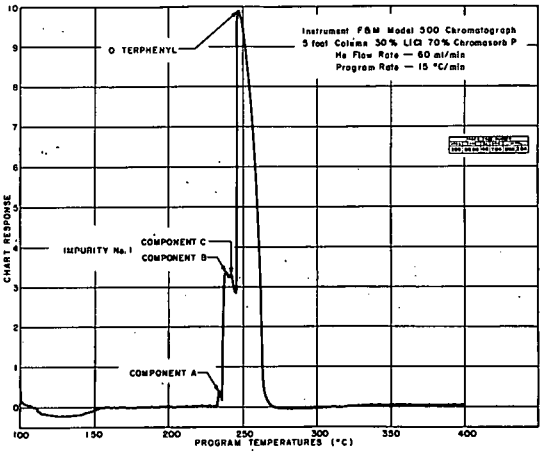

Fig. 55 Chromatogram showing impurities in o-terphenyl.

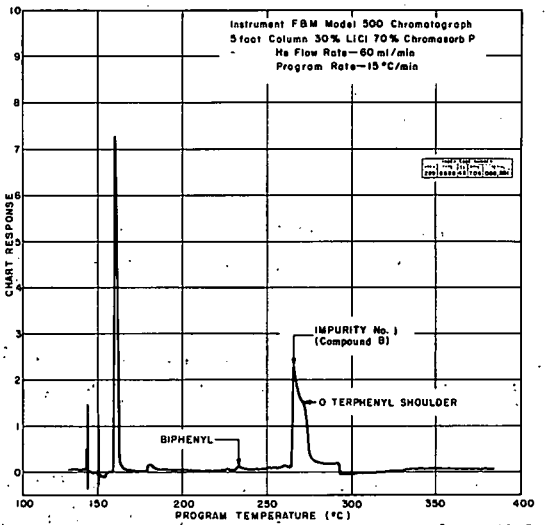

Fig. 56 Chromatogram showing preferential removal of o-terphenyl by elution chromatography.

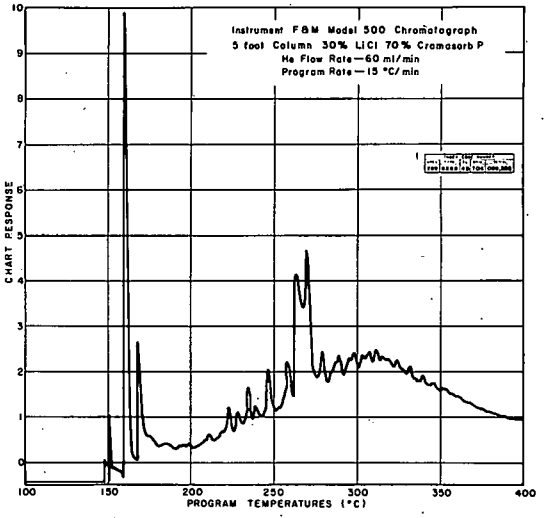

Fig. 57 Chromatogram of impurity No. 1, compound B.

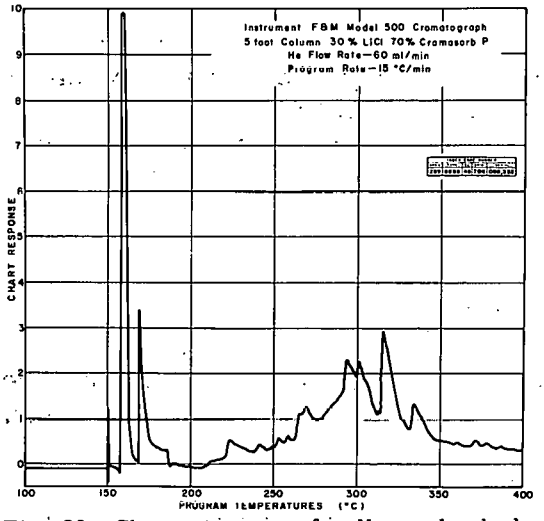

Fig. 58 Chromatogram of yellow color body present in o-terphenyl.

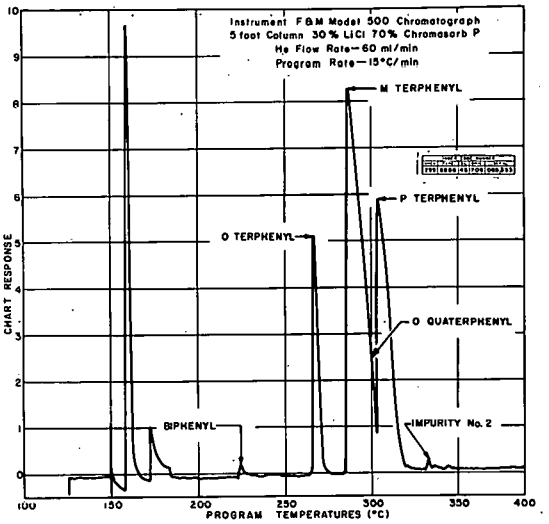

Fig. 59 Chromatogram of Santowax OMP.

III. EOCR OPERATIONS

1. INTRODUCTION

Operations Branch personnel continued to study and evaluate the design, construction, and operability of the EOCR. This was achieved by close liaison with both the construction contractor and architect-engineer. Concurrently, branch personnel witnessed equipment component tests conducted by the construction contractor and proceeded with the preparation of plant operating and maintenance manuals.

Work commenced with preparation of a final draft of the EOCR Safety Analysis Report (previously referred to as the Final Hazards Evaluation Report). Testing of a prototype control rod and rod drive mechanism continued.

2. EOCR DESIGN AND CONSTRUCTION

2.1 Construction Status

Alignment and leveling of the reactor pressure vessel was completed. The vessel was water-filled and a successful hydro-test was made at a pressure of 570 psig.

Installation of the wash cells and final wiring of the wash cell control console was begun. Work continued on steam tracing and primary coolant process piping throughout the building.

Excavation for the building foundation for the relocated Control Rod Test Facility (EOCRT) was completed. As of June 30, 1962, overall completion of the basic EOCR was approximately 90 percent.

2.2 Radiography and Inspection of Organic Piping

According to previously established criteria for radiographic examination of organic piping [26], inspection and repair of piping throughout the primary organic systems continued. As of June 20, 1962, for example, 2661 radiographs had been made. Of these, 1816 showed acceptable welds while 845 indicated defects that would require repair.

3. FIELD TESTING

Inspection and testing of components by the construction contractor, the architect-engineer, and Phillips Petroleum Co continued in several areas.

3.1 Component Inspection

Several reactor components were received by Phillips for inspection and/or modification.

The grid plate, No. 1 spider, No. 2 spider, and hold-down tubes were inspected and no major discrepancies were found. The driver fuel element extension pieces were checked and found not to meet specifications in that the mating portions of the two extension pieces were out of round. Present plans call for the extensions to be returned to the fabricator. The No. 1 spider was drilled and tapped for future installation of thermocouple leadouts and junction boxes.

3.2 Plant Component Testing

Branch representatives continued to witness component testing ("A" tests) of plant equipment as performed by the construction contractor. Component tests which were witnessed during the report period were:

A-200 Primary coolant pump & decay loop pumps

A-202 Primary cooler

A-207 Water tube boilers

A-208 Cooling water cooler

A-209 Fire water pumps

Data recorded during these tests must be evaluated and approved before the tests will be accepted as complete.

3.3 Nuclear Instrumentation

The reactor nuclear instrumentation was released to Phillips for component bench testing with the following results:

3.31 Start-up Channel. This channel generally performed well. There were, however, some deviations from specifications: The fission chamber has a sensitivity of 1.8 cpm/nv as compared to a sensitivity specified of 0.4 cpm/nv, and poor resolution time causes an inaccuracy of 33 percent as compared to a specified allowable inaccuracy of 6 percent.

3.32 Intermediate Log N Period Channel. The output of the channel does not go to zero for a zero input. In addition, inaccuracy at the lowest decade was found to be 13 percent rather than the specified allowable 6 percent. The channel is considered unacceptable and will be returned for modification.

3.33 Flux Level Amplifier. In general the amplifier was acceptable; however, there is no alarm or protective action in the event of high voltage power supply failure. This is not in conformance with the specifications.

3.34 Automatic Control Channel. This channel was acceptable.

3.35 Magnet Power Supply and Logic Channel. This channel was acceptable.

3.4 Plant Systems Testing

Operations personnel maintained readiness to begin testing plant systems as soon as construction progress permitted. It was anticipated that testing would commence on or about June 1, 1962; however, the facilities were not complete and no testing was initiated during the quarter.

A review of existing systems test procedures ("R" tests) was initiated, for the purpose of determining:

(1) If the general scope of test procedures, as written, is adequate. If not, supplements to the procedures must be prepared.

(2) If existing tests adequately cover specific hazards considerations; ie, are test commitments in the Safety Analysis Report actually covered by existing test procedures.

(3) What equipment must be procured or special preparations made for Phillips to conduct the tests as written.

(4) Adequacy of test data sheets; specifically, if they are designed to readily show if test results, in fact, meet design specifications and operating requirements.

Several meetings were held between IDO-AEC, C. F. Braun Co, Fluor Corp, and Phillips to clarify responsibilities and coordinate efforts in the performance of Field Test Procedure R-150, Reactor Vessel Dimensional and Component Test.

4. OPERATIONAL PLANNING

Operational planning continued to be directed toward procuring materials and hardware, and initiating design proposals or design changes required to make the plant operational. A substantial manpower effort is still being expended in preparation of plant operating manuals, and training and maintenance manuals. A portion of this work is summarized below.

4.1 Safety Analysis Report

Representatives from IDO-AEC, Washington-AEC, and Phillips met for an informal review of the first completed draft of the Safety Analysis Report. Final drafting of the report is now in progress, and will incorporate suggestions offered during the informal review.

4.2 Operating Manuals

The plant operating manual will be published in three separate volumes, viz:

Part I – Utilities

Part II – Process systems

Part III – Reactor systems

The first volume, Part I – Utilities, was completed and published during the quarter. Work is in progress on initial drafts of 11 sections of Parts II and III. Work is continuing with the preparation of operating and maintenance manuals for the reactor nuclear instrumentation.

4.3 Plant Requirements

Design and procurement of essential reactor facilities proceeded. Design work was completed on the following items:

Aqueous waste monitoring system

Control rod limit switch brackets

Fuel storage racks

In addition, design and procurement were either initiated or continued on several other projects, for example:

Neutron source and handling tools

Reactor and canal handling tools

Canal cleaning equipment

Tool washing facility

Start-up instrumentation thimbles

Rabbit facility

A Phillips proposal to modify the reactor shutdown extension tank and fabricate an improved working platform was authorized by IDO-AEC. This will facilitate, and improve from a safety aspect, reactor shutdown operations.

4.4 Procurement of Organic Coolant

The successful bidder to supply the organic coolant for initial operation of the EOCR was Monsanto Chemical Co. Monsanto will deliver 386,000 pounds of terphenyl coolant at a rate of 100,000 pounds per month. Initial shipments were made June 27, 1962.

4.5 Reactor Fuel Procurement

The fabricator for the EOCR fuel, Metals and Controls Inc, is in advanced stages of component procurement from commercial sources and specialty machine shops. A dummy element made of aluminum and steel to simulate an actual driver assembly has been received for use in checking out reactor handling equipment. Delivery of non-uranium-bearing dummy driver assemblies will be made next quarter and uranium-bearing (live) elements the following quarter.

4.6 Estimated Start-up Schedule

Due to unforeseen construction delays, plant systems testing did not get underway when anticipated. Based on the current construction schedule, a revised estimated schedule for plant start-up is graphically illustrated in Figure 60.

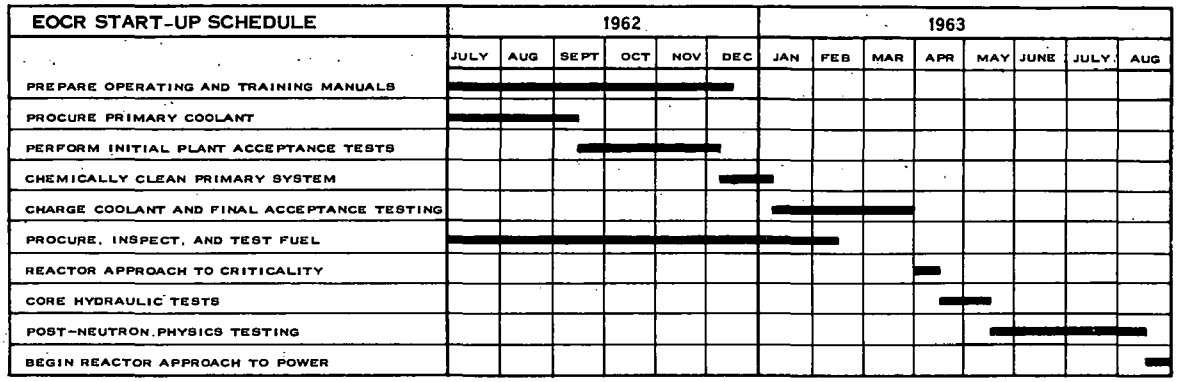

Fig. 60 Graph of plant start-up schedule.

5. COMPONENT HYDRAULIC TESTING

Sufficient testing was completed to determine that the EOCR control rod, as designed, was questionable with respect to its safe performance in the reactor under certain operating conditions. Testing of additional orifice and slot combinations for regulation of flow through driver fuel assemblies continued. Findings are summarized below.

5.1 Control Rod Testing

Testing of the reactor control rod continued (in 132°F water) and the test data analyzed. It was concluded that the rod, as designed, did not perform with a satisfactory margin of safety for operation in the reactor. Under certain flow conditions the rod failed to seat, and once seated, could be lifted from its seat when uncoupled from the drive.

Further tests of rod behavior were undertaken to locate the source or sources of excessive drag noted during some phases of rod insertion. A plexiglass viewing port was installed on the hydraulic test vessel and visual observations of rod behavior were made. Tests, performed under two different conditions, are summarized as follows:

(1) The first series of observations was made with the rod initially seated and the seat light on. The driver was unlatched from the rod and held at the 36-inch (withdrawn) position. The loop flow control valve was set to give a predetermined flow rate. The circulating pump was then started and the rod behavior noted. Results were:

Flow @ 640 to 755 gpm – The control rod lifted 1/2 inch or less, resulting in loss of the seat light.

Flow @ 756 gpm – The rod lifted approximately 13 inches.

Flow @ 810 gpm – The rod lifted 18 inches. At this position the top of the rod was in contact with the scram spring.

Flow @ 880 gpm – The rod lifted approximately 23 inches. At this position the scram spring was compressed 5 inches.

(2) A second series of observations was made with the control rod latched to the drive and held at the 36-inch (withdrawn) position. With the flow at a desired rate, the rod was scrammed with the following results:

Flow @ 660 gpm – The rod inserted to the 9-1/2-inch position in one second and then to within 1/2 inch of the seat in 40 minutes. The seat light was not actuated.

Flow @ 700 gpm – The control rod inserted to the 14-inch position in one second, inserted another 4 inches in 3 minutes and inserted no farther in the next 15 minutes.

Flow @ 735 gpm – The control rod inserted to the 17-inch position in one second and inserted no farther in the next 15 minutes.

Flow @ 775 gpm – The control rod inserted to the 18-inch position in approximately 5 seconds and inserted no farther in the next 15 minutes.

In attempting to locate the sources of drag during rod drop, the spring-loaded seal shoes were adjusted to limit their maximum dimension to the boot minimum internal dimension of approximately 4.125 inches. Significantly, the maximum flow rate attained with satisfactory rod seating was increased from the previously reported 550 gpm [27] to 680 gpm.

The rod was then ballasted with a weight of 112 pounds. One hundred successful scrams were made at a further increased flow rate of 760 gpm. The seal shoes were then further restricted to a maximum dimension of 4.106 inches. Satisfactory seating of the weighted rod was then obtained at a flow rate as high as 810 gpm. This retraction of the seal shoes did not increase leakage around the rod significantly.

Further testing of various rod configurations was conducted. Rod drop times were measured. As shown in Table XXX, the modified rod (112-pound ballast, retracted shoes) seated in 1.38 seconds at a flow of 810 gpm. The rod did not lift from its seat until a flow of 880 gpm was attained.

In order to minimize impact stresses incurred when the rod seats following a scram, modifications to the snubber piston were made and tested. Under the most severe condition (zero flow through the control rod), the modified snubber piston reduced the rod impact velocity from 5 feet per second to 1.5 feet per second. The tests were conducted with 112-pound ballast and scram spring installed. Since impact stress varies as the square of impact velocity, the modified piston significantly reduces the impact stress on the rod.

5.2 Driver Fuel Element Testing

Testing of different orifice and slot size combinations continued to calibrate flow rates through driver fuel assemblies. Table XXXI represents orifice and slot combinations with measured flow rates determined (using 132°F water) for

TABLE XXX

EOCR PROTOTYPE-CONTROL-ROD[a] DROP TIMES AND PRESSURE DIFFERENTIAL

Conditions: Tests performed in 132°F H_2O for 36-in. drop (msec).

	As-built Modified Piston, No Deflector							Pressure Differential (psi), 1.309-in. Boot Orifice		
Flow Rate (gpm)	1.25-in. Boot Orifice, No Ballast, Full Shoe	1.25-in. Boot Orifice, 125-lb Ballast, Full Shoe	1.25-in. Boot Orifice, 112-lb Ballast, Full Shoe	1.309-in. Boot Orifice, No Ballast, 4.125-in. Shoe	1.309-in. Boot Orifice, 112-lb Ballast, 4.125-in. Shoe	1.309-in. Boot Orifice, 112-lb Ballast, 4.106-in. Shoe	No Scram Spring, 1.309-in. Boot Orifice, 112-lb Ballast, 4.106-in. Shoe	(gpm)	Rod (ΔP)	Vessel (ΔP)
0	560	—	545	540	525	525	568	0		
300	710	—	625	653	617	602	663	300	-3.5	-8.2
400	823	710	665	722	628	646	758	400	-5.9	-14.6
500	940	808	800	848	705	714	982	500	-9.0	-22.5
600	—	1000	980	1095	808	798	1062	600	-12.5	-32.5
660	—	1175	1200	1600 at 675 gpm	≈ 900	≈ 890	≈ 1147	660	-15.0	-39
660 (14 in.)	480	≈ 450	475	480 at 675 gpm	≈ 430	≈ 420	575	660	-15.0	-39
700	—	1380	1460	—	995	960	1557	700	-16.8	-44
800	—	—	—	—	—	1384	No seat	800	-21.7	-57
800 (14 in.)	—	—	—	—	—	—	≈ 1293	800	-21.7	-57
900	—	—	—	—	—	—		900	-27	-71
Maximum rate for seating (gpm)	550	700	700 to 725	680	760	810				
14-in. insertion time (msec)	—	—	—	—	485 at 760 gpm	515 at 800 gpm				
Total drop time (msec)	2120	1380	> 1460	1600	1250	1380				
Vessel, ΔP (psi)	—	—	—	—	50	58				
Lift-off flow rate (gpm)	765	—	—	770	880	880				
Control rod, ΔP (psi)	—	—	—	—	25.5	25.5				

[a] Rod dry weight = 410 lb, rod wet weight = 358 lb, rod dry weight with 112-lb ballast = 522 lb, rod wet weight with 112-lb ballast = 456 lb.

various reactor positions. This work completes driver fuel testing in the existing test facility.

TABLE XXXI

DRIVER FUEL ORIFICE AND SLOT VALUES

Driver Fuel Position	Calculated Flow (gpm)	Measured Flow[a] (gpm)	Monitor Tube[b] Measurement (psi)	Orifice Number[c]	Orifice Hole Size (in. Diameter)	Number of Holes	Slot Number[c]	Slot Size (in.)
D-1	430	475	32.5	5	9/16	8	1	1/4 diameter hole
D-2	680	690	25	3	7/8	8	2	0.291 x 3.000
D-3	780	770	20.5	6	39/64	8	2	0.291 x 3.000
D-4	780	770	20.5	6	39/64	8	2	0.291 x 3.000
D-5	680	690	25	3	7/8	8	2	0.291 x 3.000
D-6	780	770	20.5	6	39/64	8	2	0.291 x 3.000
D-7	970	990	9	8	(d)	8	4	1.125 x 3.000
D-8	750	755	16.5	5	9/16	8	2	0.291 x 3.000
D-9	430	475	32.5	5	9/16	8	1	1/4 diameter hole
D-10	970	990	9	8	(d)	8	4	1.125 x 3.000
D-11	970	990	9	8	(d)	8	4	1.125 x 3.000
D-12	550	580	28.5	1	43/64	8	1	1/4 diameter hole
D-13	750	755	16.5	5	9/16	8	2	0.291 x 3.000
D-14	970	990	9	5	9/16	8	2	0.291 x 3.000
D-15	750	755	16.5	5	9/16	8	2	0.291 x 3.000
D-16	680	690	25	3	7/8	8	2	0.291 x 3.000
D-17	780	770	20.5	6	39/64	8	2	0.291 x 3.000
D-18	780	770	20.5	6	39/64	8	2	0.291 x 3.000
D-19	680	690	25	3	7/8	8	2	0.291 x 3.000
D-20	430	475	32.5	5	9/16	8	1	1/4 diameter hole

(a) 132°F, H_2O test media, 40 psi test vessel differential.

(b) Monitor tube pressure minus vessel outlet pressure.

(c) Phillips' number.

(d) Elongated hole 0.625 in minor axis, 0.841 in major axis (0.442 in ^{2} per hole).

5.3 Control Rod Drive Testing

Two production control rod drive units were installed and tested at the flow test facility. Minor problems were encountered with operation and adjustment of the rod position indicators and the rod position limit switches. Some modifications will be required to correct these problems.

IV. REFERENCES

1. Organic Coolant Reactor Program Quarterly Report, 1st Qtr 1962, IDO-16787, p 10 (1962).

2. A. J. Moffat and P. W. Solomon, The Gas-Solid Chromatographic Separation of Polyphenyls on Lithium Chloride-Firebrick, IDO-16732 (November 1961).

3. G. R. Vavasour, Ed, Proceedings of the Tripartite Conference on Transport of Materials in Pressurized Water Nuclear Systems, AECL-1265 (June 1961).

4. Organic Coolant Reactor Program Quarterly Report, 3rd Qtr 1961, IDO-16734, p 9 (1961).

5. P. H. Emmett, Catalysis, p 242, New York, Reinhold Publishing (1956).

6. P. de Radzitzky and J. Hanotier, "Clathration of Hard-to-Separate Aromatic Mixtures With New Werner Complexes", I. & E. C. Process Design and Development 1, No. 1, p 10 (January 1962).

7. W. M. Hutchinson et al, Relationship Between Yields of Dimers of a Polyphenyl and Its Partial Reaction Rates, IDO-16706 (August 7, 1961).

8. P. L. Southwick and D. I. Sapper, "4-Styrylthiazoles. Syntheses and Relationships Among Ultraviolet Absorption Spectra", J. Org. Chem. 19, p 1926 (1954).

9. G. R. Ames and W. J. Davey, J. Chem. Soc., p 3480 (1937).

10. F. Arndt, Organic Syntheses, Collective Vol. II, pp 165, 461, New York, Wiley (1943).

11. E. E. Marler and E. E. Turner, "Orientation Effects in the Biphenyl Series. IX. Nitration of 4-chloro-4'-fluoro——and 4-bromo-48 fluorobiphenyl", J. Chem. Soc., p 1359 (1931).

12. F. H. Case, "A Further Study of the Bromination of the Nitrodiphenyls", J. Am. Chem. Soc. 60, p 424 (February 1938).

13. Organic Coolant Reactor Program Quarterly Report, 1st Qtr 1962, IDO-16787, p 42 (1962).

14. Organic Coolant Reactor Program Quarterly Report, 3rd Qtr 1961, IDO-16734, p 44 (1961).

15. E. H. Kober et al, Synthesis of Nitrogen-Containing and Heterocyclic Fluid Systems. Part II. The Preparation of Triazine, Quinoline and Tertiary Amino Derivatives, WAPD-TR-60-315 (Part II) (November 1960).

16. F. H. Case and E. Koft, "The Synthesis of Certain Substituted 1,3,5-Triazines Containing the Ferroin Group", J. Am. Chem. Soc. 81, p 905 (1959).

17. "Thiazoles", O. Hromatka (to Merck & Co.) U. S. 2,160,867 (June 6, 1939). "Thiazole Derivatives", Firma E. Merak (O. Hromatka, inventor), Ger. 670,131 (January 12, 1939).

18. E. P. Hart, "Naphthyridines. Part 1. The Chemistry of 1:5-Naphthyridine", J. Chem. Soc., p 1879 (1954).

19. A. Albert, "Naphthyridines. Ionization Constants and Spectra of Four Parent Substances", J. Chem. Soc., p 1790 (1960).

20. Organic Coolant Reactor Program Quarterly Report, 1st Qtr 1962, IDO-16787, p 75 (1962).

21. O. A. Hougen, "Engineering Aspects of Solid Catalysts", Ind. Eng. Chem. 53, p 509 (1961).

22. Organic Coolant Reactor Program Quarterly Report, 1st Qtr 1962, IDO-16787, p 96 (1962).

23. Ibid, p 51.

24. Ibid, p 68.

25. Ibid, p 79.

26. Ibid, p 127.

27. Ibid, Table LIII, p 132.

PHILLIPS
PETROLEUM
COMPANY

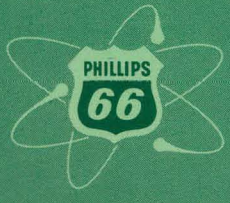

ATOMIC ENERGY DIVISION